From the Institute of Normal and Pathological Physiology
Philipps-University Marburg
Faculty of Medicine
Germany
Director: Prof. Dr. Dr. J. Daut

in collaboration with

School of Pharmacy, Texas Tech University Health Sciences Center,
Department of Pharmaceutical Sciences,
Amarillo, Texas, U.S.A.
Dean: A. A. Nelson, R.Ph., Ph.D.

Drug Delivery of Oligonucleotides at the Blood-Brain Barrier:
a Therapeutic Strategy for Inflammatory Diseases
of the Central Nervous System

Inaugural-Dissertation for attaining the degree
of Doctor of Human Biology (Dr. rer. physiol.)
submitted to the Faculty of Medicine
Philipps University Marburg

Berit Osburg
of Erfurt/Germany

Marburg 2003

To Uli and Jördis

Table of Contents

List of abbreviations used in this script

AEC	aminoethylcarbazol
APC	antigen presenting cell
Atm	atmosphere
ATP	adenosine tri phosphate
AUC	area under the curve
AZT	azidothymidine
BBB	blood-brain barrier
BCA	bicinchoninic acid
BDNF	brain derived nerve growth factor
BFGF	basic fibroblast growth factor
bioPEGPEI	biotinylated PEGPEI
bp	base pairs
BSA	bovine serum albumin
cAMP	cyclic adenosine monophosphate
CD	cluster of differentiation
cDNA	complementary DNA
Ci	Curie
CNS	central nervous system
COX-2	cyclooxygenase-2
cpm	counts per minute
°C	degree Celsius
Da	Dalton
DALDA	Tyr-D-Arg-Phe-Lys-NH2
dATP	desoxy adenosine tri phosphate
dCTP	desoxy cytosine tri thphosphate
dGTP	desoxy guanine tri phosphate
DHP	dihydropyridine
DMEM	Dulbecco's minimal essential medium
dNTP	desoxy nucleotide tri phosphate
dpm	decays per minute
dTTP	desoxy thymidine tri phosphate
DMSO	dimethylsulfoxide

DNA	desoxy ribonucleic acid
ds	double stranded
DTT	dithiothreitol
EAE	Experimental Autoimmune Encephalomyelitis
E. coli	Escherichia coli
EDTA	ethylene diamine tetra acetate
EGF	epithelial growth factor
ELAM-1	endothelial leukocyte adhesion molecule-1
EMSA	electrophoretic mobility shift assay
et al.	et alii
FCS	fetal calf serum
FPF	folate-PEG-folate
FPLC	fast protein liquid chromatography
g	gram
GAPDH	glycerinaldehydephosphodehydrogenase
GLUT	glucose transporter
h	hour
HABA	2(4'-hydroxyazobenzene)benzoic acid
HBSS	Hank's buffered saline
HIV	human immunodeficiency virus
HMW	high molecular weight
HPLC	high pressure liquid chromatography
ID	injected dose
IGF	insulin like growth factor
IgG	immuno globulin G
IκB	inhibitory κB
IL	interleukin
iNOS	inducible nitric oxide synthetase
IPTG	isopropyl β D thiogalactoside
i.v.	intravenous
l	liter
kb	kilo bases
kDa	kilo Dalton
LB medium	Luria-Bertani medium

LDH	lactate dehydrogenase
LDL	low density lipoprotein
LFA-1	lymphocyte function associated antigen-1
LMW	low molecular weight
LNAA	large neutral amino acid
LPS	lipopolysaccharide
M	molar
m	milli
MAb	monoclonal antibody
MBP	myelin basic protein
MDR	multi drug resistance
Me-ODN	methylphosphonate ODN
MHC	major histocompatibility complex
min	minute
MOPS	morpholino propan sulfonic acid
MS	Multiple Sclerosis
MTT	3-(4,5-dimethylthiazol-2-yl)-2,5-diphenyl tetrazolium bromide
MW	molecular weight
μ	micro
mRNA	messenger RNA
n	nano
NF-κB	nuclear factor-κB
NGF	nerve growth factor
NHS	N-hydroxy-succinimide
NMR	nuclear magnetic resonance (spectroscopy)
NO	nitric oxide
OD	optical density
ODN	oligodesoxynucleotides
PAGE	polyacrylamide gel electrophoresis
PCR	polymerase chain reaction
PEG	polyethylene glycol
PEI	polyethylenimine
PFA	paraformaldehyde

PG	prostaglandin
PHPMA	N-(2-hydroxypropyl)-methacrylamide
PLA	poly(lactic acid)
PNA	peptide nucleic acids
PO-ODN	phosphodiester ODN
PS	permeability- surface area
PS-ODN	phosphorothioate ODN
RHB	Ringer-HEPES buffer
RNA	ribo nucleic acid
rpm	rotations per minute
RT	room temperature
RT-PCR	reverse transcription PCR
SA	streptavidin
SDS	sodium dodecyl sulfate
SIV	simian immunodeficiency virus
SSC	saline sodium citrate
ss	single stranded
S-SMPB	Succinimidyl-4-(p-maleimidophenyl)butyrate
SSPE	saline sodium phosphate EDTA
TBE	tris boric acid EDTA
TCA	trichloro acetic acid
TCR	T cell receptor
TE	tris EDTA
Tf	transferring
TF	transcription factor
TfR	transferrin receptor
TGE	tris glycine EDTA
TNF	tumor necrosis factor
U	units
UV	ultraviolet
V	volt
VCAM-1	vascular cell adhesion molecule-1
VD	volume of distribution
VIP	vasointestinal peptide

VLA-4   very late activation antigen-4

X-Gal   5-bromo-4-chloro-3-indolyl-β-D-galactoside

1.   Introduction

The blood-brain barrier (BBB) is the interface of peripheral circulation and central nervous system (CNS). It plays a crucial role in the supply of nutrients to the brain and in the exchange of information. The BBB is closely involved in many disease processes affecting the CNS. In addition, its control function in the passage of drugs to brain tissue is an important factor in the development of more specific and potent neuropharma-ceutical agents. The following discourse introduces aspects of BBB biology, pharmacology and pathology, which are relevant to the research carried out for this thesis: First, an overview of drug delivery approaches is given. Second, the transcription factor NF-κB is described as a target for oligonucleotide-based anti-inflammatory drugs. Third, the vehicle for delivery of oligonucleotides used here, the cationic polymer polyethylenimine (PEI), is explained. Fourth, the neuroinflammatory disease Multiple Sclerosis (MS) is portrayed as one example of a disease with inflammatory damage to the BBB, which could be a therapeutic target for the drug delivery strategy developed in this project.

1.1.   Drug delivery strategies through the blood-brain barrier

The presence of the BBB has major implications for the passage of compounds into the brain that are either hydrophilic or relatively large (> 400 - 600Da). Due to complex tight junctions, the paracellular transport across the cerebral endothelium, which forms the morphological substrate of the BBB, is limited. As a result, even the passive entry of certain low molecular weight nutrients (amino acids, glucose) is restricted. Several transport mechanisms have been characterized, including passive processes (diffusion), facilitative or carrier mediated transport, and active (energy requiring) processes. The diffusion of compounds across the endothelial cells of the BBB is dependent on several factors like lipid solubility, molecular weight, and electrical charge. There are three different classes of transport systems within the BBB: carrier-mediated transport systems, receptor-mediated systems, and active efflux transporters (Pardridge, 2002). Glucose and amino acids are transported into the brain by selective carrier mechanisms. For example, GLUT1 is a stereospecific facilitative carrier system, which transports glucose and other hexoses (galactose, mannose, 2-deoxyglucose, 3-O-methylglucose) with high affinity (Farrell and Pardridge, 1991). Nine distinct high affinity amino acid carrier systems have been described at the BBB for transport of small or large neutral

amino acids, of basic amino acids, and of acidic amino acids, respectively (Smith, 2000). Further carrier systems exist for the transport of amines (e.g., choline), nucleosides (e.g., adenosine), purine bases (e.g., adenine), monocarboxylic acids (e.g., pyruvate), and thyroid hormones (e.g., T3) (Smith, 1993).

Receptor-mediated transport systems at the BBB include the transferrin receptor. Its expression at the BBB was first described by Jefferies et al. using a mouse anti rat IgG_{2a} monoclonal antibody (OX26) (Jefferies et al., 1984). These receptors are responsible for transport of transferrin (and thus iron) into brain tissue. Several other receptors for peptides and proteins are present at the BBB, such as the insulin receptor (van Houten and Posner, 1979), leptin receptor (Bjorbaek et al., 1998; Golden et al., 1997), IGF-1 and –2 receptors (insulin-like growth factors) (Frank et al., 1986), and LDL receptor (low density lipoprotein) (Meresse et al., 1989).

The BBB also prevents entry of many substances, including potential neuropharmaceuticals, by active efflux systems. These mediate the ATP-dependent efflux of small molecules from brain to blood. The prototype of these efflux transporters is p-glycoprotein, which is the product of the multidrug resistance gene (MDR) that is known to have a broad substrate specificity (Borst, 1998). Immunoreactive p-glycoprotein was first described at the brain microvasculature by Cordon-Cardo and colleagues (Cordon-Cardo et al., 1989).

The development of non-invasive brain drug-targeting technologies for delivery of small and large drugs across the BBB is a pressing need. About 98% of all small-molecule drugs do not cross the BBB, and the uptake of large-molecule drugs through the BBB is completely hindered (Pardridge, 2002). Whereas small-molecule drugs provide symptomatic relief for brain disorders such as epilepsy and affective disorders, large-molecule drugs possess the potential to cure many neurological disorders such as stroke, Alzheimer's disease, ataxias, and brain tumors (Pardridge, 2002). The physiological transport systems at the BBB may be utilized for delivery of chemically very different neuropharmaceuticals. Carrier-mediated transport and active efflux systems are of importance for delivery of small-molecule drugs, while large-molecule drugs (peptide-based therapeutics, antisense drugs and genes) may be transported by receptor-mediated systems via endocytosis and transcytosis.

1.1.1. Small molecule drugs

Two main factors determine, whether small molecules cross the BBB: the molecular weight (400 – 600Da) of a drug and its lipid solubility – the number of hydrogen bonds, which are formed by this molecule with water. For example, negligible transport would be expected, if the drug forms more than ten hydrogen bonds (Lipinski et al., 2001). Manipulations of small molecule drugs for drug delivery purposes will be performed mainly on hydrophilic compounds by blocking of hydrogen bond-forming functional groups (Pardridge and Mietus, 1979) or by increasing the number of methylene groups within a molecule (Diamond and Wright, 1969). Another way to increase transport properties of a drug is the so-called lipidization by chemical alteration of a molecule (Higuchi and Davis, 1970). One of these carriers is dihydropyridine (DHP) (Bodor and Simpkins, 1983). Further candidates are free fatty acid lipid carriers (Shashoua and Hesse, 1996) and adamantane (Tsuzuki et al., 1994). While the rate of influx of drug across the BBB may be improved, as apparent by a higher permeability-surface area product (PS), other pharmacokinetic properties, such as the area under the plasma concentration curve (AUC), may be adversely affected, i.e. decreased. Because the amount of drug delivered to brain is calculated as the product of $[PS_{BBB}]$ x $[AUC_{plasma}]$, the net effect of lipidization on brain delivery may be minimal (Pardridge, 1998).

1.1.2. Carrier-mediated transport of drugs

In order to use nutrient transport systems for drug delivery, the drug must have structural characteristics mimicking the nutrient normally transported by these carriers. Transporters bind their substrate molecule and change their conformation or temporarily open up a pore, allowing passage across the plasma membrane. L-DOPA is a pro-drug used for treatment of Parkinson's disease. It utilizes the large neutral amino acid transporter (LNAA) at the BBB (Wade and Katzman, 1975). Inside the brain L-DOPA will be decarboxylated to dopamine – the active substance. Other examples of carrier-mediated BBB transport of small molecules include the uptake of amino acid-based anticancer agents melphalan and acivicin by LNAA (Killian et al., 2000). Drugs exhibiting high affinity for the carrier can be specifically designed to enhance brain uptake. Takada et al. showed that the regional brain uptake of the amino acid derivative D, L – NAM exceeded that of the clinically used analogue, melphalan, by greater than 20-fold (Takada et al., 1992).

The characteristics of the active efflux pump p-glycoprotein explain experimental observations that some molecules with a MW > 400 - 600Da do not cross the BBB despite considerable lipophilicity. Drugs like cyclosporine, vinblastine and vincristine are subject to p-glycoprotein mediated efflux (Begley, 1996; Pardridge, 1998).

1.1.3. Nanoparticles and Liposomes

Solid or vesicular drug containers are being scrutinized for their potential in the delivery of both small molecules and macromolecules.

Nanoparticles. Up to this time point the transport mechanisms of nanoparticles across the BBB are controversially discussed. Nanoparticles have sizes in the range of 100 – 400nm, and therefore, they should not be able to pass the tightly sealed endothelial cell membrane. Further problems arise from the rapid clearance of systemically injected nanoparticles from the bloodstream, the opsonization by plasma proteins and the phagocytotic activity of the reticuloendothelial system (Gref et al., 1994; Schroeder et al., 1998). In order to prevent the release of the drug from the nanoparticle, the transport system must be coated with stabilizers, such as polysorbate, poloxamers or poloxamines (Troster et al., 1990). Kreuter and colleagues reported the brain delivery of poly(butylcyanoacrylate) nanoparticles, which were sequentially coated with polysorbate 80 and apolipoprotein B or E. The authors observed antinociceptive pharmacological effects when the nanoparticles were loaded with an opioid analog, the synthetic hexapeptide dalargin (Kreuter et al., 2002). The mechanism of entry into brain remained unknown. A receptor-mediated endocytosis by LDL receptors of these lipoprotein-mimicking particles was proposed. However, it is known that polysorbate 80 (Tween 80) as a detergent causes the disruption of the BBB due to solvent destabilization of this barrier (Azmin et al., 1985). Therefore, opening of the BBB could also be the reason for a nanoparticle uptake observed by these authors.

Liposomes exist as unilamellar vesicles with a diameter of 40 – 80nm or as multilamellar vesicles in a range from 0.3 - 2μm, which encapsulate the drug that has to be transported. However, classical liposomes do not show significant transport through the BBB because of their size and the rapid clearance from the circulation (Gref et al., 1994; Sakamoto and Ido, 1993; Schackert et al., 1989). After conjugation of liposomes with polyethylene glycol (PEG) increased circulation times were observed (Papahadjopoulos et al., 1991). PEG on the liposome surface prevents the absorption to cells of the reticuloendothelial system ("stealth" liposomes) and increases the half life of

the circulating liposome in blood (Papahadjopoulos et al., 1991) Receptor-mediated endocytosis/transcytosis was observed by coupling these PEG-liposomes to a vector such as a monoclonal antibody directed against the transferrin receptor (Huwyler et al., 1996) (see 1.2. below).

1.1.4. Peptide-based neuropharmaceuticals

Due to their hydrophilicity and size, peptides are generally excluded from passage through the BBB by simple diffusion. The methods under investigation for peptide and protein drug delivery may be divided in three principal strategies:

a) Invasive procedures by either direct intraventricular administration of the drug or by temporary disruption of the BBB by injection of hyperosmolar solutions into the carotid artery. Approaches like intraventricular injection of a drug are used when the disease process is close to the brain surface, for example the delivery of glycopeptide and aminoglycoside antibiotics in meningitis (Nau et al., 1998). In addition to the invasive character of this method it must be considered that drug distribution within the brain is diffusion-limited (Jain, 1990), and due to the continuous turnover of the cerebrospinal fluid the clearance of the drug from the ventricle occurs rapidly.

The temporary opening of the BBB by disruption of the tight junctions by infusion of hyperosmolar solutions like 2M mannitol into the carotid artery (Neuwelt and Rapoport, 1984) is also an invasive procedure. There is evidence for chronic neuropathologic changes inside the brain (Salahuddin et al., 1988) because of entry of neurotoxic substances and plasma proteins (Nadal et al., 1995).

b) Strategies that increase delivery of systemically injected drugs to brain by **chemical manipulation** (increased lipophilicity, see 1.1.1.), or inclusion of the compound into small liposomes (see 1.1.3.).

c) Physiologic-based strategies, which exploit the various transport mechanisms at the BBB for nutrients, peptides, and plasma transport proteins (Bickel et al., 2001), which will be described in detail in section 1.2.

1.1.5. Antisense drugs

The principle of antisense oligodeoxynucleotides (ODN) is the selective inhibition of gene expression by binding to specific mRNA, thus preventing translation into a protein. Generally, ODNs are most effective inhibitors when they are targeted to the translation initiation site (Daaka and Wickstrom, 1990). Current research focuses on the mode of

action of antisense drugs, their specificity, stability, cellular uptake in cell culture as well as organ distribution and pharmacologic action *in vivo*. Unmodified phosphodiester ODNs (PO-ODN) with their strong negatively charged backbone have an excellent solubility in aqueous solutions and good hybridization characteristics. However, *in vivo* applications are limited due to the presence of 3'-exonucleases in serum leading to degradation of ODN (Sands et al., 1994; Shaw et al., 1991). Structural alterations of ODN, e.g. substituting the backbone oxygen by a sulfur atom (PS-ODN) improve the properties regarding exonuclease stability. The half-life of these phosphorothioates increases to > 18h in pure fetal calf serum (FCS) compared to 5min for PO-ODNs (Shaw et al., 1991). PS-ODN show enhanced cell uptake by binding to multiple cellular proteins in cell culture (Beltinger et al., 1995). The disadvantage of this binding behavior is an increased affinity to plasma proteins (albumin, α_2-macroglobulin), which causes a loss of the bioavailability of the PS-ODN in the circulation (Soker et al., 1993). Moreover, neurotoxic properties of phosphorothioates were reported (Whitesell et al., 1993). In methylphosphonate ODNs (Me-ODN), the negatively charged oxygen of the phosphodiester bond is replaced by a neutral methyl group. They are also highly resistant against nucleases, and due to their lipophilic character are taken up by cells by passive diffusion or pinocytosis. Limitations in their application result from a lower water solubility and poor duplex formation due to their steric conformation. Therefore, to achieve the inhibition of a specific target sequence, 20-100-fold higher concentrations of Me-ODN compared to PS-ODN are needed (Maher and Dolnick, 1988). Peptide nucleic acids (PNA) are another example of very stable and neutral DNA analogues. PNAs retain high affinity for complementary RNA or DNA, but show poor cellular uptake without suitable delivery methods (Koppelhus and Nielsen, 2003).

Due to size and/or charge, antisense drugs do not cross the BBB. Therefore, *in vivo* therapeutic effects in the CNS after systemic application of free drugs cannot be expected. While they are efficiently taken up by nervous tissue when applied directly into the cerebrospinal fluid (Schlingensiepen and Heilig, 1997), this invasive method is unsuitable for clinical applications.

Efforts are made to create delivery vehicles for antisense drugs. A multitude of cationic lipid carriers are commercially available (e.g., lipofectin, DOTMA) and are used successfully in cell culture (Bennett et al., 1992; Schlingensiepen and Schlingensiepen, 1997). However, non-specific carrier effects have to be excluded, as shown in a study with colon tumor cells (Yeoman et al., 1992). Immuno-liposomes and polymeric

nanoparticles were investigated regarding their delivery characteristics. Liposomes encapsulate ODNs and protect them very securely from extracellular nucleases. By linkage of liposomes to antibodies, targeting to specific tissues can be reached (Zelphati et al., 1993). Polymers such as lactose- or polyalkylcyanoacrylate polymers were used to protect ODNs from nuclease digestion (Chavany et al., 1992). Linear polyethylenimine (PEI) delivered antisense oligodeoxynucleotides into liver hepatocytes *in vitro* and *in vivo* (Chemin et al., 1998). These approaches are considered in detail below (1.2.).

1.2.   Receptor-mediated delivery of "chimeric peptides"

1.2.1. "Chimeric peptide" strategies

Chimeric peptides are synthetic constructs, which are designed to improve drug delivery through the BBB (Pardridge et al., 1987b). They are formed by chemical conjugation of a transport vector to a peptide or protein (potential neuropharmaceutic drug), which by itself would be unable to pass through the BBB. The vector represents a peptidomimetic MAb, which undergoes receptor-mediated endocytosis / transcytosis. Especially well-characterized receptors at the BBB are the insulin and transferrin receptor, which under physiological conditions mediate transport of insulin and transferrin-bound iron.

Because of its high expression, the transferrin receptor (TfR) is widely used for peptide / protein delivery across the BBB (see 1.2.2.). The "chimeric peptide" transport system binds to exofacial epitopes of the receptor, not competing with binding of the endogenous ligand (Pardridge, 2002). An efficient conjugation of vector and drug can be achieved by biotin-(strept)avidin technology that is known to retain the biological activity and good pharmacokinetic characteristics of these complexes (Pardridge, 1998). **Figure 1** shows a BBB drug-targeting vector.
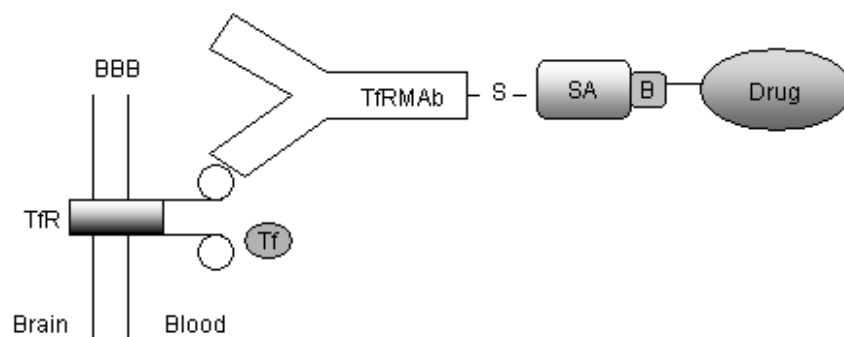
Figure 1: Scheme of a chimeric peptide targeted to the TfR. Abbreviations: SA = streptavidin, B = biotin, -S- = thioether bridge, TfRMAb = transferrin receptor monoclonal antibody

Table 1 gives an overview of various applications of the anti rat MAb OX-26, anti mouse MAb 8D3, and anti human/primate MAb 83-14 as vectors for delivery of peptides, proteins, liposome coated drugs or genes.

Vector/Species	Drug/Category	Target	Reference
OX-26/anti rat	Methotrexate/Small MW drug	TfR	(Friden et al., 1991)
OX-26/anti rat	AZT/Small MW drug	TfR	(Tadayoni et al., 1993)
OX-26/anti rat	VIP/Peptide	TfR	(Bickel et al., 1993) (Wu and Pardridge, 1996)
OX-26/anti rat	NGF/Protein	TfR	(Kordower et al., 1994) (Backman et al., 1995) (Charles et al., 1996) (Backman et al., 1996) (Albeck et al., 1999)
OX-26/anti rat	DALDA/Peptide	TfR	(Bickel et al., 1994b)
OX-26/anti rat	BDNF/Protein	TfR	(Pardridge et al., 1994) (Pardridge et al., 1998) (Wu and Pardridge, 1999) (Zhang and Pardridge, 2001a) (Zhang and Pardridge, 2001b)
OX-26/anti rat	PO-ODN/Oligodeoxynucleo-tide	TfR	(Kang et al., 1995)
OX-26/anti rat	K7DA/Peptide	TfR	(Bickel et al., 1995)
OX-26/anti rat	PNA/Oligodeoxynucleotide	TfR	(Pardridge et al., 1995)
OX-26/anti rat	A beta 1-40/Peptide	TfR	(Saito et al., 1995)
OX-26/anti rat	PS-ODN/Oligodeoxynucleo-tide	TfR	(Wu et al., 1996)
OX-26/anti rat	Daunomycin/Liposome	TfR	(Huwyler et al., 1996)
OX-26/anti rat	GDNF/Protein	TfR	(Albeck et al., 1997)
OX-26/anti rat	EGF/Protein	TfR	(Deguchi et al., 1999) (Kurihara et al., 1999)
OX-26/anti rat	Gene/Liposome	TfR	(Shi and Pardridge, 2000)
OX-26/anti rat	BFGF/Protein	TfR	(Song et al., 2002) (Wu et al., 2002)
OX-26/anti rat	PLA/Nanoparticle	TfR	(Olivier et al., 2002)

8D3/anti mouse	Gene/Liposome	TfR	(Shi et al., 2001)
			(Zhu et al., 2002)
8D3/anti mouse	A beta 1-40/Peptide	TfR	(Lee et al., 2002b)
8D3/anti mouse	PNA/Oligodeoxynucleotide	TfR	(Lee et al., 2002a)
83-14/anti primate/human	A beta 1-40/Peptide	Insulin rec.	(Wu et al., 1997)
83-14/anti primate/human	Gene/Liposome	Insulin rec.	(Zhang et al., 2002)

Table 1: Recently used BBB vector-targeting systems

1.2.2. The transferrin receptor system

Transferrin (Tf) is a glycoprotein with a molecular weight of 80kDa (Laurel and Ingelman, 1947), whose function is the transport of iron (Fe^{3+}) in plasma and its delivery to cells. Iron is an essential component of many enzymatic functions and is a requirement for oxidative metabolism. At neutral pH, Tf uptake into cells is triggered by receptor mediated endocytosis (Baldwin et al., 1982). It has been observed that brain endothelial cells express more transferrin receptors (TfR) than other vascular beds of major organs (Jefferies et al., 1984) with exception of liver (Soda and Tavassoli, 1984), which is also the principal producer of plasma Tf. TfR were found on the surface of the luminal site of the brain capillary endothelial cell (Jefferies et al., 1984). TfR are disulfide-linked homodimers with a molecular weight of 190kDa, possessing an extracellular portion of 88% (Jing and Trowbridge, 1990). After binding of the iron-Tf complex (holotransferrin) to this receptor, the complex is internalized into an acidic intracellular compartment (endocytosis), where the iron will be released and utilized or stored by the cell. Following release of iron, most of the empty binding protein (apotransferrin) can be recycled to the blood plasma, the rest is catabolized by the cell (Taylor and Morgan, 1990). A fraction of internalized holotransferrin will be transcytosed into the brain interstitium (Fishman et al., 1987; Pardridge, 1988; Pardridge et al., 1987a). The mechanisms of endocytosis and transcytosis are controversial (Moos and Morgan, 2000). Alternative possibilities have been suggested for the process of transcytosis of iron: the transcytotic pathway via holotransferrin must avoid an iron release in the endosomal compartment of the endothelial cells, otherwise a different carrier protein would be required to deliver Fe^{3+} ions across the abluminal membrane (Raub and Newton, 1991). The free apotransferrin is thought to either undergo exocytosis across the endothelial plasma membrane back to

the blood, or to return to the circulation via the cerebrospinal fluid, or to be degraded within the brain tissue (Crowe and Morgan, 1992).

Strong support for the transcytosis pathway derives from a number of brain uptake studies using the monoclonal antibody (OX-26, subtype IgG2a) (MAb) directed against the rat TfR, which was shown to bind preferentially to brain capillary endothelial cells after intravenous injection (Jefferies et al., 1984). These reports are summarized above (1.2.1.). Selective binding of OX-26 to the TfR at the BBB was shown by systemic injection of antibody. The antibody was also rapidly taken up by the liver, where it reached its saturation 1h after injection. In contrast, brain constantly extracted OX-26 from the bloodstream over a time frame of 5h. Specific accumulation of antibody in heart, lung or kidney was not seen (Pardridge et al., 1991). Friden and colleagues (Friden et al., 1991) demonstrated a time-dependent transcytosis of radiolabeled OX-26 using capillary-depletion experiments, which separate brain microvessels and brain parenchyma, and showed increase of uptake into brain compared to capillaries over time. Electron microscopy of an OX-26-colloidal gold conjugate revealed binding of conjugate to the luminal membrane of endothelial cells, accumulation in endocytotic vesicles (50-100nm), and release of gold particles to the extracellular space at the abluminal membrane of the endothelial cell (Bickel et al., 1994a).

1.3. The transcription factor NF-κB and its regulation via inflammatory stimulation

Transcription factors bind to the promoter region on the DNA to initiate gene transcription, supporting the function of RNA polymerases. NF-κB regulates the transcription of genes of a multitude of inflammatory mediators, like cytokines, chemokines, adhesion molecules, growth factors and other proteins that participate in the production of prostaglandins, leukotrienes and Nitric Oxide (NO) (Baeuerle and Baltimore, 1996; Baldwin, 1996), see **Table 2**. NF-κB family members are usually heterodimeric proteins – assembled from monomer subunits containing the 300-amino-acid Rel domain at their N-terminus, which binds to specific recognition sequences on DNA, and to other Rel proteins (Rungeler et al., 1999). These specific DNA sequences are also called consensus sequences with the following structure: 5'-GGGACTTTCC-3'. This sequence motif has been found for the first time in the enhancer of the immunoglobulin light chain κ of B-lymphocytes (Max et al., 1981; Sen and Baltimore, 1986). Up to this time point five NF-κB proteins have been identified in mammalian cells:

p65 (RelA), c-Rel, RelB, p50/p105 and p52/p100. p105 and p100 represent precursor molecules of which the smaller proteins p50 and p52 are separated off after proteolysis of the C-terminus (Beg and Baldwin, 1993; Lin and Ghosh, 1996). The most stable combination of known NF-κB proteins constitutes the p50/p65 heterodimer. NF-κB exists in the cytoplasm of most cells in its inactive form, where it is bound to inhibitory factors, like IκB (IκBα, IκBβ, IκBε), Bcl-3, p100 (IκBδ) and p105 (IκBγ) (intramolecular IκB) (Baldwin, 1996). The activation of NF-κB is regulated in the cytoplasm; cellular activation in response to a variety of inducers leads to the rapid release of NF-κB from IκB.
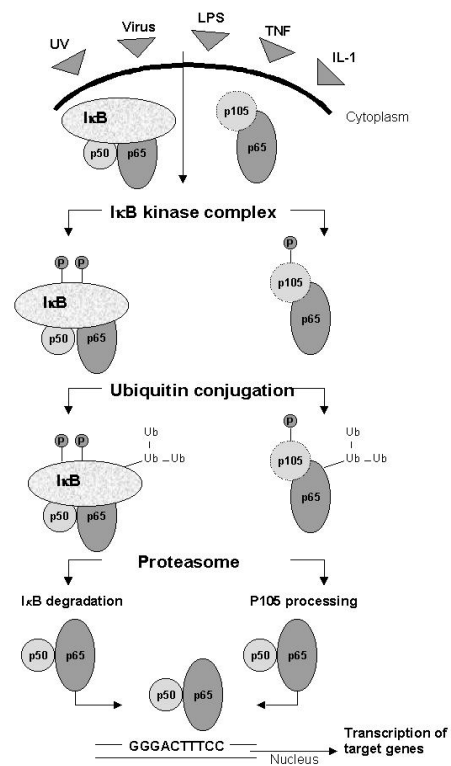
Figure 2: NF-κB signal transduction pathway. Activation of nuclear factor kappa b (NF-κB) involves the phosphorylation-dependent ubiquitinylation of the inhibitor IκB and the subsequent degradation of IκB by proteasomes. The liberated NF-κB translocates to the nucleus, where it activates the transcription of various genes.

Uncomplexed NF-κB rapidly translocates to the nucleus, and transcriptional activation of NF-κB regulated genes occurs within minutes after exposure to an inducing agent and can be considered as an important stress sensor. Cellular activation triggers an intracellular cascade of protein kinase activity – including protein kinase C, cAMP dependent protein kinase and casein kinase II (Baeuerle and Henkel, 1994) - which lead

to site-specific phosphorylation of two serines (Ser 32 and Ser 36) of IκBα, conjugation with ubiquitin, and proteasome-mediated degradation of IκB (Chen et al., 1996; Scherer et al., 1995) (**Figure 2**). Other isoforms of IκB have been identified, however, and the interaction of each IκB isoform with NF-κB may be regulated by different mechanisms (Baeuerle and Baltimore, 1996).

Gene regulation by NF-κB also plays an important role in the central nervous system. Numerous extracellular and intracellular agents or events leading to an increase in gene expression in glial and neural cells have been described:

- Neurotrophin (NGF)
- Neurotransmitter (Glutamate)
- Depolarization
- Neurotoxid peptide (Aβ)
- Developmental changes
- Oxidative stress
- Ceramide (C2-ceramide)
- Cytokines (IL1, TNF)
- Phorbolester (PMA)
- Re-oxygenation
- Lipopolysaccharide (Lipid A)

adapted from (O'Neill and Kaltschmidt, 1997)

Genes in/for	*Examples*
Viruses	Human Immunodeficiency Virus Typ 1 (HIV-1) Simian Immunodeficiency Virus (SIV) Simian Virus 40 (SV40) Adenovirus E3 Region
Immunoreceptors	Immunoglobulin k light chain Interleukin-2 receptor α chain T cell receptor ß2 Major Histocompatibility Complex I (MHCI) Platelet activating Factor Tissue factors CD11b, CD48, CD69
Cell adhesion molecules	Endothelial leukocyte adhesion molecule 1 (ELAM-1) Vascular cell adhesion molecule 1 (VCAM-1) Intercellular cell adhesion molecule 1 (ICAM-1)
Cytokines and Growth factors	β-Interferon

	Tumor Necrosis Factor α (TNFα)
	Lymphotoxin (TNFβ)
	Interleukins (IL-1β, IL-2, IL-6, IL-8)
	Granulocyte/Macrophage colony stimulating factor (GM-CSF)
	Granulocyte colony stimulating factor (G-CSF)
	Makrophage colony stimulating factor (M-CSF)
	Proenkephalin
Acute phase proteins	Angiotensinogen
	Serum Amyloid A precursor protein
	C reactive protein
	Lipopolysaccharide binding protein (LPS-BP)
Transcription factors and sub units	c-rel
	NF-κB precursor p105 and p100
	IκBα
	p53
	c-myc
	Interferon regulating factor 1
Enzymes/Proteins at oxidative stress	NO synthase
	Cyclooxygenase-2
	12-Lipoxygenase
	Phospholipase A$_2$

Table 2: Target genes for NF-κB. Modified according to (Baeuerle and Baichwal, 1997)

A pathophysiological role of NF-κB in neurological diseases, in which inflammatory reactions in the CNS are important, such as Multiple Sclerosis (MS) and Alzheimer's disease, is likely. For example, the amyloid peptide Aβ, which is deposited in senile plaques in the brain of Alzheimer's disease patients, was shown to activate NF-κB in neuronal cell culture and to be neurotoxic (Behl et al., 1994). On the other hand, a neuroprotective role of NF-κB activation in response to Aβ has been suggested (Kaltschmidt et al., 1997). When Tumor Necrosis Factor α (TNFα) or antisense treatment against IκB synthesis were used to induce NF-κB dependent gene expression, neurons exposed to Aβ showed an enhanced survival (Barger et al., 1995).

Kaltschmidt and colleagues also investigated the immunoreactivity for the DNA-binding subunit p50 and for the DNA-binding and transactivating subunit p65 in an animal model of MS, Experimental Autoimmune Encephalomyelitis (EAE) (Kaltschmidt et al., 1994). Strong immunoreactivities for p50 and p65 were detected at the peak of clinical disease in microglial cells.

Important in the context of the present work is the fact that early activation of the NF-κB system is seen in endothelial cells of the BBB under inflammatory conditions (Laflamme and Rivest, 1999; Quan et al., 1997). Moreover, considerable evidence has accumulated showing that proinflammatory effects at the BBB are mediated via a NF-κB pathway in neuroinflammatory disease, such as Multiple Sclerosis (see 1.6.).

Therefore, it should be possible to develop drugs with neuroprotective actions that are based on activation or repression of NF-κB.

1.4.   NF-κB decoys as pharmacological tools and potential drugs

Transcription factor decoys are short double-stranded oligodeoxynucleotides (ODN), which contain so-called consensus binding sequences for a specific transcription factor – in this case NF-κB. Decoys corresponding to this "cis"- binding sequence (6-10bp) (Mann and Dzau, 2000) prevent the cis-trans interaction that occurs normally between transcription factors and the promoter region of their target genes (**Figure 3**).

A correct regulation of gene expression is necessary for perfect development and function of the organism. The decoy approach is a variant *in vivo* gene therapy, as it strives to treat diseases by modulation of endogenous transcriptional regulation (Gambarotta et al., 1996; Schmedtje et al., 1997).

There are a number of published reports of *in vitro* and *in vivo* work, in which the transcription factor decoy approach proved to be effective as a gene modulating method. The first *in vitro* studies were performed by inhibition of NF-κB dependent activation of the human immunodeficiency virus (HIV) enhancer in a transiently transfected B cell line and by inhibition of interleukin-2 (IL-2) secretion in Jurkat T leukemia cells (Bielinska et al., 1990). E2F decoys directed against transcription factors influencing genes responsible for cell cycle progression and cell growth are the most extensively investigated. They have been applied successfully as inhibitors of neointimal hyperplasia in coronary artery bypass grafts in several preclinical studies, followed by phase I/II human trials (Ehsan et al., 2001; Mann et al., 1999). Recently, an AP-1 (activator protein-1) decoy has been tested *in vitro* and in animals for the same indication (Ahn et al., 2002).

Principle of action of a transcription factor (TF)
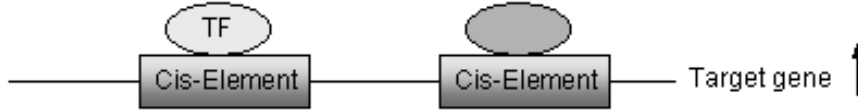
Manipulation of gene action by inhibition with decoy ODN
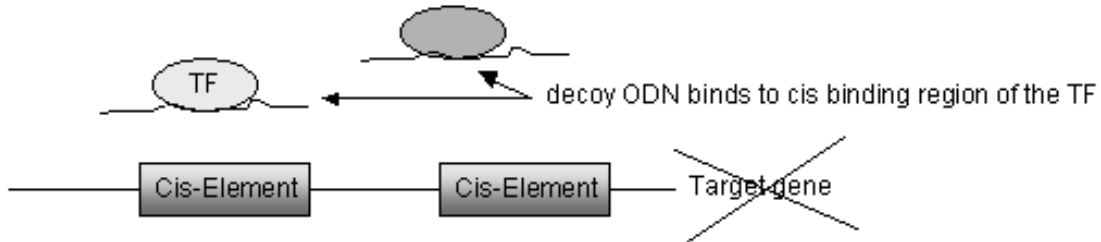
Figure 3: Transcription factor binds to the cis-element in the promoter region of its target gene → gene activation, Binding of decoy ODN to the transcription factor prevents activation of target gene

NF-κB directed decoys are able to manipulate a variety of genes, including those for cytokines, adhesion molecules, cAMP and protein kinase C activation, and Ig expression during inflammatory responses (Collins et al., 1995). Compared to the antisense approach, decoys may be advantageous because of their better ability to inhibit constitutively expressed factors by reducing their promoter activity, and to block multiple transcription factors binding to the same cis-element (Morishita et al., 1998). Moreover, investigation of endogenous gene regulation at the pre-transcriptional and transcriptional level can be studied by application of decoys (the antisense approach induces "loss of function" at the translational level) (Morishita et al., 1998).

Limitations of this approach arise from the fact that a variety of transcription factors are responsible for the regulation of one gene, and on the other hand one transcription factor is involved in the regulation of a multiplicity of target genes. This wide-ranging effect may not be desired in all applications. Therefore, a well thought-out and careful selection of decoy sequences is an important concern. Equally critical are the problems of stability and targeted delivery (Dzau, 2002). Highly efficient cellular delivery to target cells and sparing of non-target cells are the two goals here. Just as in the case of antisense ODNs and gene delivery, development of non-invasive delivery strategies is required to eventually achieve clinical utility of the decoy strategy. A promising non-viral carrier system for DNA delivery is introduced in the next section.

1.5.   Characterization of Polyethylenimine

1.5.1. Role of PEI and its advantage over viral delivery strategies

In recent years gene therapy using non-viral gene delivery systems, such as cationic lipids or cationic polymers, received increasing attention because of several advantages over viral gene delivery. Depending on the specific vector used, viral systems offer high transfection efficiency, and/or potential integration into the host genome. However, the problems of immunogenicity and pathogenicity are far from being solved, as recent incidents in clinical trials have demonstrated. (Somia and Verma, 2000; van der Eb et al., 1998). Most non-viral synthetic vectors are essentially based on the complexation by electrostatic interactions between negatively charged phosphate groups of the DNA and positively charged amino groups of the polymers, thus protecting the DNA from exposure to serum proteins, in particular from nuclease degradation. A major problem is the poor solubility of formed complexes with cationic carriers and deoxynucleotides and their tendency to aggregate in aqueous solutions. (Kircheis et al., 2001b; Vinogradov et al., 1998). Several approaches have been described to overcome these problems, e.g. the synthesis of graft copolymers with nonionic polymers like polyethylenglycol (PEG), which could form a water-soluble corona around complexes and keep them in solution (Kabanov et al., 1995).

1.5.2. Structure and synthesis

Among the various synthetic vectors, polyethylenimines (PEIs) have emerged as particularly promising due to high transfection efficacy in cell culture as well as in a variety of *in vivo* applications. PEI exists in two forms: linear and branched (**Figure 4**). Linear PEI results from cationic polymerization of 2-substituted 2-oxazoline monomer followed by a hydrolyzation to yield the linear product. In contrast, branched PEI is produced by cationic polymerization of aziridine monomers via a chain-growth mechanism and the reaction is terminated by an intramolecular macrocyclic ring formation (Godbey et al., 1999b).

Linear PEI   **Branched PEI**

H₃C-CH₂-NH—[CH₂-CH₂-NH]ₙ—CH₂-CH₂-NH₃⁺
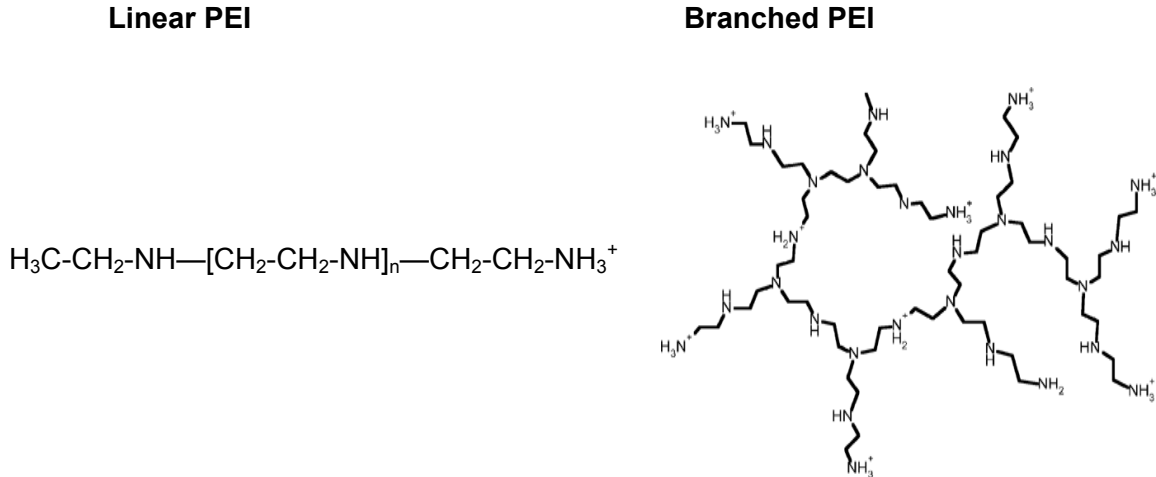
Figure 4: Structures of linear and branched PEIs

PEI possesses a very high charge density potential – every third atom is an amino nitrogen, which can be protonated to an overall protonation of 20 - 45% (at pH values of 7 and 5, respectively). At physiological pH only every fifth or sixth amino nitrogen is protonated (Suh, 1994).

Besides their structure, polyethylenimines differ from each other by their molecular weight. A variety of PEIs are commercially available, e.g., 700Da, 2kDa, 22kDa (linear), 25kDa, 50kDa, 70kDa, 800kDa. Efforts are being made to optimize the properties of PEI regarding transfection efficiency and cytotoxicity.

1.5.3. DNA condensation and particle size

PEI and DNA (plasmids / antisense deoxynucleotides) condense spontaneously by forming electrostatic ionic bonds as mentioned above. Atomic force scanning microscopy pictures of PEI-induced condensation of supercoiled plasmid DNA 5 - 7kb show that in presence of PEI (22kDa or 25kDa) the structure of saturated complexes is globular and often surrounded by folded loops of DNA (Dunlap et al., 1997). Size measurements performed by dynamic light scattering show particles of 90 - 130nm in diameter (25kDaPEI / plasmid) (Tang and Szoka, 1997). The surface charge of complexes can be determined by measuring of the ζ potential. Values of 30 - 35mV were reported at a nitrogen/phosphate (N/P) ratio > 4, which is usually required for complete complexation, compared to a potential of 37mV of PEI alone (Godbey et al., 1999a; Ogris et al., 1999). The surface charges of PEI/DNA play a major role in the

association with the negatively charged lipids of the plasma membrane (Godbey et al., 1999b).

1.5.4. Cellular uptake and intracellular trafficking

The uptake mechanism of positively charged polycation/DNA is mediated by nonspecific adsorptive endocytosis via electrostatic interactions with the cell membrane (Leonetti et al., 1990). The trafficking route of the complex from the endosome to the nucleus is not fully understood. This process could be the limiting step in efficient transfection. Due to the buffering ability of PEI protons will be bound and do not alter the pH in the endosomes, thus preventing a degradation of DNA by inhibition of degrading enzymes (Boussif et al., 1995). At the same time an influx of Cl^- relieves this H^+ gradient. As a result of increasing osmolarity, passive water uptake disrupts endosomal membranes and DNA reaches the cytoplasm (Godbey et al., 1999b). The transport of complex through the cytoplasm may involve diffusion in combination with trafficking along the cytoskeleton of the cell. The uptake into the nucleus itself seems to be mediated by formation of vesicles either from the nuclear envelope or the lysosomal membrane (Godbey et al., 1999b). Experiments injecting naked DNA or DNA in complex with PEI into the cytoplasm revealed that naked DNA could not reach the nucleus; complexes, on the other hand, were taken up by the nucleus (Pollard et al., 1998). Bieber and colleagues (Bieber et al., 2002) proved that transcription of a gene is possible, even if DNA remains integrated into its PEI complex. Therefore, effectiveness of DNA delivery does not depend on disintegration of DNA/PEI complexes.

1.5.5. *In vivo* gene delivery

While *in vitro* applications have shown very promising results, *in vivo* gene delivery has to overcome additional hurdles, such as anatomical size restrictions, interactions with biological fluids, binding to a variety of non-target cells, and extravasation into the targeted tissue (Kircheis et al., 2001b). Moreover, biological systems including the immune system of the body, the complement system and the reticuloendothelial system act as natural defense mechanisms to prevent attacks by foreign bodies. *In vivo* delivery is differentiated into local administration of drug (e.g., directly into tumors, or specific organs – brain, kidney, lung), and systemic application by injection of the drug into the blood stream. Intraventricular administrations of PEI/DNA complexes showing gene expression in brain were applied by several authors (Abdallah et al., 1996; Boussif et al.,

1995; Goula et al., 1998; Lemkine et al., 1999). Systemic application to the lung for example, was investigated by Zou and colleagues, who found that a bolus injection of 50μg DNA in 400μl glucose into the mouse tail vein led to transfection of alveolar cells, primarily because of vascular leakage around the lung alveoli (Zou et al., 2000). However, for *in vivo* applications, the amount of DNA and the bolus volume injected to prevent aggregation of PEI/DNA complexes must be reduced.

Furthermore, there are also reports about application to the liver (Robaczewska et al., 2001), kidney (Boletta et al., 1997) and subcutaneously growing tumor grafts (Kircheis et al., 2001a; Kircheis et al., 1999).

1.5.6. Modifications of PEI

To improve the properties of cationic polymers, especially for applications in *in vivo* gene transfer, modifications of PEI have been intensely investigated. With respect to two of at least four existing barriers for *in vivo* gene delivery (systemic circulation, biodistribution, endosomal escape, transfer to nucleus), different newly synthesized co-polymers have been suggested.

The first barrier to systemic gene delivery is to maintain the integrity and stability of injected DNA in the circulation. Several groups used polyethylene glycol (PEG) to develop long-circulating polyplexes. This hydrophilic polymer shields polymer/DNA complexes. Strongly reduced plasma protein binding and erythrocyte aggregation of PEG-g (grafted)-800kDaPEI/DNA could be shown in comparison to non-modified PEI (Ogris et al., 1999). After systemic application of PEGylated complexes with PEI 25kDa or 800kDa Oupicky and colleagues observed a steric stabilization by increased resistance of complex to salt-induced aggregation. Moreover, they showed for the first time a prolonged half-life after shielding their complex with the multivalent N-(2-hydroxypropyl)-methacrylamide (PHPMA). Half life in mice increased from < 5min to > 90min after injection (Oupicky et al., 2002). To investigate the influence of the molecular weight of PEG, several PEGs (550Da to 20kDa) were combined with 25kDa PEI. Co-polymers with 20kDa PEG yielded small, highly condensed particles of 51 ± 23nm, while using the 550Da PEG resulted in larger and diffuse structures of 130 ± 60nm. 550Da PEG did not prevent erythrocyte aggregation due to incomplete shielding of the positive charge of PEI. Cytotoxicity seemed to be independent of the molecular weight of PEGs. However, for *in vitro* gene expression studies 550Da PEG proved to be most efficient (Petersen et al., 2002).

The second hurdle is to efficiently deliver the gene complex to specific cells or tissues. Target specific application of molecules requires identification of cell surface receptors and the use of appropriate ligands for receptor-mediated endocytosis into tissue. Attachment of folic acid improved PEI-mediated transfection efficiency in the presence of serum, whereas the same effect could not be obtained with other anionic compounds such as cholic acid, citric acid, EDTA, or glutamic acid (Guo and Lee, 2001). Folate-PEG-Folate-g-PEI was investigated regarding its transfection efficiency and cytotoxicity in colon adenocarcinoma cells and oral epidermoid cells. An optimal transfection and low cytotoxicity were achieved using a ratio of FPF/PEI = 5.2 : 1 at neutral polymer amine/DNA phosphate charge (Benns et al., 2002). The same group synthesized PEI derivatives with terminal galactose-g-PEG, which binds to asialoglycoprotein receptors in liver and could improve the transfection efficiency compared to the polyplex alone (Sagara and Kim, 2002). An epithelial growth factor (EGF)-PEG-g-PEI derivative was successfully applied was in human carcinoma cell lines. It is known that EGF receptors are overexpressed in a high percentage in different human cancer tissues (Blessing et al., 2001).

1.5.7. LMW-PEI as preferred polymer

Extensive use of different PEIs for *in vitro* and *in vivo* gene delivery is often limited due to high toxicity or unsatisfying transfection rates of the applied polymer (Chollet et al., 2002; Fischer et al., 1999). Fischer et al. describe the synthesis of a low molecular weight polymer, LMW PEI, with favorable features, such as a low degree of branching, low cytotoxicity, small aggregate formation, high transfection efficiency, and insensitivity against serum compared to the commercially available high molecular weight 800kDa PEI (Fischer et al., 1999). Using size exclusion chromatography in combination with light scattering techniques and NMR-spectroscopy, they synthesized a polymer with a MW of 2,700Da (referred to Dr. D. Fischer), which is less branched than the HMW PEI because of the increased number of secondary NH-groups. The formation of primary and tertiary NH-groups is responsible for branched polymers. In vitro cytotoxicity of LMW PEI was tested using the LDH release and the MTT-assay. No membrane damaging effect of LMW PEI was measured with ECV 304 endothelial cells or L929 fibroblasts by LDH assay after 30 or 60min. In contrast, HMW PEI (500μg/ml) released LDH into the medium after incubation for the same time. Electron microscopy showed HMW PEI polymer precipitates adhering to the cell surface in large clusters (2 - 6μm). The reaction

was followed by a necrosis of affected cells. On the other hand, LMW PEI aggregates in the range of 10-50nm could be detected on the plasma membrane, and endocytic vesicles of 350nm were visible inside the cell. In terms of transfection efficiency, the authors showed a 100fold increase of expression of luciferase using LMW PEI compared to HMW PEI at a N/P ratio = 26.67. This positive transfection behavior could be further improved up to a N/P ratio of 66.66. For HMW PEI transfection levels increased up to a N/P ratio of 13.33; higher ratios showed lower transfection due to cytopathic effects. Because of its favorable properties, the polymer used in this project was based on LMW PEI.

1.6.   Multiple Sclerosis – an inflammatory disease of the central nervous system

1.6.1. Multiple Sclerosis as an autoimmune disorder

The etiology of Multiple Sclerosis (MS) still has to be resolved, but it is known that it is a multifactorial disease. MS is very variable in onset and progression. Common symptoms include impaired vision due to an optic neuritis, paresis and paralysis, deficits in sensation, ataxia and fatigue (Al-Omaishi et al., 1999). There is strong evidence that autoaggressive T cells enter the CNS and attack the myelin sheaths surrounding neuronal cells (Hafler and Weiner, 1995). A second factor is a genetic disposition, which is seen in first grade relatives possessing an increased risk compared to the general population (Kantarci et al., 2002; Oksenberg and Hauser, 1997). Environmental circumstances are also being discussed (Rosati, 2001).

The inflammatory reactions within the CNS affect the white matter, leading to multiple lesions associated with decreased conductive properties of the neurons. Periventricular brain areas are primarily affected. The brain tissue is characterized by perivascular mononuclear infiltrations and presence of myelin debris inside of macrophages (de Vries et al., 1997).

1.6.2. Pathophysiological changes at the BBB under inflammatory conditions and MS

An early step upon activation of brain microvasculature is the secretion of several mediators. Cytokines such as tumor necrosis factor α (TNFα), interleukin-1 (IL-1) and interleukin-6 (IL-6), which are present within the CNS, are of crucial importance for the

development of the inflammatory response. The secretion of cytokines leads to an alteration of properties of the BBB. They can increase its permeability, and trigger the release of mediators important for manifestation of an inflammation, such as eicosanoids, the derivatives of arachidonic acid. Arachidonic acid can be converted through the action of cyclooxygenase into prostaglandins (PGs) and thromboxane A_2. One possible site of synthesis of these factors seems to be the endothelial cell itself (de Vries et al., 1995): after systemic administration of endotoxin or proinflammatory cytokines (e.g. TNFα) the expression of numerous pro-inflammatory proteins in brain endothelial cells is upregulated. These include the CD14 LPS receptor (Lacroix et al., 1998), interleukin-1 (Quan et al., 1998b), TNF receptors p60 and p80 (Nadeau and Rivest, 1999; Osburg et al., 2002), cyclooxygenase-2 (Quan et al., 1998a), inducible nitric oxide synthase (iNOS) (Wong et al., 1996), and the adhesion molecules ICAM-1 and VCAM-1 (Henninger et al., 1997). The promoter regions of these genes contain binding sites for the transcription factor NF-κB.

BBB dysfunction is of paramount importance in MS. MRI scans unveil newly developing lesions by detection of BBB damage, complementing the standard clinical diagnostic criteria (McDonald et al., 2001). It had long been known from the EAE model that BBB damage precedes the onset of clinical symptoms (Claudio et al., 1989; Daniel et al., 1983).

Although the etiology of MS still remains elusive, studies in EAE revealed that a crucial event in the pathogenesis is a transmigration of activated T lymphocytes across the BBB (Wekerle et al. 1986; Hickey et al. 1991). Subsequent research into the role of adhesion molecule expression on BBB endothelium showed an increased expression of ICAM-1 (Sobel et al. 1990) and VCAM-1 (Brosnan et al. 1995) in MS lesions compared to control brain tissue. Similar conditions were observed in EAE (Dopp et al. 1994; Steffen et al. 1994). The latter studies also uncovered that expression of the adhesion molecules preceded clinical disease by several days. Dr. Engelhardt's group delineated the interaction of α4-integrin (VLA-4) on encephalitogenic T lymphocytes and VCAM-1 on the BBB both *in vitro* and *in vivo* (Laschinger et al. 2000; Vajkoczy et al. 2001). Highlighting the importance of adhesion molecules on lymphocytes and endothelial cells in MS is the recent success in a clinical trial with an antibody to α4-integrin, natalizumab (Miller et al., 2003).

2.   Objective of this work

The aim of this project is to explore the potential of a novel vascular targeting strategy for future treatment of Multiple Sclerosis (MS). It is known that the blood-brain barrier (BBB) endothelial cells are intimately involved in early steps of pathogenesis of neuroinflammatory diseases. The inflammatory process starts with the transmigration of activated lymphocytes from the peripheral circulation into brain tissue (Hickey et al., 1991; Wekerle et al., 1986) and leads to a functional breakdown of the BBB. During this process a number of vascular markers are being expressed, i.e. the adhesion molecules ICAM-1 and VCAM-1, which mediate the entry of autoaggressive T cells into the brain, and enzymes with pro-inflammatory effect (cyclooxygenase 2, COX-2, and inducible nitrous oxide synthase, iNOS).

Hypothesis of this project: Upregulation of adhesion molecules and other pro-inflammatory proteins in brain vascular endothelial cells can be inhibited by delivery of a NF-κB decoy ODN/PEI complex applying the transferrin receptor-mediated delivery strategy.

Experimental aims:

1.   Chemical conjugation of the rat anti mouse transferrin monoclonal antibody 8D3 to the ODN/PEI complex using the streptavidin-biotin linker technology

2.   Physico-chemical characterization of the delivery vehicle bioPEGPEI

3.   Measurement of cellular uptake and pharmacological effects of NF-κB decoy (vector system) in an *in vitro* model

4.   Determination of the pharmacokinetics of vector mediated delivery of ODN after systemic administration *in vivo*

2.   Material and Methods

2.1.   Material

2.1.1. Instruments

β-radiation Counter LS6000SC	Beckman
Centrifuge Rotina 48	Hettich
DNA Sequencer ABI PRISM™310	Perkin Elmer
Electrophoresis apparatus:	
Power supply: Power PAC 1000	BIO-RAD
Mini Sub Cell GT System 7x7cm	BIO-RAD
Sub Cell GT System 15x15cm	BIO-RAD
ELISA reader Spectrofluor Plus	Tecan
Gel dryer Model 583	BIO-RAD
Glass Teflon Homogenizer 1ml	
Handcounter Model 3	Ludlum
Heating plate	Heidolph
High speed Centrifuge Avanti J-25I	Beckman
HPLC columns	TosoHaas
HPLC LC module I plus	Waters
Hybridization oven Shake'n'Stack	Hybaid
Incubator	Forma
	Scientific
Intensifying Screen	Kodak
Laminar flow	Nuaire
Magnetic stirrer	Heidolph
Microfuge 5415D	Eppendorf
Phase contrast microscope TS100	Nikon
pH meter 443i	Corning
Phosphoimager	BIO-RAD
Photometer UV/VIS 918	GBC
Quartz cuvette 10mm	Fisher
Rotor JA-10	Beckman
Software analysis program (Molecular Analyst)	BIO-RAD

Submicron particle sizer Model 380/ZLS	Nicomp Instr. Corp.
Surgical lamp KL750	Schott
Surgical microscope	Zeiss
Thermo cycler GeneAmp PCR system2400	Perkin Elmer
Tissue homogenizer Wheaton-Tenbroeck 94x20mm, Wall distance 0.25mm	neolab
Transscreen CassetteBioMax, 20x25cm	Kodak
UV illuminator FBTIV-816	Fisher Scientific
Vacuum pump	Gast
Vortexer Reax top	Heidolph
Water bath 1083	GFL$^{®}$

2.1.2. Chemicals

Chemicals were purchased from Sigma, GIBCO Life Technologies, Mallinckrodt, Fisher Scientific, BioRad, Promega, and Pharmacia, if not otherwise mentioned. The degree of purity of all chemicals was "p.a." (pro analysii). All radioactive chemicals were obtained from NEN/Perkin Elmer or Amersham Pharmacia.

2.1.3. Enzymes

T4 polynucleotide kinase   Promega
catalyzes the transfer of the terminal $[\gamma^{32}P]$ phosphate of
ATP to the 5'-terminus of polynucleotides or to mononucleotides
bearing a 5'-phosphate group.
Reaction buffer10x: 700mM Tris HCl (pH 7.6), 100mM $MgCl_2$, 50mM DTT
Conditions of incubation: 30min at 37°C.

Klenow polymerase (5-10U/μl)   Promega
DNA polymerase I Large (Klenow) Fragment Mini Kit
The 5′→3′ polymerase activity of Klenow Fragment can be used
to fill in 5′-protruding ends with unlabeled or labeled dNTPs.
Reaction Buffer10X: 500mM Tris-HCl (pH 7.2 at 25°C), 100mM
$MgSO_4$, 1mM DTT. Incubation temperature: 1 hour at 37°C

Super-Script II-Reverse Transcriptase (200U/µl)   GIBCO
The enzyme catalyzes the synthesis of first strand cDNA.
Buffer: 5x first strand buffer
Reducing agent: DTT 0.1M

Taq DNA polymerase (5U/µl)   Promega
Taq DNA Polymerase catalyzes the incorporation of dNTPs into
DNA. It requires a DNA template, a primer terminus, and the
divalent cation Mg^{++}. *Taq* Polymerase contains a polymerization
dependent 5'-3' exonuclease activity.
Buffer: 10x PCR buffer

T4 DNA Ligase (3 Weiss U/µl)   Promega
T4 DNA Ligase (1-3U/µl) catalyzes the joining of two strands
of DNA between the 5'-phosphate and the 3'-hydroxyl groups
of adjacent nucleotides in either a cohesive-ended or blunt-ended
configuration.
Reaction buffer: 10x 300mM Tris-HCl (pH 7.8), 100mM $MgCl_2$,
100mM DTT, 10mM ATP
Conditions of incubation: 16 hours at 4°C.

Restriction enzyme
Bst ZI (10U/µl)   Promega
Isochizomers: Eag I, Ecl XI, Xma III, Eco 52I
Restriction site: 5'...C↓GGCCG...3'
                    3'...GCCGG↑C...5'
Incubation buffer: 6mM Tris HCl pH 7.9, 150mM NaCl,
                    6mM $MgCl_2$, 1mM DTT
                    + Acetylated BSA (10mg/ml)
Incubation temperature: 3 hours at 50°C

2.1.4. Buffers and Solutions

Synthesis of 8D3-SA
8D3 in PBS
Recombinant Streptavidin lyophilized from 20mM K_2PO_4 pH 6.5;   Sigma
36mg dissolved in1mL water
0.32M Sodium borate/1mM EDTA pH 8.0
0.16M Sodium borate/1mM EDTA pH 8.0
Traut's reagent 1.38mg/mL 0.16M Sodium borate   Pierce
Glycine 7.5mg/mL water
0.02M PBS pH 7.0/1mM EDTA
S-SMPB 4.58mg/mL Dimethylformamide (DMF)   Pierce
Iodoacetamide 3.7mg/ml water   Pierce
d-[8,9-^{3}H(N)]-biotin   NEN
Coomassie   Pierce

i.v. pharmacokinetics
RHB: 10mM HEPES
                                2.8mM $CaCl_2$
                                1mM NaH_2PO_4
                                1mM $MgSO_4$
                                141mM NaCl
                                4mM KCl

10mM D-Glucose
pH 7.4

Capillary depletion
32% dextran in RHB

Immunohistochemistry
ABC-Elite (Vector Lab):   2 drops A per 5ml PBS + 2 drops B per 5ml PBS
AEC stock solution: 1.6mg/ml in DMSO
AEC working solution: 6ml AEC stock solution
                            50ml Sodium acetate 0.02M pH 5.1
                            4ml 3% H_2O_2

Retardation assay
Electrophoresis buffer: TAE 50x stock solution
                            1M Tris base
                            1M Acetic acid
                            50mM EDTA
                            pH 8.5

Stability tests
Polyacrylamide gel electrophoresis
Electrophoresis buffer: TBE 10x
                            890mM Tris base
                            890mM Boric acid
                            20mM EDTA
                            pH 8.0

Gel: 20% 15ml
                            10ml 37:1 Acrylamide/Bis acrylamide
                            3ml TBE 5x
                            1.85ml water
                            135μl 10% APS
                            10.5μl TEMED

Extraction of nuclear fragments for NF-κB gel shift assay
Buffer A: 10mM HEPES pH 7.9
                            1.5mM $MgCl_2$
                            10mM KCl
                            1mM DTT

Buffer C: 20mM HEPES pH 7.9
                            25% glycerol
                            0.42M NaCl
                            1.5mM $MgCl_2$
                            1mM DTT

Buffer A + 0.1% Triton X-100

NF-κB gel shift assay

Binding buffer: 12mM HEPES pH 7.9
                                   4mM TrisHCl
                                   60mM KCl
                                   1mM EDTA
                                   1mM DTT

Gel: 60ml
                                   12ml TGE 5x
                                   15ml 19:1 Acrylamide/Bis-acrylamide
                                   30ml water
                                   150μl 30% APS
                                   72μl TEMED

Electrophoresis buffer: TGE 5x
                                   50mM Tris HCl
                                   380mM glycine
                                   2mM EDTA
                                   pH 8.5

mRNA isolation

2x binding buffer: 20mM Tris HCl pH 7.5
                                   1M LiCl
                                   2mM EDTA

Lysis and binding buffer: 100mM Tris HCL pH 8.0
                                   500mM LiCl
                                   10mM EDTA pH 8.0
                                   1% SDS
                                   5mM DTT

Washing buffer with SDS: 10mM Tris Hcl pH 8.0
                                   0.15M LiCl
                                   1mM EDTA
                                   0.1% SDS

Washing buffer: 10mM Tris HCl pH 8.0
                                   0.15M LiCl
                                   1mM EDTA

Elution buffer: 10mM Tris pH 7.5

Reconditioning solution: 0.1M NaOH

Storage buffer: 250mM Tris HCl pH 8.0
                                   20mM EDTA
                                   0.1% Tween-20
                                   0.02% Sodium azide

Northern blotting

Formaldehyde gel electrophoresis

Electrophoresis sample buffer 10x:

	50% Glycerol (87%)
	0.2M EDTA pH 8.2
	0.25% Bromo phenol blue
	0.25% Xylene cyanol

Electrophoresis buffer: MOPS 10x stock solution
                                 0.2M MOPS
                                 50mM Na-acetate
                                 10mM EDTA pH 7.0

Denaturating buffer: 10ml Formamide
                                 3.5ml Formaldehyde 37%
                                 2ml 5x MOPS

Sample buffer: 50% Glycerine 87%
                                 0.25% Bromo phenol blue

Formaldehyde gel: 1% Agarose
                                 85% purified water
                                 water and agarose are boiled in a microwave and
                                 cooled down to 60°C in a water bath
                                 10% 10x MOPS
                                 2.5M Formaldehyde 37%
                                 0.05% Ethidium bromide (500μg/ml)

Blotting
SSC 20x: 3M NaCl
                                 0.3M Na-citrate pH 7.2

Pre and Hybridization
Prehybridization buffer: 11.1M Formamide
                                 30% 20x SSPE
                                 0.5% SDS
                                 14% purified water
                                 1% denaturated salmon sperm DNA (10mg/ml)

Hybridization buffer: prehybridization buffer with labeled probe

SSPE 20x: 3M NaCl
                                 200mM NaH$_2$PO$_4$
                                 20mM EDTA pH 7.4

Blot storage buffer: 0.5x SSPE, 1% SDS
Stripping buffer: 0.05x SSPE, 0.3% SDS

For several purposes

PBS: 20mM Sodium phosphate
                                  150mM NaCl pH 7.4

2.1.5. Media

LB (Luria Bertani) media   10g Tryptone
                                  5g Yeast extract
                                  5g NaCl
                                  pH 7.0

fill up to 1L with purified water; autoclave for 30min at 121°C and 1atm
for agar: 1L LB media and 15g Agar; autoclave for 30min at 121°C and 1atm
Addition of Ampicillin 100µg/ml
IPTG (Isopropyl-β-D-thiogalactoside) 0.1M, and X-Gal (5-bromo-4-chloro-3-indolyl-β-D-galactoside) were spread over the surface of a LB-Ampicillin plate, Absorption time 30min at 37°C.

SOB media   2g Tryptone
                                  0.5g Yeast extract
                                  1ml 1M NaCl
                                  0.25ml 1M KCl

SOC media   SOB media and
                                  1M $MgCl_2 \cdot 6H_2O$
                                  1M $MgSO_4 \cdot 7H_2O$

Tryptone, Yeast extract, NaCl, and KCl are given to 97ml sterile water. The reaction mix is autoclaved and cooled down. 2M Mg^{2+} stock solution and 2M Glucose are added to a final concentration of 20mM. The media is filled up to 100ml and passed through a sterile 0.2µm filter unit. The media should have a pH of 7.0.

8D3 cell culture

DMEM +   10% FCS   PAA
                                  1% Penicillin/Streptomycin
                                  1% Non essential amino acids
                                  1% Sodium pyruvate
                                  2% L-Glutamine
                                  0.4% β-Mercaptoethanol

Stock solutions: 10000U/ml/10000µg/ml Penicillin/Streptomycin
                                  100x Non essential amino acids
                                  100mM Sodium pyruvate
                                  200mM L-Glutamine
                                  0.1% β-Mercaptoethanol in DMEM

Washing buffer: 1x HBSS

	25mM HEPES	
	15% FCS	

Freezing medium:	30% FCS	
	10% DMSO	
	60% DMEM +	

Serum free medium:	Ex-cell 610-HSF	JRH Biosciences
	2% L-Glutamine	
	1% Penicillin/Streptomycin	
	1% Sodium pyruvate	
	1% Non essential amino acids	

bEnd5 cell culture

DMEM +:	10% FCS
	1% Non essential amino acids
	1% Penicillin/Streptomycin
	1% Sodium pyruvate
	2% L-Glutamine
	0.4% β-Mercaptoethanol

Stock solutions:

10000U/ml/10000μg/ml Penicillin/Streptomycin
100x Non essential amino acids
100mM Sodium pyruvate
200mM L-Glutamine
0.1% β-Mercaptoethanol in DMEM

Washing buffer I:	25mM HEPES
	10% FCS
	90% DMEM +

Washing buffer II:	1x HBSS
	5mM EDTA
	40mM HEPES

Freezing media:	10% DMSO
	50% FCS
	40% DMEM +

Trypan blue 0.4%
Trypsin 0.25%/EDTA 1mM

2.1.6. Primers and Oligodeoxynucleotides

Hybridization of transcription factor decoys

The oligodeoxynucleotides were obtained from MWG Biotech in HPSF purified condition.

NF-κB 1:
5' - CCT TGA AGG GAT TTC CCT CC – 3'

NF-κB 2:
5' – GGA GGG AAA TCC CTT CAA GG – 3'

Reverse Transcription

Random Primer Hexamer –5'- pd (N)$_6$ (500ng/μl)   Pharmacia

50 A260 units 1unit = 26.5μg
               50units = 1.325mg
stock solution 1mg/ml
working solution 500μg/ml

PCR
Primers for Northern blotting probes:

Name			mRNA sequence	Fragment size
ICAM-1	Forward primer: GCTCAGGTATCCATCCATCC		137 - 156	505 bp
	Reverse primer: CTGAGATCCAGTTCTGTGCG		642 - 623	
VCAM-1	Forward primer: TGAAATGCCTGTGAAGATGG		12 - 31	268 bp
	Reverse primer: CTCAAAACTGACAGGCTCCA		279 - 260	
iNOS	Forward primer: ATGTCCGAAGCAAACATCAC		2291 - 2310	449 bp
	Reverse primer: TAATGTCCAGGAAGTAGGTG		2740 - 2721	
COX-2	Forward primer: GTGCCAATTGCTGTACAAGC		1341 - 1360	540 bp
	Reverse primer: TTACAGCTCAGTTGAACGCC		1918 - 1894	
IκBα	Forward primer: AGCAAATGGTGAAGGAGCTGC		193 - 213	323 bp
	Reverse primer: CCAGCTTTCAGAAGTGCCTCAG		516 - 495	
IκBβ	Forward primer: GCAGAATGACCTAGGCCAAACA		349 - 371	328 bp
	Reverse primer:		677 - 656	

	TAGCCTCCAGTCTTCATCACGC		
GAPDH	Forward primer: ACCTCAACTACATGGTCTAC	156 - 175	801 bp
	Reverse primer: TTGTCATTGAGAGCAATGCC	957 - 938	

2.1.7. DNA markers

100 bp ladder 50μg   Promega

2.1.8. Bacteria and Plasmids

High efficient competent cells from E. coli JM 109   Promega

Transformation efficiency: 1 x 10^8 cfu/μg DNA

T/A cloning: pGEM$^{®}$ -T- vector (50ng)   Promega

2.1.9. Animals

Male BALB/c mice 20-25g   Charles River

2.2.   Methods

2.2.1.   Characterization of the 8D3-SA vector complex

2.2.1.1. 8D3 hybridoma culture

8D3 hybridoma cells were grown under addition of mouse feeder cells (abdominal macrophages) and thymus lymphocytes in DMEM+ in T75 cell culture flasks. After two days cells were split into T175 flasks and fed until a total volume of about 1.2L was reached. The cells were centrifuged at 250g for 10min at 4°C and transferred into four 850cm^2 roller bottles containing serum free medium. Cells rotated for about one week at 150rpm and 37°C/5% CO_2 and were harvested by centrifugation at 6000g and 4°C for 30min. Antibody supernatant was precipitated with ammonium sulfate (330g/L supernatant) at 4°C over night and centrifuged for 45min at 6000g at 4°C. The resulting pellet was resuspended in about 10ml PBS and dialyzed using a dialysis tubing with a molecular weight cut-off of 10,000Da (Sigma). The antibody was further purified by a HiTrap protein G column (Pharmacia), concentrated on Centriprep 30 columns (Millipore) and protein content was measured by BCA method (Pierce, Rockford, IL). The antibody was stored in aliquots at -80°C.

2.2.1.2. Synthesis of 8D3-SA

For thiolation the 8D3 antibody was mixed with Traut's reagent (2-Iminothiolane) and incubated for 60min at RT on a magnetic stirrer. At the same time S-SMPB (Succinimidyl-4-(p-maleimidophenyl)butyrate) was added to streptavidin and reacted under the same conditions as the antibody. Glycine was added to quench both reactions for further 30min. The reaction mixtures were purified over a PD 10 column (Pharmacia) and protein peaks collected. 8D3 and streptavidin peaks were combined and incubated under gentle stirring on ice for two hours. The reaction was quenched with 10% iodoacetamide for 10 - 20min and ^{3}H-biotin was added and the mixture transferred onto Superdex 200 HR 10/30 for purification. 1mL fractions were collected and 5μl aliquots were counted in a β-counter, and compared with peaks obtained in UV-detection. The 8D3 : streptavidin = 1 : 1 fractions were pooled and a rechromatography was performed using the size exclusion column TSK 3000 SWXL. The samples were concentrated and the protein measured as mentioned above.

Reaction mechanisms:

a)   Thiolation of 8D3 with 2-Iminothiolane

The imidoester group reacts with amines to form a stable, charged linkage, while leaving a sulfhydryl group available for further coupling.


b)   Activation of Streptavidin with sulfo-SMPB (Succinimidyl-4-(p- maleimido-phenyl)butyrate)

The reagent has an amine-reactive N-hydroxy-succinimide (NHS) ester on one end and a sulfhydryl-reactive maleimide group on the other end. It possesses a negatively charged sulfonate group that lends considerable hydrophilicity to the molecule. The NHS ester can react with primary amines in proteins to form stable amide bonds, while the maleimide end nearly exclusively reacts with sulfhydryl groups to create stable thioether linkages.
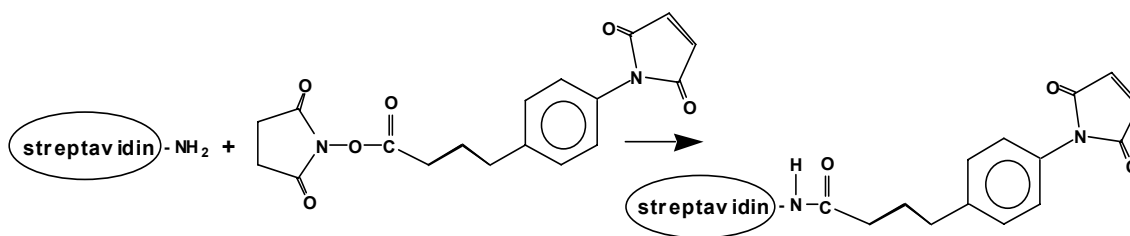
c)   Coupling of Streptavidin to the 8D3 monoclonal antibody

Interaction between the sulfhydryl group of the antibody and the maleimide group of the activated streptavidin under formation a stable thioether bond.
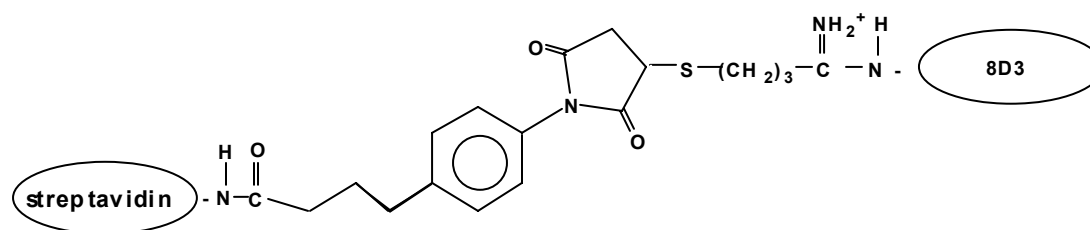
2.2.1.3. i.v. pharmacokinetics of ^{3}H-biotin-8D3-SA

BALB/c mice were anesthetized with ketamine (100mg/kg) and xylazine (4mg/kg) intramuscularly and the right common carotid artery was retrogradely catheterized with PE10; 70µl of RHB pH 7.4/0.1%BSA containing 1.7µCi of ^{3}H-biotin-8D3-SA (10.6µg) were injected into the jugular vein and arterial blood was withdrawn from the carotid artery at 0.25, 1, 2, 5, 10, 20, 30 and 60min after injection of the isotope solution. The blood samples were centrifuged (1500g, 10min) and plasma was counted for total radioactivity. Mouse brains were taken at 60min, solubilized in 1ml Scintigest and counted in a beta counter. Pharmacokinetic parameters were estimated by fitting plasma radioactivity data to a bi-exponential equation with a derivative-free nonlinear regression analysis (WinNonlin, BMDP-AR). The area under the plasma concentration curve (AUC) was calculated. The organ volume of distribution (Vd) of ^{3}H-8D3-SA MAb was estimated from the ratio of radioactivity of the tissue (counts per minute per gram) and plasma concentration (cpm/ml). The brain permeability-surface area (PS) product was calculated as follows:

$$PS = (V_d - V_0) \cdot C_P (60min)/AUC_{0 \to 60min}$$

where C_P (60min) is the terminal plasma concentration and V_0 is the plasma volume of the brain. The brain concentration (without intravascular content) was expressed as percentage of injected dose (ID)/g of brain, and was determined as follows:

$$\%ID/g = PS \cdot AUC_{0 \to 60min}$$

2.2.1.4 Capillary depletion

The pharmacokinetic studies were performed as described under i.v. pharmacokinetics. After 60min the brain tissue was removed and homogenized in ice-cold physiological buffer (RHB) for capillary depletion analysis. The total brain homogenate was fractionated into the capillary pellet and the postcapillary supernatant by a dextran (16% final concentration, equal volumes of homogenate and 32% dextran) density centrifugation at 4,300g for 15min at 4°C in a swinging bucket rotor. 0.5ml aliquots of homogenate, postcapillary supernatant and the capillary pellet were digested in Scintigest and counted in a beta counter. V_d values for the different fractions were calculated as follows:

$$V_d = (cpm/g\ brain)/C_p(t)$$

Where $C_p(t)$ are the counts per minute per microliter of plasma at brain sampling time (t).

2.2.1.5. Cell culture of bEnd5 cells

The cell line used in these experiments is a mouse brain endothelioma line bEnd5. Cells were rapidly thawed at 37°C and seeded into 6-well culture dishes in 2ml of medium. Typically, a cell count of about 1×10^6 cells/well was reached after day 6. The bEnd5 cells were grown in DMEM (high glucose) medium containing 10% fetal calf serum, 1% nonessential amino acids (10mM), 100 units/ml penicillin, 100 µg/ml streptomycin, 1% sodium pyruvate (100mM), 2% L-glutamine (200mM) and 0.4% ß-mercaptoethanol at 37°C in a 5% CO_2 atmosphere. Cells were fed all two days until confluence (approximately 6 days).

2.2.1.6. Binding and internalization experiments

For *in vitro* uptake studies the mouse brain endothelioma cell line bEnd5 was cultured in 6-well dishes for 5 days at 37°C and 5% CO_2 to grow confluent. After washing the cells with ice-cold serum free DMEM the following tracer solutions were added:

a) 50µl of 0.35µg 8D3-SA and 0.05µCi ^{3}H-biotin diluted in DMEM/1%BSA to 2ml serum free DMEM+

b) 50µl of solution a) and additional 80µg (about 240fold excess) of uncoupled 8D3

c) 50µl of solution a) and additional 80µg of the mouse anti-rat antibody OX 26

The binding and uptake capacity was measured at 0, 15, 30 and 60min at 37°C solubilizing cells in 1N NaOH and counting in a beta counter. In order to remove the surface bound ^{3}H-8D3SA and to calculate the internalization an acid wash step was performed by a 5-min-incubation of cells with HEPES/DMEM pH 3.0. The receptor binding was expressed in %bound/mg cell protein.

2.2.1.7. Immunohistochemistry

bEnd5 cells were grown in 96-well plates for 2 days and fixed with 3% PFA for 3min. Endogenous peroxidase and unspecific staining were blocked with 0.3% H_2O_2 (5min) and 3% BSA (30min), respectively. The cells were incubated either with 10µg/ml 8D3 or 8D3-SA. As a secondary antibody a biotinylated rabbit anti mouse antibody (5mg/ml, Vector Lab) was used. Visualization was performed with the avidin-biotin-peroxidase method (Vector Lab), using aminoethylcarbazol (AEC) as a substrate (20 - 30min at 37°C).

2.2.2.   Physico-chemical properties of bioPEGPEI/ODN or 8D3SA-bioPEGPEI/ODN

2.2.2.1. Hybridization of transcription factor decoys

The complementary single stranded oligodeoxynucleotides (transcription factor decoys), were dissolved at a concentration of 1μg/μl in water, and were hybridized in a thermo cycler under the following incubation conditions: 5min at 95°C, 1h at 60°C, 1h at 35°C and 30min at RT. The annealed double strands were stored at -20°C.

2.2.2.2. HABA (2(4'-hydroxyazobenzene) benzoic acid) assay

The incorporation of biotin into the PEGPEI copolymer at the tip of the PEG^{3400} was determined with the streptavidin-HABA assay. A 0.7ml mixture of HABA (0.005M) in 0.01M NaOH and streptavidin (0.05mg/ml) in 0.05M Na$_2$HPO$_4$ / 0.15M NaCl pH = 6.0 was added to a spectrophotometer microcuvette. The absorbance at 500nm was measured and 2μl - 5μl increments were successively added of either 0.167mM biotin standard in 0.05M PBS pH 6.0, buffer control PBS pH 7.4, 0.147mM bioPEG^{3400}, or 0.355mM bioPEG^{3400}PEI. The decrease in absorbance at 500nm caused by biotin displacement of HABA from streptavidin was recorded with each successive addition of 4 - 6 aliquots of either biotin standard or experimental sample. The results were analyzed by linear regression analysis (Δ A$_{500}$ vs. μl sample or buffer volume).

2.2.2.3. Complex formation

4μg of double stranded NF-κB decoys (1μg/μl) and the appropriate amounts of bioPEGPEI (MW 6,400 Da) (0.1μg/μl) were added to 20mM PBS pH 7.4 to yield a total volume of 50μl. The mixture was pipetted thoroughly and incubated for 10min at RT for complex formation.

2.2.2.4. Polyacrylamide gel electrophoresis (PAGE)

Free single and double stranded ODNs were compared with bioPEGPEIODN complexes incubated in 10mM PBS pH 7.4 and DMEM+ with 20% rat serum at 37°C for 0min, 30min or 2h. The stability of N/P ratios from 3:1 to 10:1 was investigated on a native 20% PAGE 16 x 20cm with cooling function. DNA was stained after electrophoresis with SYBR GOLD (Molecular Probes).

2.2.2.5. Retardation assay

The 50μl complex mixture was loaded onto a 15 x 15cm 1% agarose gel stained with ethidium bromide. Electrophoresis was carried out at 140V for 2h in 1x TAE running buffer. The gel was visualized and photographed under UV-detection.

2.2.2.6. Binding characteristics of 8D3-SA to its ligand bioPEGPEI/NF-κB

Another approach to verify the binding behavior of the vector 8D3-SA to its ligand bioPEGPEI/NF-κB can be performed by incubation of both components followed by separation on an agarose gel. 8D3-streptavidin and NF-κB were radioactively labeled with ^{3}H-biotin or ^{32}P-γ-ATP, respectively and incubated for complex formation. 1μl or 0.5μl of double stranded NF-κB decoys (1μg/μl), about 20,000cpm of ^{32}P-NF-κB and the appropriate amounts of bioPEGPEI (MW 6,400Da) (0.1μg/μl) were mixed to yield N/P ratios of 3:1 and 6:1, respectively. After a 10min incubation time 8D3-SA (1.3μg/μl) was added to the preformed complex to form 8D3-SA/bioPEGPEI/NF-κB ratios of 1/1, 1/3, 1/9 and 1/27. The complexes were incubated at RT for another 30min. Samples were loaded onto a 15 x 15cm 1% agarose gel and separated at 90V for 3h in 1x TAE electrophoresis buffer. Each lane was cut in 13 equal pieces (piece 6 was original pocket with sample), each piece was digested in 2ml of Soluene (Packard) at 37°C over night and counted in organic Scintillation fluid in a beta counter.

2.2.2.7. Interaction of FITC-NF-κB decoys with bEnd5 cells

Cells were grown in DMEM+ with 10%FCS on 16-well chamber slides (2500 cells/well) for 24h prior to treatment. bEnd5 cells were exposed to 0.5μM or 2μM NF-κB decoy complexed with bioPEGPEI at a ratio of 6:1 (N/P). The evaluated time points were 2, 4, 8, 12, and 24h at 37°C in serum-free media. The cells were washed twice after treatment in ice-cold PBS pH 7.4 and fixed in 4% paraformaldehyde/PBS for 5min. Cells were dehydrated in a graded series of alcohol (70 - 100%) for 1min each. After that, cellular accumulation was examined using an epifluorescence microscope.

2.2.2.8. Particle sizing

Complex size, either of bioPEGPEIODN or 8D3SA-bioPEGPEIODN, in different solutions was investigated by photon correlation spectroscopy using a Submicron Particle Sizer, Model 380/ZLS. The average particle size distribution was determined by

intensity-based Gaussian or multimodal so-called 'Nicomp' (non-Gaussian) fit to raw data, which had been collected over 15min at 23°C at an angle of 90°. Complex solutions were prepared in 10mM PBS pH 7.4, in 10mM PBS pH 7.4 + 10% human plasma and DMEM+ without plasma, respectively and measurements started after 10min, 1h, 2h, 4h, 8h, 24h and 1week. The complex formation was carried out as described under 2.2.2.3. in a total volume of 0.2ml containing an ODN concentration of 10μg/ml. Various N/P ratios were evaluated, ranging from 3:1 to 60:1.

2.2.2.9. Stability tests

Stability tests were performed to show the durability of various complexes under different conditions and at different time points. Several methods were choosen to confirm the obtained results.

Microcentrifugation and trichloro acetic acid (TCA) precipitability

After labeling of ODNs by T4 polynucleotide kinase radioactive NF-κB decoys were complexed with unlabeled ODNs and bioPEGPEI as described under 2.2.2.3. Complexes were incubated in DMEM+ for different periods (10min, 1h, 4h, 24h) at 37°C or in DMEM+ on bEnd5 cells at 37°C and analyzed by their TCA precipitability. TCA precipitation was carried out using 10μl of a carrier DNA (salmon sperm DNA 10mg/ml), 100μl of 500μl sample and 500μl 20% TCA. The mixture was vortexed and incubated on ice for 10min. A centrifugation step was performed at 13,000g for 5min at 4°C and the supernatant transferred into 3ml of Econosafe for counting in a beta counter. The pellet was dissolved in 500μl of 1N NaOH by vortexing and counted. Another experimental series used the combination methods of centrifugation through Ultrafree MC filters (Millipore) at 5,000g for 10min and following TCA precipitability both in 10mM PBS pH 7.4 and DMEM+ with 10% FCS to analyze the extent of dissociation of ODN from its complex. Free ODN passes the filter membrane to almost 100%. However, complex bound DNA adheres to the membrane.

2.2.3. Stimulation experiments with LPS or TNFα and inhibition of activation

After a growing period of 6 days bEnd5 cells were either stimulated with Lipopolysaccharide of E. coli serotype 0111:B4, LD_{50} = 12.3mg/kg (1μg/ml) or with recombinant TNFα (50ng/ml) diluted in DMEM+ medium over a time course of 30, 60,

120, 240, and 360min for Northern blot experiments, or for the following periods for isolation of nuclear fragments: 1, 5, 10, 60, 120, 240, and 360min. During the stimulation periods bEnd5 were incubated at 37°C in a 5% CO_2 atmosphere.

For Northern blot experiments bEnd5 cells were treated with bioPEGPEI/NF-κB or 8D3SA-bioPEGPEI/NF-κB, respectively, and incubated with different NF-κB concentrations (0.1μM - 5μM) over several time frames (4h – 48h) (see 3.3.3.). After treatment the medium was aspirated and new DMEM+ with 10% FCS added containing the TNFα (50ng/ml). After 4hours of incubation the medium was aspirated and the cells prepared for mRNA isolation.

2.2.3.1. Extraction of nuclear fragments and NF-κB gel shift assay

bEnd5 cells were harvested, washed in icecold phosphate-buffered saline, centrifuged at 1,850g for 10min and the pellet resuspended in 500μl of buffer A. A recentrifugation step was performed at 1,850g for 10min. Cells were resuspended in 80μl buffer A containing 0.1% TritonX-100 by gentle pipetting. After incubation for 10min on ice, the homogenate was centrifuged and the nuclear pellet was washed once with buffer A and resuspended in 70μl of ice-cold hypertonic buffer C. This suspension was incubated for 30min on ice followed by centrifugation at 13,000g for 30min. The resulting supernatant was stored at –80°C as nuclear extract. Protein concentrations were determined by the BCA (Pierce) method. To minimize proteolysis, all buffers included 1μl/500μl of a protease inhibitor cocktail (SIGMA).

The NF-κB decoys were 5`-end-labeled with T4 polynucleotide kinase in the presence of [γ-^{32}P]ATP (NEN) according to Promega's protocol.

For the electrophoretic mobility shift assay, 5μg of nuclear protein were incubated with 80,000cpm of ^{32}P labeled double-stranded oligodesoxynucleotides in a binding buffer, and 1μg of poly (dG:dC) (Pharmacia) for 30min at room temperature. Competition studies were performed by adding a 80-fold molar excess of unlabeled double stranded oligodesoxynucleotides (1μg) to the binding reaction. Resulting protein-DNA complexes (18μl) were resolved on native 5% polyacrylamide gels (20 x 20cm) using a high ionic strength buffer (50mM Tris HCl, 380mM glycine, and 2mM EDTA, pH 8.5). The gels were run at 250V for 180min, dried under vacuum (55min), and subjected to autoradiography (BioMax Kodak).

2.2.3.2. mRNA isolation

After a growing period of 6 or 7 days, respectively, bEnd5 cells were harvested in ice-cold 20mM PBS pH 7.4 from 6-well plates by using a cell scraper and centrifuged at 250g for 10min at 4°C. The pellet was then homogenized by pipetting with 1ml lysis buffer and genomic DNA was sheared and fragmented through a 21G cannula. The cell lysate was centrifuged for 1min at 16,000g and the polyA-RNA directly bound to Dynabeads Oligo(dT)$_{25}$ – paramagnetic, polystyrene beads containing 25 nucleotide long chains of deoxythymidylate covalently attached to the bead via a 5` linker group (Dynal). The magnetic beads were bound to their magnetic stand, the supernatant was taken off and the magnetic beads with the polyA RNA were washed twice in washing buffer and once in the same washing buffer without addition of SDS, respectively. Elution of mRNA was achieved in 10μl elution buffer for 2min at 65°C.

2.2.3.3. RT-PCR

One microgram of bEnd5 cell total RNA was reverse transcribed with Superscript II-reverse transcriptase (GIBCO, BRL) and pd (N)$_6$ random primer hexamers (Pharmacia) for 90 min at 42°C. 2μl of reverse transcription product (cDNA) was used for PCR without further purification. PCR was a hot start PCR with addition of 2.5U Ampli Taq polymerase (5U/μl) at 94°C, and PCR was performed in a total volume of 50μl containing 1x PCR buffer II (PE Applied Biosystems) with 2.5mM MgCl$_2$, 0.3mM dNTP mix (Pharmacia) and 5'- or 3'-primers each of 0.8mM. 35 amplification cycles were performed with annealing temperatures of 55°C and annealing time of 40sec. After that 10μl of PCR products were resolved by electrophoresis on a 1.5% agarose gel. Ethidium bromide-stained gels were photographed using a video camera and the Molecular Analyzer Software (BioRad) and interpreted. PCR products were purified with the QIAquick PCR purification kit according to the instructions of the manufacturer (QIAGEN). All amplified and purified DNA probes were sequenced by the Sequencing Core Facility at Texas Tech University in Lubbock.

2.2.3.4. pGEM-T vector cloning

All PCR products were T/A cloned into the pGEM-T vector (Promega) using the polyA overhangs of the probe produced by the AmpliTaq Polymerase (PE) and the polyT overhangs of the vector. The ligation into this vector was carried out by a T4-DNA ligase included in the pGEM-T vector kit (Promega). Vectors were transformed in highly

efficient competent cells (E. coli, JM 109, Promega), grown on agar plates and white colonies were selected and amplified in LB medium. All protocols were performed according to Promega instructions. E. coli were lysed and vector DNA purified with the QIAGEN Miniplasmid and Maxiplasmid preparation kits. Selected clones were digested by the restriction enzyme BstZI and the cDNA stored at –80°C for further labeling procedures.

2.2.3.5. Northern blotting - denaturing formaldehyde gel and hybridization

The polyA RNA probes were denaturated in denaturation buffer at 65°C for 10min. 2.5-5µg enriched polyA RNA were separated by electrophoresis in 1x MOPS in denaturating agarose gels (1.5% Agarose, 1x MOPS, 2.2M Formaldehyde), transferred to nylon membranes (Nytran SuPerCharge, Schleicher & Schuell) by capillary action in 20x SSC using the downward transfer system by Schleicher & Schuell over night, and cross-linked by baking at 80°C for 2h.

Membranes were pre-hybridized in a solution of 50% formamide, 6x SSPE, 0.5% SDS, and 100µg/ml of denatured salmon sperm DNA for 3 - 4 hours at 42°C. The hybridizations were performed with the following ^{32}P-labeled complementary DNA probes: All probes were BstZI - BstZI digested fragments complementary to the corresponding mouse polyA RNA sequences (ICAM-1, VCAM-1, iNOS, COX-2, IκBα, IκBβ and GAPDH). BstZI cut on both polylinker sites of the pGEM vector (Promega). The probe labeling procedure was carried out through a random primer labeling kit (Prime-it RmT^{TM}, Stratagene) and radioactive labeled [α^{32}P]dCTP (NEN). The probe hybridized in a hybridization oven at 42°C for 24 hours. The nylon membranes were washed under stringent conditions in 6x SSPE, 0.3% SDS for 15min at 42°C, in 2x SSPE, 0.3% SDS for 15min at 42°C, in 1x SSPE, 0.3% SDS for 15min at 42°C and in 0.5x SSPE, 0.3% SDS for 30min at 50°C. Autoradiographic signals were analyzed by a phosphoimager (BIORAD), in combination with densitometric software (Molecular Analyzer Software, BIORAD). For photographic reproduction, autoradiograms were developed after exposure to x-ray films (Biomax, Kodak). All data were corrected for variability in loading by calculation as a ratio to the values obtained with GAPDH.

2.2.4. i. v. pharmacokinetics of bioPEGPEI/NF-κB and 8D3SA-bioPEGPEI/ NF-κB

BALB/c mice were anesthetized with ketamine (100mg/kg) and xylazine (4mg/kg) intramuscularly and the right common carotid artery was retrogradely catheterized with PE10; 70μl of RHB pH 7.4/0.1%BSA containing either 1μCi of ^{3}H-NF-κB (0.93μg) or the combination of 1μCi of ^{3}H-NF-κB (0.93μg) and bioPEGPEI/NF-κB (0.78μg) or 1μCi of ^{3}H-NF-κB (0.93μg) and bioPEGPEI/NF-κB (0.78μg) -8D3-SA (25.6μg) were injected into the jugular vein and arterial blood was withdrawn from the carotid artery at 0.25, 1, 2, 5, 10, 20, 30 and 60min after injection of the isotope solution. The complex was formed at a N/P ratio of 6:1 and a 8D3-SA/bioPEGPEI ratio of 1:1. The blood samples were centrifuged (1,500g, 10min) and plasma was counted for total radioactivity. Mouse brains were taken at 60min, solubilized in 2ml Soluene and counted in a beta counter. Pharmacokinetic parameters were estimated as described under 2.2.1.3.

3.   Results

3.1.   Synthesis and characterization of a vector for brain delivery in the mouse

3.1.1. Production and purification of 8D3 hybridoma

The 8D3 rat hybridoma was generated by Dr. Britta Engelhardt and colleagues at the Max Planck Institute for Physiological and Clinical Research, Bad Nauheim, Germany. This antibody of the rat IgG_{2a} isotype was obtained by immunization of rats with a murine endothelioma cell line and specifically recognizes an antigen on cerebral vessels, which has been shown to be the mouse transferrin receptor (Kissel et al., 1998). The hybridoma is best grown in serum free media in roller culture and then the antibody was purified in 2 steps by ammonium sulfate precipitation followed by affinity chromatography on a Protein G column. The final IgG preparation was >95% pure as demonstrated by size exclusion HPLC and SDS-PAGE, with a final yield of approximately 20mg/L of culture supernatant.

3.1.2. Coupling of the 8D3 antibody to recombinant streptavidin

An efficient linker strategy between vector and drug moiety is crucial for drug delivery applications. The avidin-biotin technology facilitates coupling due to the extremely high binding affinity (K_D = 10^{-15} M^{-1}) and to its versatility. The same vector can be used to deliver a wide variety of biotinylated ligands. For our experimental procedures a 1:1 molar conjugate of 8D3 and recombinant streptavidin (SA) was used. Pharmacokinetic advantages for *in vivo* applications of conjugates with neutralized forms of avidin or with streptavidin over the strongly cationic native avidin have been described (Bickel et al., 1994). The linkage was achieved with commercial chemical coupling reagents (Pierce, Rockford, IL) as published for the anti rat-transferrin receptor monoclonal antibody OX26 (Bickel et al., 1993) and described in detail in the 'Methods' section. The final reaction mixture contained a major fraction of the desired 1:1 molar conjugate, designated 8D3-SA, along with some higher molecular weight conjugates and residual free 8D3 and streptavidin. The FPLC purification on Superdex 200HR was monitored by UV at 280nm absorbance and labeling with a trace amount of ^{3}H-biotin on columns. **Figure 5** depicts a typical chromatographic result. The yield of 8D3-SA is approximately 25 - 30% on a protein basis, calculated from the initial amounts of antibody and SA.
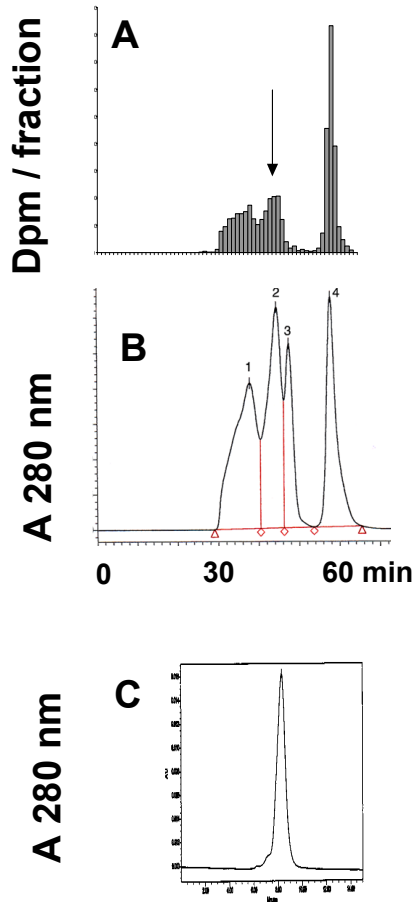
Figure 5: Purification of 8D3-SA on 2 Superdex 200 HR 10/30 in series (A, B). A = radioactivity in the collected fractions, B = corresponding UV-absorbance at 280 nm (peak #1 = higher molecular weight conjugates, peak #2 = the desired 1:1 molar conjugate (arrow in A), peak #3 = uncoupled 8D3, peak #4 = uncoupled SA. The elution profile in C is an analytical rechromatography on TSK gel 3000SW$_{XL}$ to verify the purity of peak #2 in B.
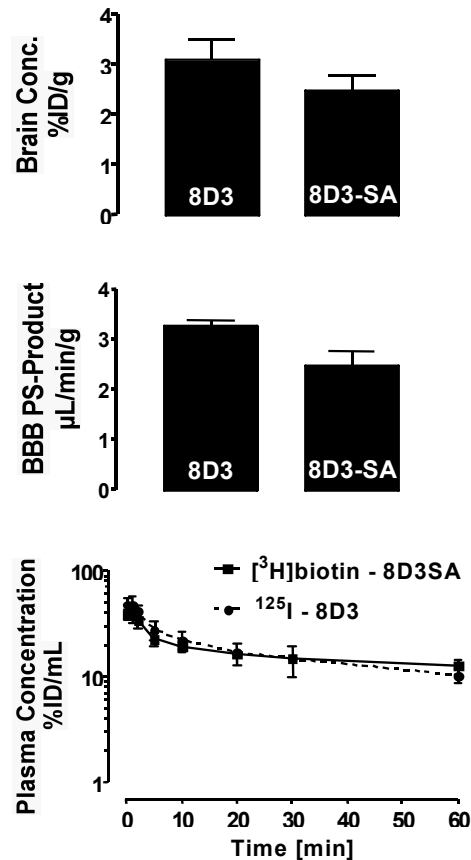
Figure 6: Pharmacokinetics of 8D3-SA in mice as determined by i.v. bolus injection of 8D3-SA labeled with ^{3}H-biotin. The brain concentration after 60min, the calculated PS-product, and plasma concentrations are shown side by side with corresponding data for ^{125}I-8D3. Data are means $\pm$ S.E. (n=3).

3.1.3. Pharmacokinetics and brain uptake of 8D3 and 8D3-SA after i.v. administration

The properties of 8D3 as a potential brain delivery vector have been published recently (Lee et al., 2000). The pharmacokinetics after i.v. bolus injection of ^{125}I-labeled 8D3 were investigated in anesthetized mice. As published, 8D3 demonstrated high uptake into brain tissue of up to 3.1 %ID/g (percent of the injected dose per g). Here, the 8D3-SA

conjugate as a potential drug vector was investigated to characterize its pharmacological behavior after i.v. injection into BALB/c mice. In the following table pharmacokinetic parameters are compared (see also **Figure 6**). All data are means ± S.E.. In each experimental series three BALB/c mice were injected.

The pharmacokinetic values were calculated by linear regression fitting using the programs BMDP or WinNonlin, respectively.

	8D3 n=3	8D3-SA n=3
C_{brain} [% ID/g]	3.1 ± 0.4	2.5 ± 0.3
$AUC_{(0 – 60min)}$ [% ID · min/ml]	932 ± 57	1035 ± 137
PS_{brain} [µl/min/g]	3.3 ± 0.1	2.5 ± 0.3
VD_{brain} [µl/g]	263 ± 19	252 ± 28

Table 5: Comparison of pharmacokinetic parameters of 8D3 or 8D3-SA conjugate: c_{brain} = PS · $AUC_{0-60min}$, AUC – area under the plasma curve, calculated by linear regression fitting (BMDP, WinNonlin); PS – brain permeability-surface area PS = $(V_d – V_0)$ · c_p (60min) / $AUC_{0 – 60min}$; V_0 – plasma volume of the brain; c_p (60min) – terminal plasma concentration

The data revealed almost unchanged pharmacokinetic properties of 8D3-SA compared to the parent antibody. The plasma concentration time course was superimposable. Brain uptake rate and brain concentrations reached 80% of the values measured for 8D3. The values for 8D3 and 8D3-SA conjugate, respectively, are not significantly different as shown by t-test.

We also demonstrated in "capillary depletion" experiments (gentle homogenization and density centrifugation in 16% dextran) (**Figure 7**) that after one hour 33% of the total brain concentration of anti-transferrin receptor antibody-SA conjugate was associated with the capillary fraction, which is identical with a % ID/g of 0.6. The 8D3-SA could be either membrane bound or internalized. In the histogram shown, homogenate represents brain tissue and capillaries before density separation. After centrifugation the supernatant as the brain tissue and the pellet as the capillary fraction are pictured. The data are means ± S.E.. The i.v. bolus injection of the 8D3-SA conjugate was applied to three BALB/c mice (n=3).

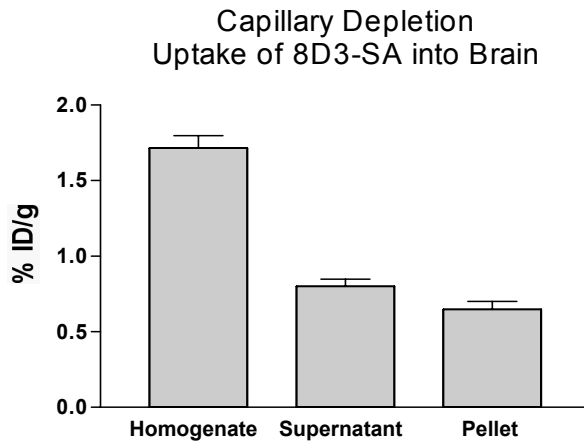Capillary Depletion
Uptake of 8D3-SA into Brain

Figure 7: shows a capillary depletion experiment 60min after i.v. bolus injection of 8D3-SA after gentle homogenization of brain and separation into capillary pellet and postvascular supernatant by dextran density centrifugation. Data are expressed as percent of the injected dose per g brain and show that 33% of total 8D3-SA vector are associated with the capillary pellet.

3.1.4. Binding and uptake studies with 8D3 and 8D3-SA using the bEnd5 brain endothelial cell line

The bEnd5 endothelioma is derived from mouse brain endothelium and was generated by immortalization with polyoma middle T oncogen (Rohnelt et al., 1997). It has been successfully used as an in vitro model of the mouse BBB, especially to investigate the role of adhesion molecules in T cell transmigration (Laschinger and Engelhardt, 2000; Reiss and Engelhardt, 1999). Therefore, the cell line represents a good model for drug delivery to brain endothelium and for measuring pharmacologic effects. Evidence for the functionality of 8D3-SA as a vector in these bEnd5 cells was obtained by immunohistochemistry and tracer binding experiments. First, we visualized the binding of 8D3 and 8D3-SA to transferrin receptors on bEnd5. **Figure 8** demonstrates that comparable labeling of bEnd5 cells with either the native antibody or with the streptavidin conjugate was obtained. Labeling experiments with 10μg/ml of the native 8D3 antibody or the synthesized 8D3-SA conjugate showed similar staining patterns. As a negative control served the incubation of the biotinylated rabbit anti rat antibody on bEnd5 cells without the primary antibody.
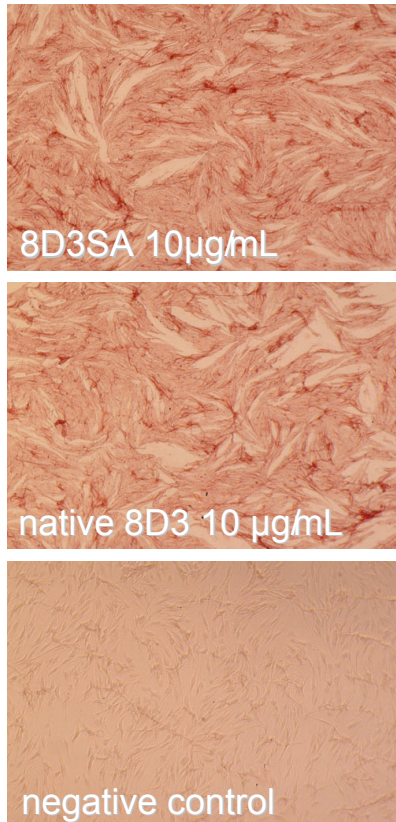
Figure 8: Immunohistochemistry on bEnd5 cells. The cells were grown in 96-well plates and fixed with 3% paraform-aldehyde. Endogenous peroxidase and unspecific staining were blocked with 0.3% H_2O_2 and 3% bovine serum albumin, respectively. The cells were incubated either with 10 µg/ml 8D3 or 8D3-SA. A biotinylated rabbit anti-rat IgG antibody was used as a secondary antibody. Visualization was performed with the avidin-biotin-peroxidase (ABC) method, using aminoethylcarbazol (AEC) as a substrate. Negative control = without primary antibody.

Second, binding and internalization was measured with ^{3}H-biotin-labeled 8D3-SA. **Figure 9** shows a representative result of a binding assay. After an incubation time of 60min a binding of 2.7%/mg protein was measured. A mild acid wash procedure revealed that the major fraction (70%) of the cell-associated radioactivity was internalized after 15min, 30min or 60min of incubation. Direct evidence for the receptor specificity of the binding and uptake was obtained by competition experiments with a 240-fold molar excess of native 8D3, which resulted in a 90% decreased amount of ^{3}H-biotin-8D3-SA associated with the bEnd5 cells. In contrast, binding/uptake could not be displaced by a corresponding molar excess of the rat-specific TfR antibody, OX26.

In combination, these results confirm the receptor-mediated uptake mechanism of the 8D3 antibody and its streptavidin conjugate by brain endothelial cells *in vitro*.
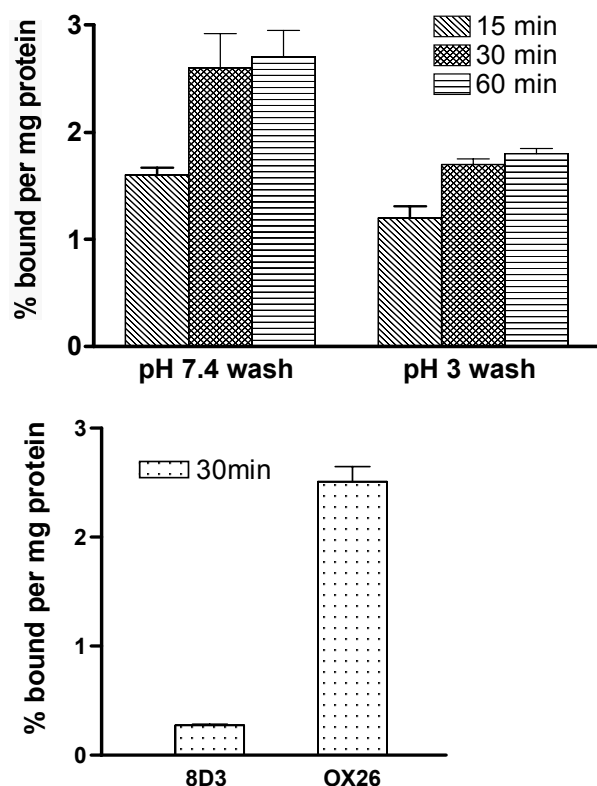
Figure 9: Binding and uptake studies with bEnd5 cells demonstrate a time dependent increase of both binding and internalization as shown by mild acid wash. After 60min a binding of 2.7%/mg protein was observed. The pH 3-solution removes cell surface bound ^{3}H-biotin-8D3SA and the results after acid wash represent internalized tracer. The internalization is expressed as a percentage of total binding. Data are standardized by the protein measurement of the solubilized cells.
Incubation of bEnd5 cells with ^{3}H- 8D3-SA and additional unlabeled 8D3 or OX26 (240-fold molar excess) for competition studies showed a 90% decrease in binding for 8D3. However, no competition by the anti-rat Ab OX26 was seen.

3.2. Polyethylenimines as carriers for oligonucleotides

3.2.1. Synthesis and characterization of low molecular weight biotinylated PEG-PEI

Dr. Kissel's group (Institute of Pharmaceutical Technology and Biopharmacy, Philipps-University Marburg, Germany) has recently developed a small, low-branched PEI (molecular weight, 2,700Da) with favorable characteristics for DNA delivery *in vitro* and *in vivo*: very narrow size distribution, superior transfection efficiency *in vitro*, and very low cellular toxicity compared to commercial PEI formulations (Fischer et al., 1999). A graft copolymer with biotinylated PEG (designated as bioPEGPEI) was synthesized. The biotin-PEG serves two purposes: (1) it enables coupling to our 8D3-SA vector. Such biotinylated PEG derivatives have been successfully used for coupling of cationic macromolecules such as brain derived nerve growth factor to streptavidin-based vectors (Wu et al., 1999). (2) as known from pharmacokinetic studies (Zalipsky et al., 1995), PEGylation improves the stability and pharmacokinetics of diverse macromolecular conjugates.

The graft copolymer was synthesized at a 1:1 molar ratio from biotin-PEG (molecular weight = 3,400Da, Shearwater Polymers) carrying a single reactive N-hydroxysuccinimide ester group (NHS) at the opposing end of the linear PEG chain, and our low molecular weight PEI (MW = 2,700Da). Equimolar amounts of biotin-PEG-CO_2NHS (3,700Da) (0.034mmol in 40ml $CHCl_3$) and Low Molecular Weight PEI (2,700Da) (0.034mmol in 25ml $CHCl_3$) were added together dropwise under vigorous stirring. The reaction mixture was boiled for 18h. No non-reacted biotin-PEG was left as determined by NMR and size exclusion chromatography of the reaction mixture. The synthesis of the bioPEGPEI was carried out in Dr. Kissel's laboratory. The spectrophotometric HABA assay demonstrated that bioPEGPEI retained full binding affinity for streptavidin (**Figure 10**).
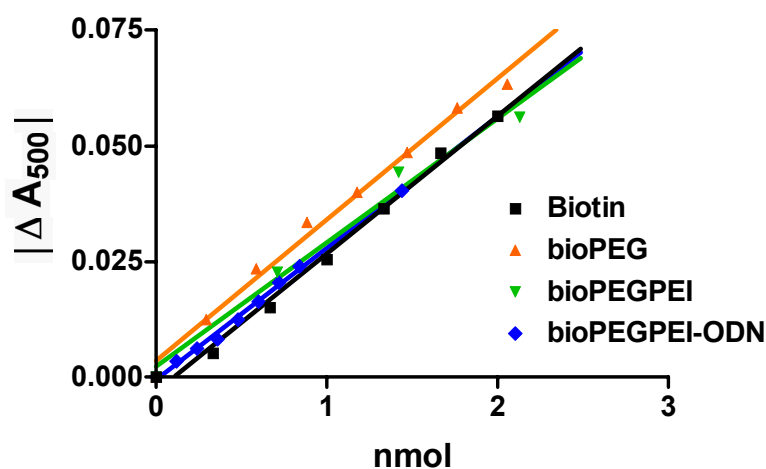

Figure 10: HABA assays for measurement of biotin concentrations. The biotin analog HABA binds weakly to streptavidin, forming a colored complex in solution. HABA can be displaced by increasing concentrations of biotin (x-axis), as detected by a proportional change in absorbance at 500 nm (y-axis). Addition in equimolar amounts of bioPEG (biotinylated PEG MW 3,400), bioPEGPEI (copolymer of bioPEG and PEI MW 2,700), bioPEGPEI-ODN (complex of bioPEGPEI with NFκB decoy ODN) resulted in comparable displacement curves. The slopes of the regression lines were not significantly different from the biotin standard (black), indicating that the biotin moiety in bioPEG and bioPEGPEI is fully available for binding, even after complex formation with the ODN.

3.2.2. Complex formation and Retardation assays

Different molar ratios of PEI amine to DNA phosphate (N/P ratio) were tested for complexation of ODN (NF-κB decoy) by bioPEGPEI and analyzed in retardation assays on polyacrylamide and agarose gels. **Figure 11** demonstrates that bioPEGPEI readily formed complexes with the ODN in 10mM PBS pH 7.4. At N/P = 3:1 virtually all ODN is

bound, and at higher N/P ratios no free ODN is detectable. ODN in complex form is protected from nucleases in plasma as shown in **Figure 11B**.
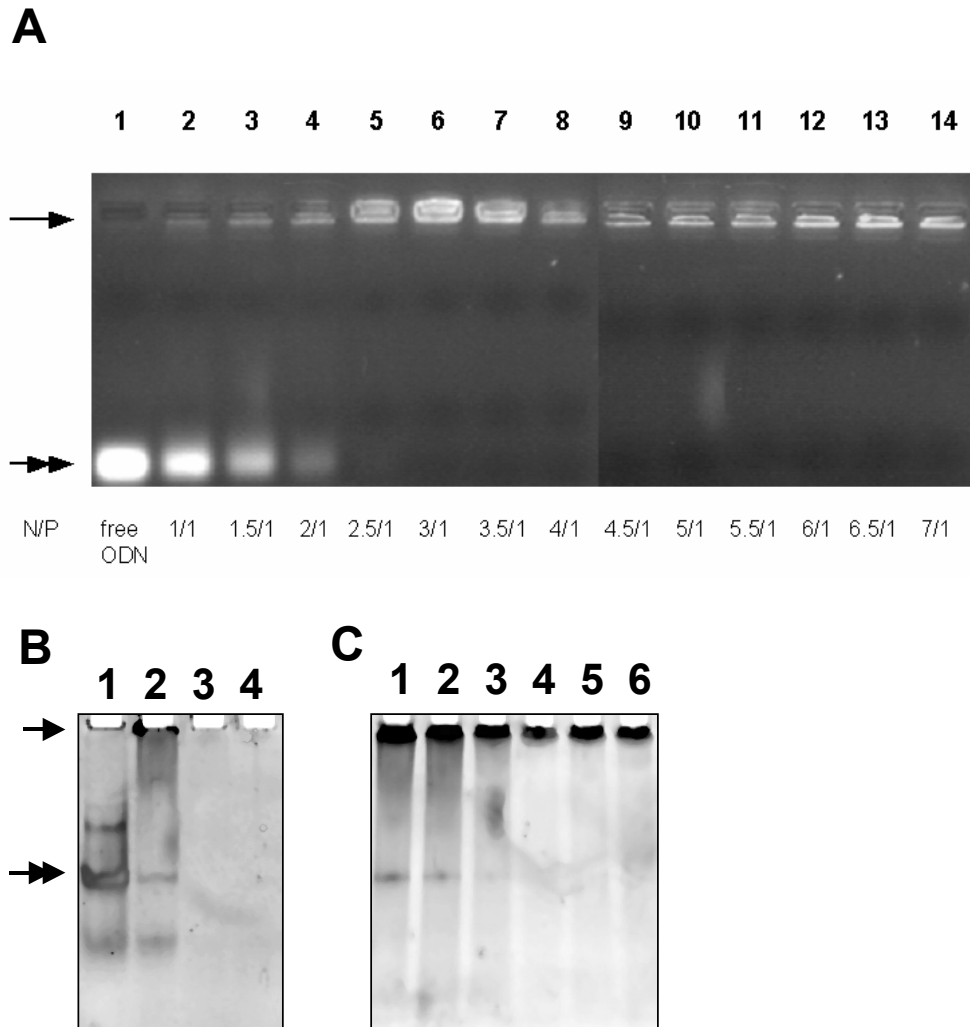
A

B

C

Figure 11: (A) Different N/P ratios ranging from 1:1 to 7:1 were investigated on an ethidium bromide stained 1% agarose gel. Lane 1 shows 4μg of a free ODN, incompletely complexed by bioPEGPEI at ratios 1:1 to 2.5:1 and completely bound at higher ratios. Pocket staining revealed neutral or cationic complexes.
Non-denaturating 20% poly-acrylamide gels stained with SYBR Gold for visualization of DNA. The samples in **(B)** were loaded as follows: lane 1 = double-stranded ODN (NF-κB decoy), 2 to 4 = bioPEGPEI-ODN complex at N/P ratios of 3:1, 6:1, and 10:1. The position where the sample was loaded is indicated by the arrow, the double arrow shows the migration of free double-stranded ODN. At N/P of 6:1 and 10:1 there was no free ODN detectable.
(C) demonstrates the stability in 20% human plasma of the bioPEGPEIODN complexes with N/P ratios of 6:1 (lanes 1-3) and 10:1 (lanes 4-6). The samples were incubated at 37°C for 0 min (lane 1 and 4) 30 min (lane 2 and 5) or 120 min (lane 3 and 6) before application to the gel.

3.2.3. Binding characteristics of 8D3-SA to its ligand bioPEGPEI/NF-κB

The targeting vector 8D3-SA was radioactively labeled with ^{3}H-biotin and conjugated with bioPEGPEI/NF-κB at different molar ratios to investigate its separation in an electric field by electrophoresis. After a 3h electrophoresis at 90V the free 8D3-SA moved from its origin (pocket, gel slice #6) and accumulated in gel slice #9 (**Figure 12**).
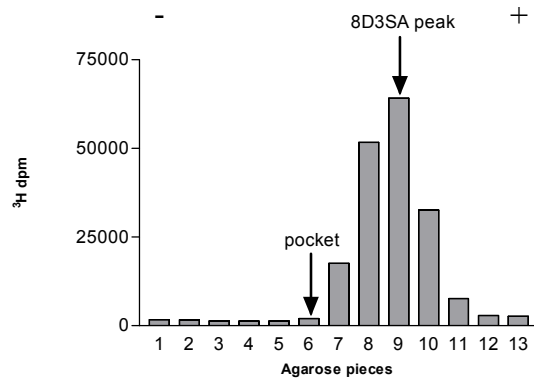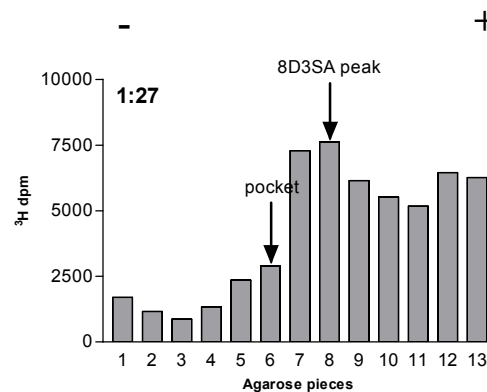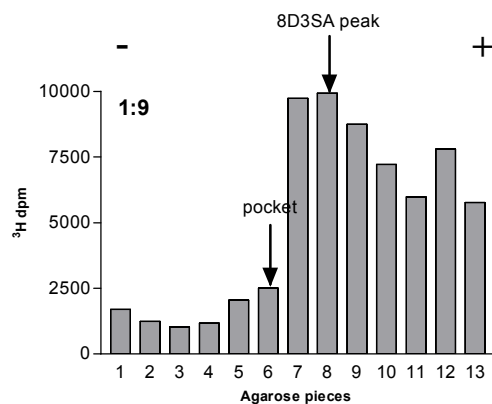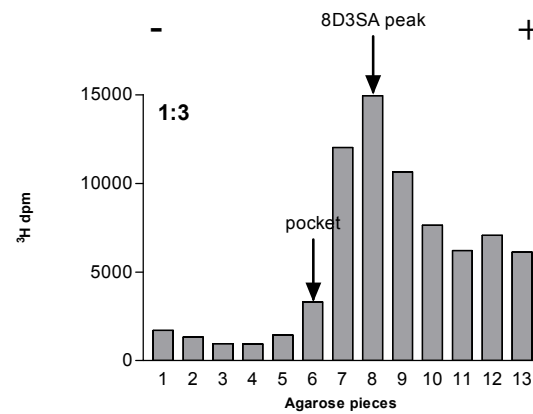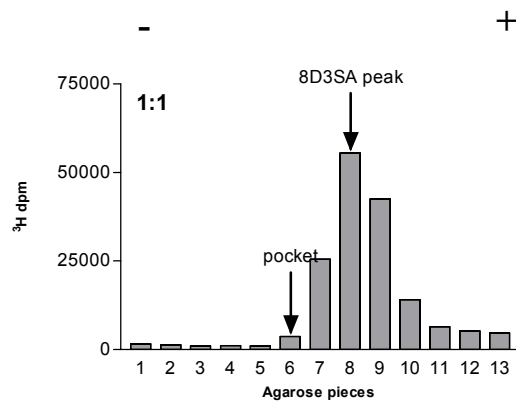
N/P = 3:1

Figure 12: Migration of 8D3-SAbioPEGPEI/NF-κB on a 1% agarose gel N/P = 3:1. The agarose gel was cut into 13 equal gel slices and each slice was measured in a beta counter. The first panel shows the 8D3-SA without conjugation, all the other panels show conjugation at a drug to antibodyconjugate ratio of 1/1, 1/3, 1/9 and 1/27.

The same studies as for the free 8D3-SA, were repeated after conjugation of vector with its ligand at the following vector/ligand ratios of 1/1, 1/3, 1/9 and 1/27. Due to the neutral/cationic characteristics of the bioPEGPEI/NF-κB at ratio 3:1, a shifting to gel slice #8 is visible. Particularly, a conjugation of 1/1 seems to form a distinct peak, whereas all the other ratios obtained more indistinct peaks reaching slices #9 to 13. We obtained similar results studying bioPEGPEI/NF-κB ratios of 6:1. Noticeable is a slight shift in mobility to gel slice #7 (**Figure 13**).
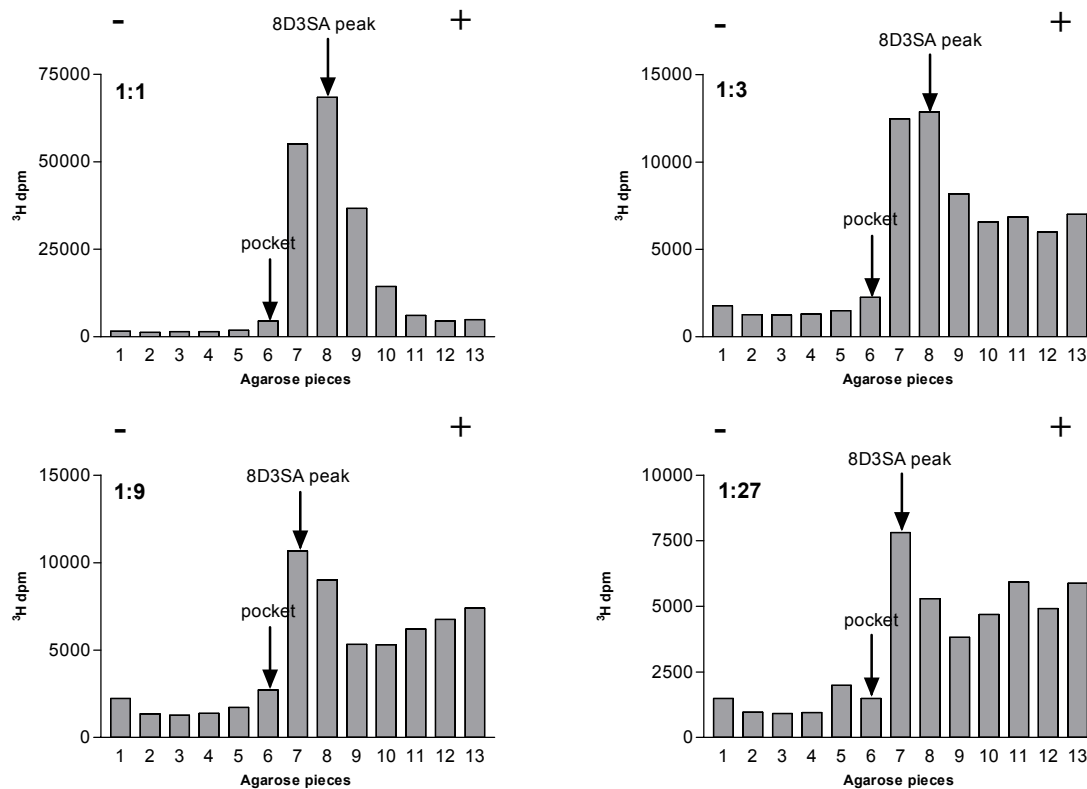
N/P = 6:1

Figure 13: Comparable binding and separation behavior of complexes is shown at a N/P ratio of 6:1. However, a shifting of the peak fraction is noticed in conjugates at ratios of 1:9 and 1:27, suggesting that increasing amounts of PEI prevent a separation as shown at ratios 1:1 and 1:3.

The same samples were analyzed by counting the radioactive labeled ^{32}P-NF-κB part of this complex in a beta counter. Broad distribution with a hardly visible peak in slice #8 is shown at 8D3SA-bioPEGPEI/NF-κB ratio of 1/1. The small amount of radioactivity in the sample could explain the lack of a prominent peak (compare cpm values to the following samples). Distinct peaks appear at ratios 1/3 and1/9 in gel slice #7, corresponding to ^{3}H-biotin counts seen at ratio 6:1, but shifted from #8 to #7, if compared to ratio 3:1. Ideally,

both radioactivities (^{3}H/^{32}P) should have their peak fraction in the same slice to proof the tight binding of all components. Due to its strong negative charge, free NF-κB would expect to appear in higher slice numbers (**Figure 14**).
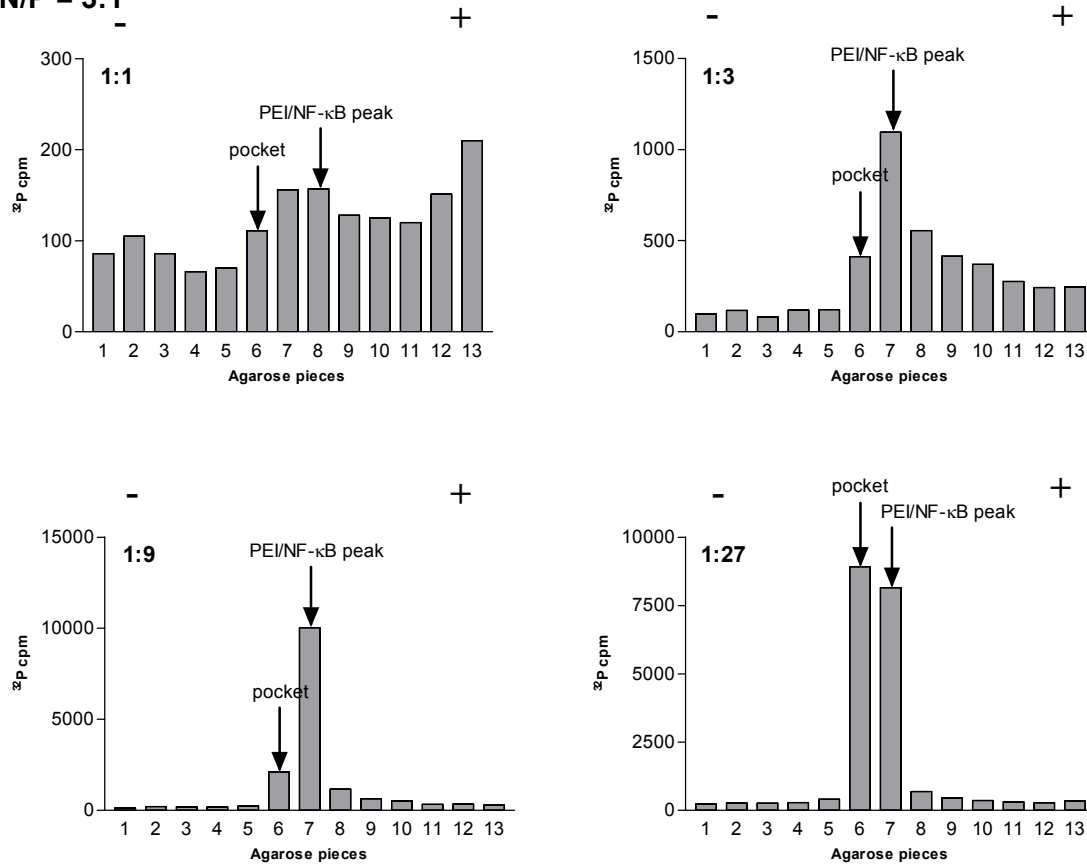
N/P = 3:1

Figure 14: ^{32}P-NF-κB cpm of each slice were counted and presented in the diagram to compare peak fractions at a N/P ratio of 3:1 and different 8D3-SA to bioPEGPEI/NF-κB ratios. The first panel reveals a relatively homogenous distribution of ODN compared to the panels at higher antibody to ligand ratio. The behavior of the ODN's in this case is not explainable, it can only be suspected that the increasing amount of PEI has a further influence on the stability of DNA in its conformation independent from the ratio, in which the DNA was complexed before (3:1). The variable cpm numbers are due to different amounts of ODN entering the conjugation reaction between antibody and ligand.

When complexes formed at the 6:1 ratio were investigated, they revealed exactly the same behavior as shown for the 3:1 ratio. Moreover, peaks in gel slices #7 show clearly, that vector and ligand are tightly associated. A PEI excess seems to have a negative influence on the separation properties of the conjugate as shown by enhanced conjugate accumulation in slice #6 (pocket) (**Figure 15**).
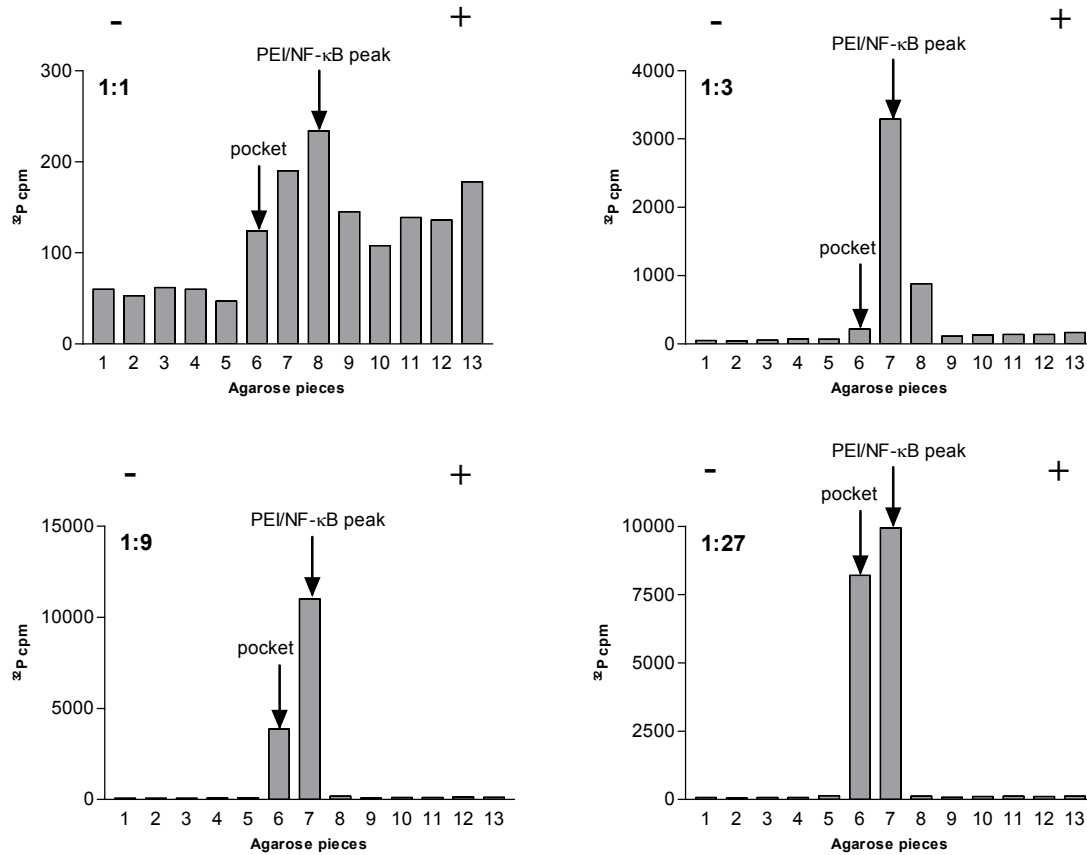
N/P = 6:1

Figure 15: Diagrams show an analogue picture as seen for N/P ratios of 3:1 in **Figure 14**. Distinct peaks are formed at antibody to ligand ratio of 1/3 and 1/9, resulting in an excess of PEI at ratio 1/27 sitting in the pocket (slice #6). Due to low amount of activity in the first panel (ratio 1/1), no distinct peak could be detected.

3.2.4. Vector-mediated increase in cellular uptake

Quantitative uptake experiments with ^{32}P-labeled ODN (5' labeling with T4 polynucleotide kinase and γ-^{32}P-ATP) were performed with bEnd5 cells in 24-well plates. The tracer was added in 0.5ml cell culture medium and incubated for various times at 37°C. **Figure 16** depicts the results of a 60min uptake study. Less than 0.2% of the activity was associated with cells when free ODN was used. The bioPEGPEIODN complex showed binding and uptake of 2%, and this was further increased 3-fold by the targeting to transferrin receptors with 8D3-SA (8D3SA/bioPEGPEIODN = 1:1). In a separate experimental series a mild acid wash at the end of the incubation was used to differentiate surface bound and internalized tracer. For bioPEGPEIODN complexes with

8D3-SA we found >90% of the total activity as internalized fraction at incubation times of more than 10 min, which is in good agreement with the data obtained for ^{3}H-biotin-8D3-SA.
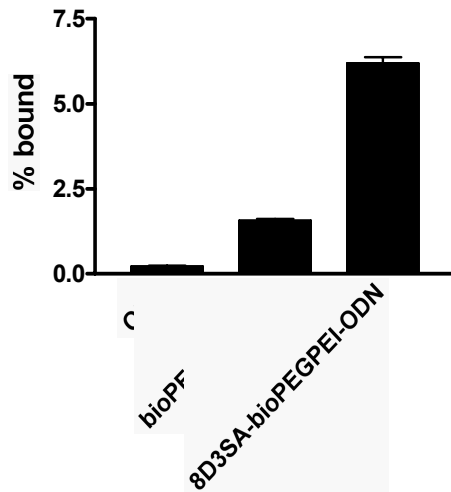

Figure 16: Uptake of ^{32}P-labeled ODN by bEnd5 cells after 60min (mean ± SD, n=3). The N/P ratio of the bioPEGPEI-ODN complexes was 3:1. The ODN tracer concentrations were adjusted to 0.2μM. After the incubation period cells were washed 3x with cold medium, solubilized in 1M NaOH and counted in scintillation fluid in a liquid scintillation counter.

3.2.5. Interaction of FITC-NF-κB decoys with bEnd5 cells

Fluorescence microscopic studies with FITC-labeled NF-κB decoys 0.5μM confirmed the cellular uptake of 8D3SA-bioPEGPEI/NF-κB by bEnd5 cells (**Figure 17**). At early times (30min incubation at 37°C) labeling of the plasma membranes, at later time points (4h, 8h) uptake of fluorescent dye into the nucleus could be observed. The pictures were taken on a Nikon inverted fluorescence microscope with a 40time lens. The same experiments were carried out without vector. At the fluorescence microscopy level we could not recognize differences in staining patterns. Also uptake studies with 2μM ODN did not display any visible differences.
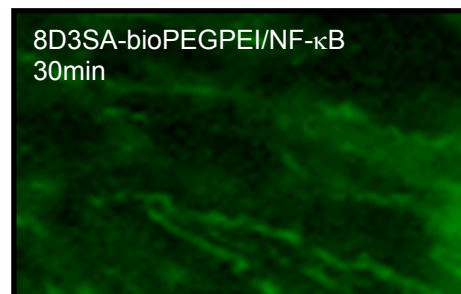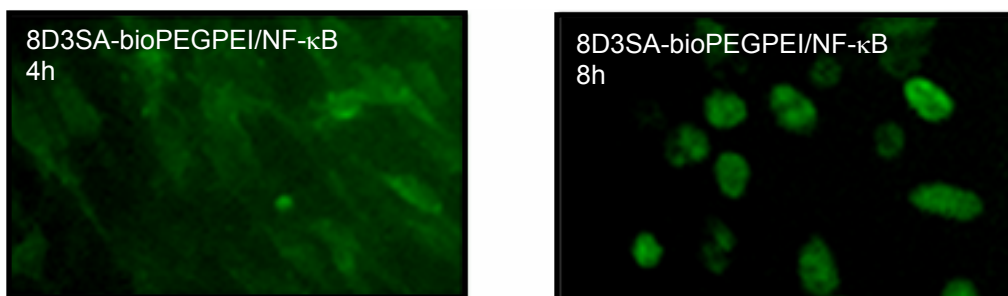
Figure 17: The fluorescence microscopy pictures show the incubation of 8D3SA-bioPEGPEI/NF-κB 0.5μM on bEnd5 cells at various incubation times. Free NF-κB decoys served as a negative control. Pictures were taken with a 40time lens.

3.2.6. Particle sizing

In the past, several experimental studies investigating particle sizes of PEI-ODN complexes under different salt conditions proved difficult, because of rapid aggregation of polyplexes with each other (Tang and Szoka, 1997). Pegylation of PEI not only improves pharmacokinetic stability *in vivo*, it also prevents the non-specific interaction with blood components, such as erythrocytes and plasma proteins (Ogris et al., 1999). Moreover, this PEI modification should enable its measurement under different incubation conditions, while preventing its aggregation. Our first measurements were performed in 10mM PBS at a pH of 7.4 and N/P ratios ranging from 3:1 to 60:1 to show a possible size change (**Figure 18**). At a ratio of 3:1 complexes seem to be very constant in size (120 - 140nm) over time. Particle sizes in this range can be expected to be compatible with the endosomal compartment. 6:1 ratio complexes proved even smaller with narrower Gaussian distribution, demonstrating a higher complexation of PEI and ODN. However, with further increasing N/P ratios the complex size increased.

Samples were stored at 4°C and a repeat measurement was carried out after 4w. There was no change in complex size.

Stability of a bioPEGPEI/NF-κB complex in PBS (pH 7.4) at different N/P ratios

3:1

| Gauss SE mean | 40.12 | 46.04 | 52.12 | 44.01 | 44.97 | 51.55 | 63.52 |

6:1

| Gauss SE mean | 34.51 | 39.67 | 40.05 | 39.34 | 52.18 | 44.40 | 40.38 |

10:1

| Gauss SE mean | 37.62 | 39.44 | 40.67 | 48.00 | 40.93 | 42.62 | 41.50 |

20:1

| Gauss SE mean | 42.62 | 48.64 | 47.74 | 50.60 | 47.55 | 47.19 | 44.45 |

60:1

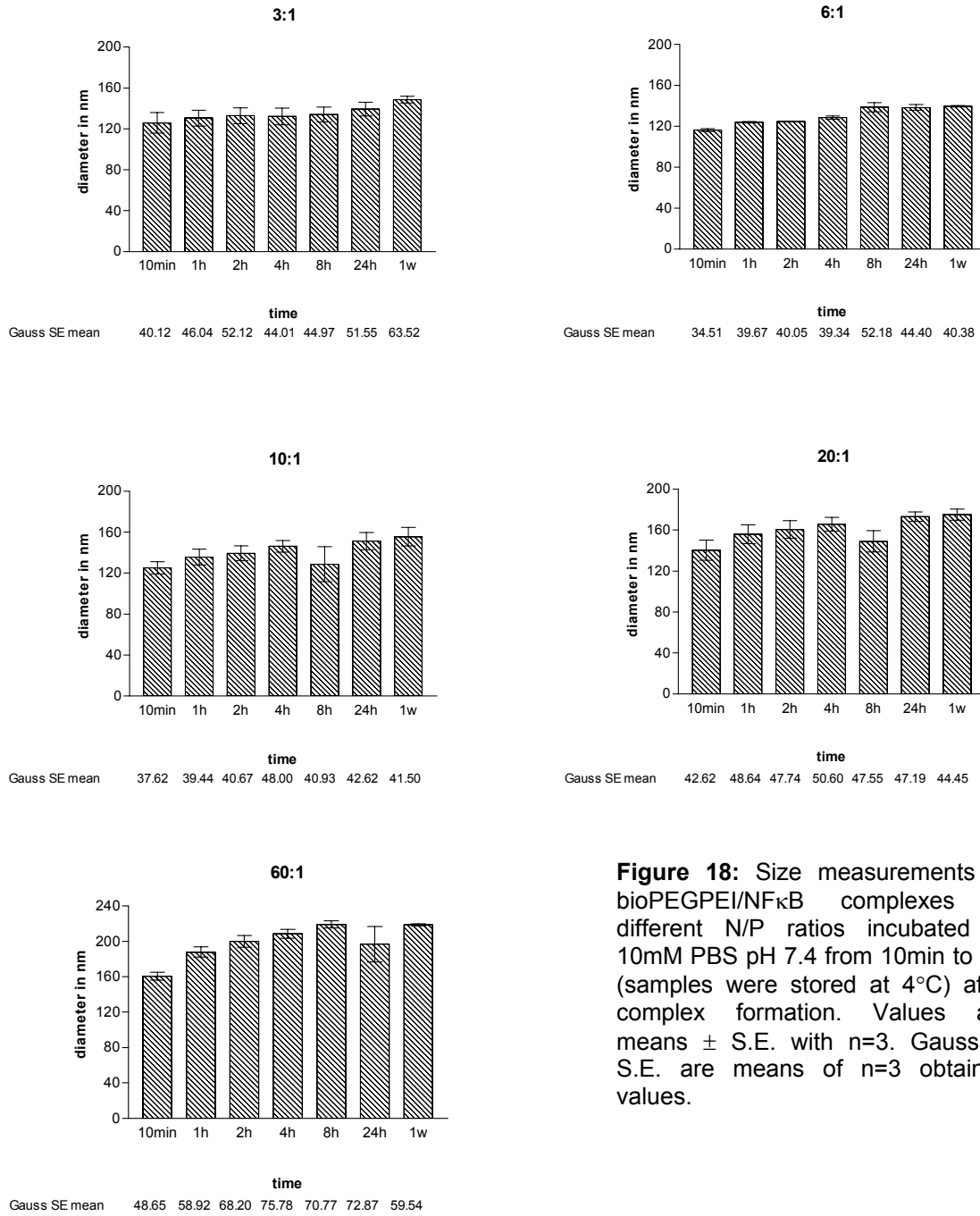| Gauss SE mean | 48.65 | 58.92 | 68.20 | 75.78 | 70.77 | 72.87 | 59.54 |

Figure 18: Size measurements of bioPEGPEI/NFκB complexes at different N/P ratios incubated in 10mM PBS pH 7.4 from 10min to 1w (samples were stored at 4°C) after complex formation. Values are means ± S.E. with n=3. Gaussian S.E. are means of n=3 obtained values.

Stability of an 8D3-SAbioPEGPEI/NFκB complex in PBS (pH 7.4) at N/P ratio of 6:1

6:1

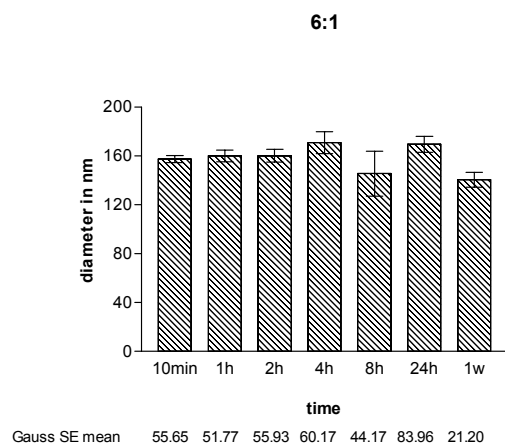| Gauss SE mean | 55.65 | 51.77 | 55.93 | 60.17 | 44.17 | 83.96 | 21.20 |

Figure 19: shows a representative picture of a size and stability test after complex formation of drug and its vector at a N/P ratio of 6:1 and molar 8D3SA/bioPEGPEI ratio of 1:1. Complex sizes appear to be constant over a time frame of 24h, after 1w smaller complexes are visible with decreasing Gaussian distribution.

In a second step we tested the influence of coupling our targeting vector to the DNA/polymer complex by incubating 8D3-SA (MW 210kDa) with bioPEGPEI/NFκB after complex formation for 15min (**Figure 19**). From the results obtained in the first study we chose the 6:1 ratio for further experiments. The diagram shows an average increase in complex size of 40nm compared to the unconjugated complex (see **Figure 18**). After 1w a moderate decrease of complex size by 30nm could be observed compared to the 24h measurement, which may be caused by loosening of complex formation rather than dissociation of vector and ligand (the dissociation time of biotin and streptavidin is 90 days).

Stability of a bioPEGPEI/NFκB complex in DMEM+ (w/o plasma) at N/P ratio of 6:1

6:1

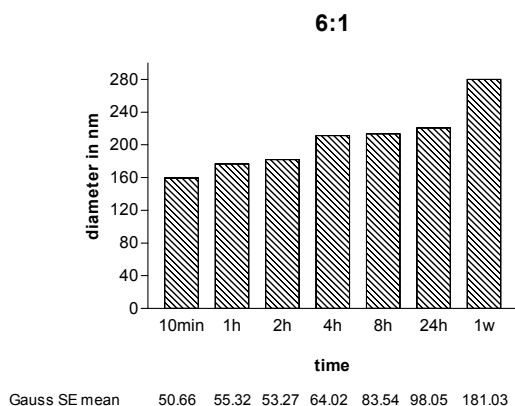| Gauss SE mean | 50.66 | 55.32 | 53.27 | 64.02 | 83.54 | 98.05 | 181.03 |

Figure 20: bioPEGPEI/NFκB complexes are shown after incubation in DMEM+ as they appear under *in vitro* conditions. The complex size increased over 1w, suggesting a time dependent uptake of salts contained in the DMEM+.

Medium salts also have an influence on size behavior as shown in **Figure 20**. In contrast to all other results obtained, sizes changed over time significantly. Starting at 160nm after 10min of complex incubation, particle sized increased to about 280nm after 1w. These findings may be explained by continuous incorporation of salt ions into the polyplex.

3.2.7. TCA (Trichloro acetic acid) precipitation and ultrafiltration

The stability tests already mentioned under 3.2.2. were extended by incubating complexes in different media and over several time frames. Ultrafiltration and trichloro acetic acid precipitation were used as analytical tools.

bioPEGPEI/NF-κB complexes were incubated either in 10mM PBS or DMEM+ with 10% FCS over 10min, 1h, 4h or 24h at 37°C and filtered through an Ultrafree MC (Millipore) unit at 5000g for 10min. Free NF-κB passes this filter to almost 100%, complexes adhere to the filter membrane (see **Figure 21**). Therefore, this method can be used to estimate the percentage of ODN, which is released from its complex after the various incubation times. A TCA precipitability test of NF-κB decoy or its complex was used to check for the purity of tracer after labeling and for the stability of the complex, respectively. The mean TCA of labeled probe after incubation in PBS was 96.4%, and after incubation in DMEM + with 10% FCS was 88.0%, yielding values of 94.8% after incubation in PBS and 89.2% after incubation in DMEM + with 10% FCS for 24h, respectively. The results of this 24h experiment show that the time and the incubation medium do not decrease stability, supporting the results of native PAGE (section 3.2.2.).

In a second experimental series the probability of alteration of the complex by incubation on bEnd5 cells was investigated. The experiments were performed in the same manner as described, incubating the complex in DMEM + 10% FCS in an Eppendorf tube or on bEnd5 cells for the same periods as above (**Figure 22**). Surprisingly, after 24h of incubation we could see an almost complete release of ODN (96.7%) from its complex caused by cell activity. Incubation times of 10min and 1h revealed similar results as obtained for experiments carried out in an Eppendorf tube.

The measurement of TCA precipitability correlated well with the filtration experiments: the TCA precipitability of freshly labeled ODN was 94%, decreasing only slightly to 92.7% after 10min and 87.5% after 24h. In contrast, incubation on cells decreased precipitability from the medium to 34.8% after 24h.
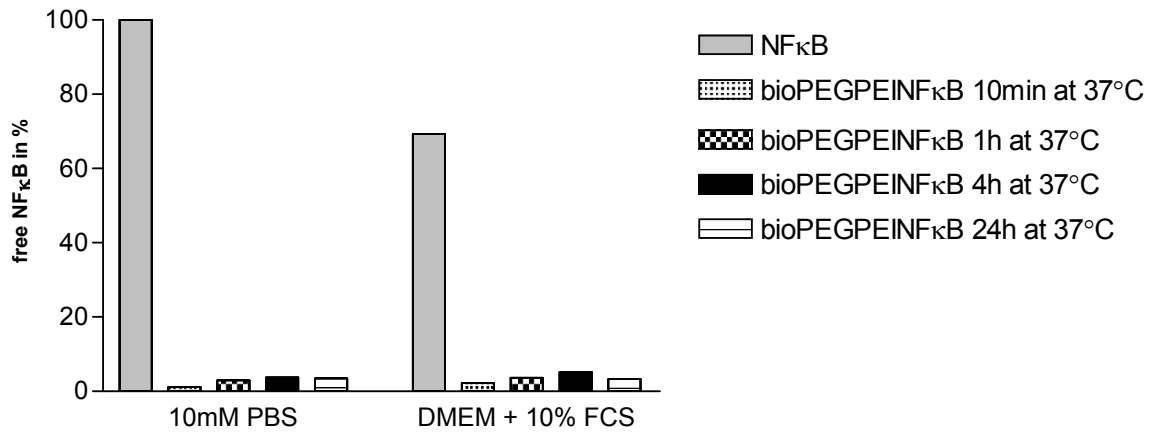
Figure 21: 100% of free NF-κB decoy incubated in PBS pass through the ultrafiltration membrane. Free ODN incubated in DMEM + 10% FCS pass to 70%, due to partial binding of ODN to plasma proteins and their retention by the filter. In contrast, only 1.1% of total ODN in complex with bioPEGPEI pass through the membrane after a 10min incubation at 37°C in PBS. There is only a minor increase to 3.4% after 24h incubation. The result is similar after incubation in DMEM with 10% FCS.

Figure 22: Comparison of complex stability after 10min, 1h, 4h and 24h of incubation either without or with bEnd5 cells.

3.3. Investigation of inflammatory markers influenced by activation of NF-κB

3.3.1. NF-κB gel shift assays

As a method to directly show the modulation of the transcription factor by stimulation with Lipopolysaccharide (LPS) or TNFα, we utilized electrophoretic mobility shif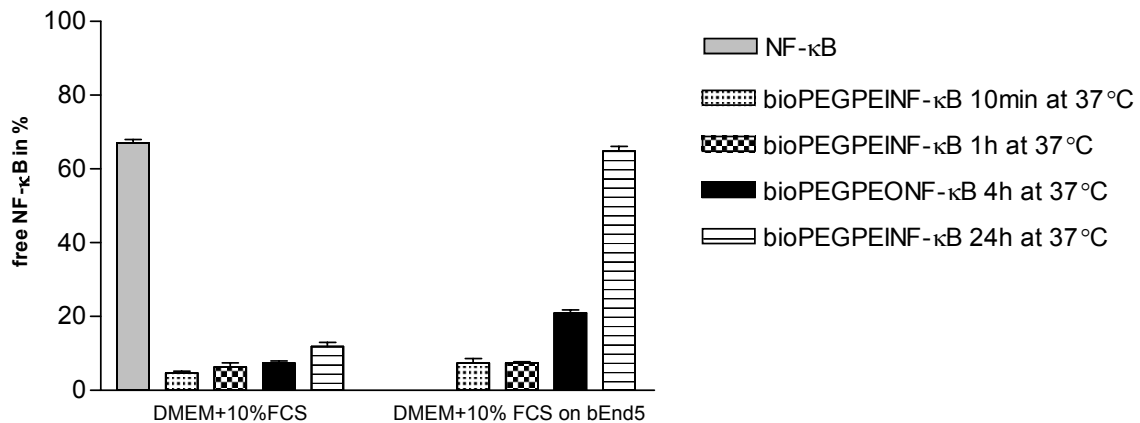t assays (EMSA). The cells were grown in 6-well plates. An inflammatory response was provoked by addition of bacterial LPS and TNFα (1µg/mL and 50ng/mL, respectively) or LPS alone to the culture media, which activates the NF-κB transcription factor. Nuclear extracts were prepared from the cells after various times and incubated with ^{32}P-labeled NF-κB decoy oligo (Bragonzi et al., 1999). The ODN sequence used in these experiments contains the NF-κB binding cis-element of the murine VCAM-1 promoter (Cybulsky et al. 1993) and is a 20-mer phosphodiester ODN with the sequence 5'-CCT TGA A**GG GAT TTC CC**T CC-3' (κB-consensus site bolded and underlined). A scrambled ODN sequence (5'-TTG CCG TAC CTG ACT TAG CC-3') was used as a control. The ODNs were custom synthesized (MWG Biotech) as single-stranded sequences and were annealed with the complementary 20-mer prior to use. The result of the binding reactions of labeled NF-κB decoy with nuclear extracts and the electrophoresis is shown in **Figure 23**. NF-κB activity was just faintly detectable in the control cells (= 0min), but showed the expected strong signals after 1min and 5min of stimulation. In the 60min and 120min samples a second peak of activity appeared. The specific bands representing NF-κB binding activity were verified by competition with unlabeled specific ODN. There was no competition with an equal excess of the scrambled ODN sequence detectable (not shown).
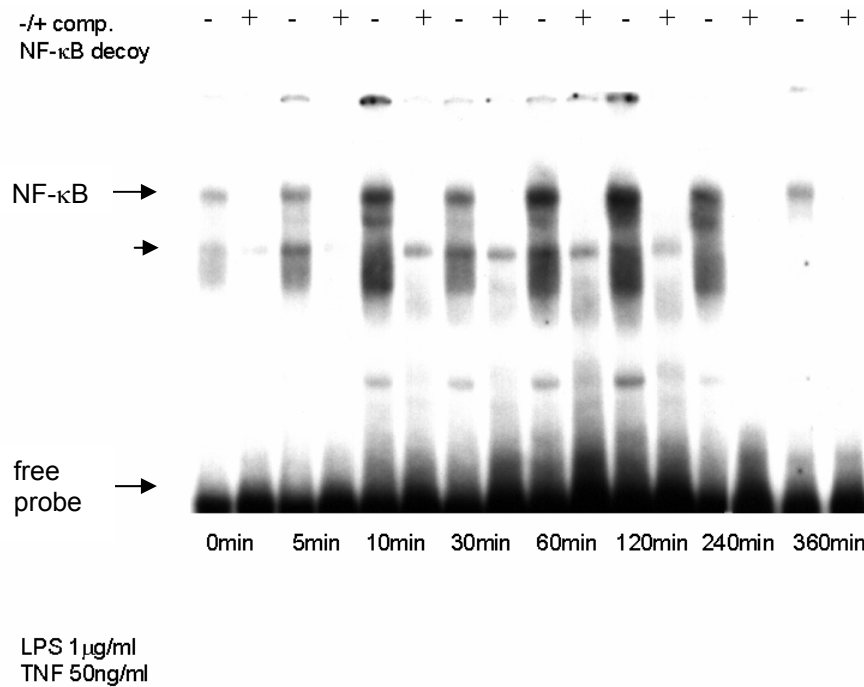
Figure 23: depicts a typical picture of an EMSA after stimulation of bEnd5 cells with TNFα (50ng/ml) and LPS (1μg/ml). NF-κB is constitutively active at a low level, its activity increases after 1min and 5min of stimulation, reaching the first peak after 5min. A second peak can be seen after 120min, followed by a decrease to almost basal levels after 360min. A 80-fold molar excess of non-labeled NF-κB decoy prevents binding of ^{32}P-NF-κB decoy to its transcription factor. However, non-specific bands (arrow heads) remain visible, supporting the specificity of the competition.

We could obtain a different activation pattern after sole stimulation by LPS. The maximum peak of activation occurred after 5min and 10min, respectively, declining to basal levels after 120min (**Figure 24**). We could not show any biphasic activation as seen after combined LPS/TNFα activation.

These results form a base for continuing investigations regarding activation/inhibition experiments after targeted treatment with 8D3SA-bioPEGPEI/NF-κB decoys.
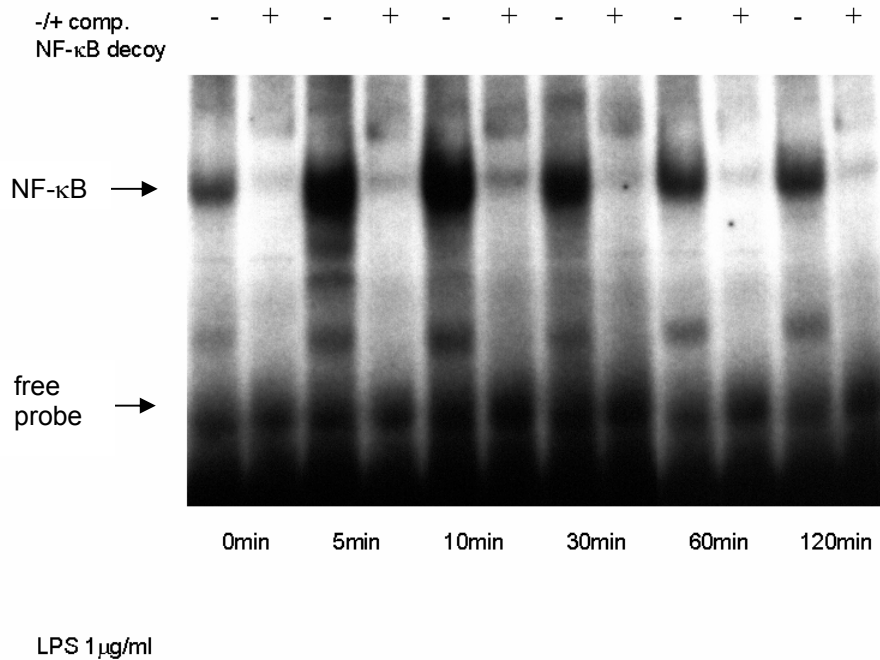
Figure 24: The autoradiogram represents an activation pattern after stimulation with LPS (1μg/ml) alone. A maximum of stimulation can be observed after 5min and 10min, respectively, resulting in a decrease after 120min. Competition studies were performed as described in the picture legend above.

3.3.2. Northern blots for quantification of gene expression related to inflammation

We generated the probes required for detection on Northern blots of a select group of transcripts involved in inflammation: adhesion molecules ICAM-1 and VCAM-1; inducible nitric oxide synthase (iNOS), cyclooxygenase-2 (COX-2), and the inhibitor components of NF-κB complexes, IκBα and IκBβ. The measurements of these mRNAs serve as quantitative parameters for the pharmacological effect of oligodeoxynucleotide drugs. Data have been obtained in the bEnd5 *in vitro* model by treatment with LPS, TNFα and TNFα/LPS as described for NF-κB shift assays. After various times of stimulation, bEnd5 cells grown in 6-well plates were harvested by scraping, lysed in 1% SDS buffer and mRNA was extracted for Northern blotting.

Our first stimulation experiments were carried out with LPS 1μg/ml. The activation patterns changed over the observed time period of 360min, reaching their peak values at 120min. In most cases, after 120min values declined to original values obtained at time 0min. The gene expression was upregulated 7.7-fold for ICAM-1 and 5-fold for VCAM-1 and IκBα. The maximum level for iNOS was reached after 240min (2-fold). Transcripts for COX-2 and IκBβ remained nearly constant. The evaluations were performed by standardization to the signal for the house-keeping gene GAPDH.

LPS

Figure 25: Northern blots of mRNA isolated from bEnd5 cells after sole stimulation with LPS 1μg/ml. Time after stimulation is given on the x-axis. The bar graphs show the ratios relative to time = 0 after standardization to the GAPDH signal. Activation peaks of investigated mRNAs appear at 120min. VCAM-1: The band at lower molecular weight represents the splice variant for the truncated GPI-anchored form (Cybulsky et al. 1993).

In addition to these observations we hybridized TNFα (50ng/ml) stimulated mRNA blots with the same probes and detected different stimulation patterns compared to LPS activation. As shown in **Figure 26** the most obvious differences in stimulation could be measured for ICAM-1 and VCAM-1, suggesting that upregulation of these adhesion molecules is more responsive to TNFα. ICAM-1 could be stimulated by LPS 7.7-fold, by

TNFα about 32-fold and VCAM-1 was activated 5-fold, as compared to a 28-fold elevation by TNFα. Most investigated genes reached their peak levels at the end of the covered time period of 360min.

Results obtained point out a major role of TNFα for upregulation of gene expression involved in inflammatory processes in this brain endothelial cell line.
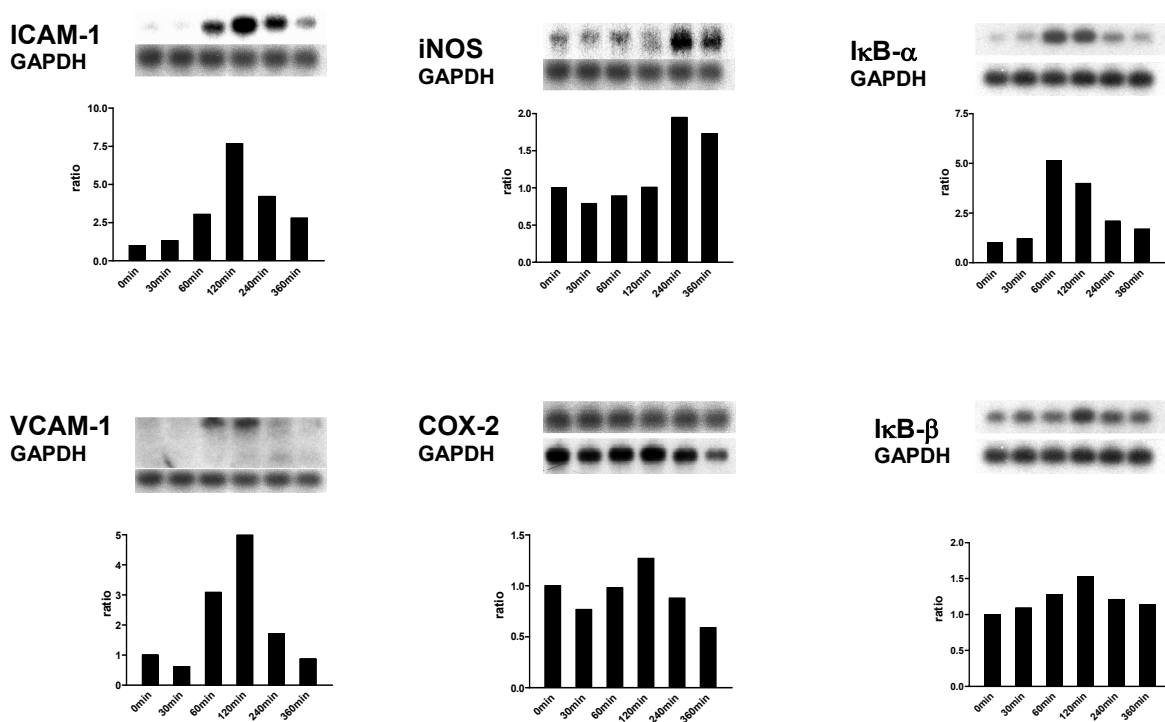
TNF

Figure 26: Northern blots of mRNA isolated from bEnd5 cells after sole stimulation with TNFα 50ng/ml. Time after stimulation is given on the x-axis. The bar graphs show the ratios relative to time = 0 after standardization to the GAPDH signal. An increasing stimulation pattern is shown for almost all mRNAs, reaching their peak levels at 360min (see also **Figure 27** for comparison studies).

Figure 27 depicts the time course found in stimulation experiments with TNFα/LPS in combination. As shown, all messages were increasingly stimulated within the time frame covered in this study (0-360 min) and could compared with results we obtained from Northern blots with sole TNFα activation. The maximum levels of stimulation for the different mRNA species, compared to baseline, ranged from 2-fold (IκBβ) to 40-fold (VCAM-1). The robust signals and the wide dynamic range seen in our experiments confirm that this system is well suited for detecting pharmacological modulations in gene

expression. We expected this selection of gene transcripts to be adequate for monitoring the effects of our NF-κB inhibitor.
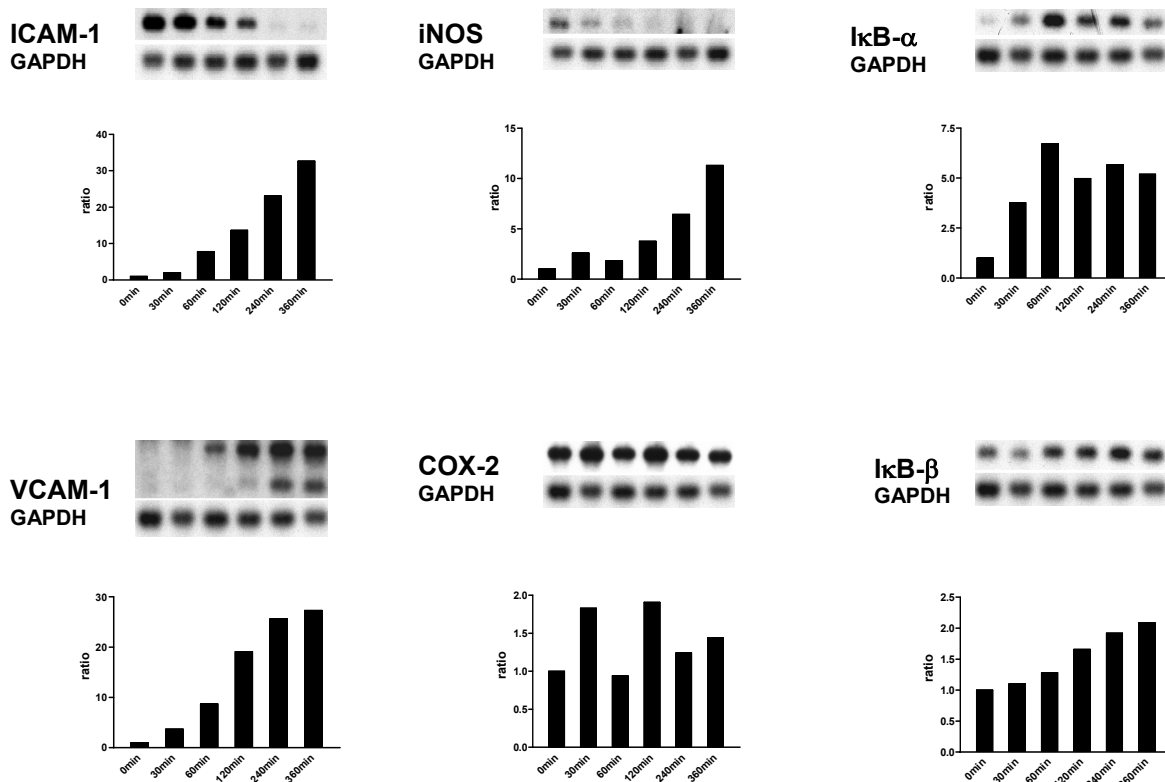
TNF/LPS
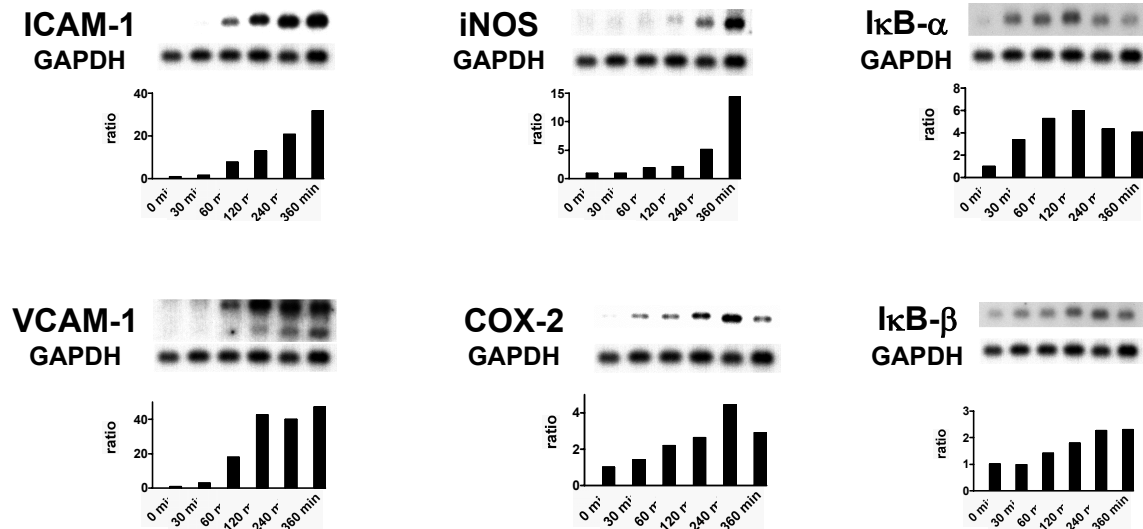
Figure 27: Northern blots of mRNA isolated from bEnd5 cells after stimulation with LPS and TNFα. Time after stimulation is given on the x-axis. The bar graphs show the ratios relative to time = 0 after standardization to the GAPDH signal.

3.3.3. Inhibition of VCAM-1 expression after NF-κB decoy treatment

To further characterize the inhibition of immune response after NF-κB decoy treatment we chose to evaluate the expression patterns of VCAM-1. VCAM-1 shows an abundant expression after stimulation with TNFα (50ng/ml) (see **Figure 26 and 27**).

Moreover, besides the predominant form of VCAM as a seven immunoglobulin domain containing transmembrane protein (Cybulsky et al., 1991), there is a second transcript containing only the first three immunoglobulin domains (Terry et al., 1993). This truncated molecule contains the message for a glycosylphosphatidylinositol (GPI)-anchored form of VCAM-1.

In our experimental studies we investigated the expression patterns of both isoforms in terms of time, concentration of applied oligodeoxynucleotides, and deprivation of FCS. First, we performed all our experiments with the non-targeted conjugate bioPEGPEI/NF-κB at a N/P ratio of 6:1. Our fluorescence microscopy studies revealed uptake of non-targeted complex into bEnd5 cells. However, with this method we could not see any significant difference of uptake between targeted (8D3 MAb) and non-targeted delivery (**Figure 17**). In **Figure 28** the incubation of cells with medium without or with FCS,

respectively, served as a control and was set to 100%. After treatment of bEnd5 cells with our drug over 4h, 12h, 24h or 48h cells were harvested and mRNA of 3 wells of a 6-well plate for each time point was isolated. Northern blot studies were performed and the density of obtained bands was calculated using the Molecular Analyst software (BIORAD). The ratios of VCAM-1 isoform1 and isoform2 were estimated after normalization to the house-keeping gene GAPDH. The concentration of NF-κB decoy applied in these series was 2μM. First, the cells were incubated with decoys as described, then the medium was removed and replaced by fresh medium containing TNFα (50ng/ml) for 4h. No activation of expression without TNFα stimulation was found, neither for isoform1 nor for isoform2. Interestingly, after treatment of cells with bioPEGPEI/NF-κB for 4h we could recognize a slight stimulation of VCAM-1 of about 20% in comparison to our control. After incubation with drug over 12h, 24h, and 48h the expression levels decreased continuously to 5 to 15% of the original value. The expression patterns for the two isoforms were similar, but activation of isoform2 was at a lower level compared to the density of bands for isoform1. We could show that the absence or presence of FCS from the medium had no influence on the ability of drug to reduce the TNFα-dependent activation.
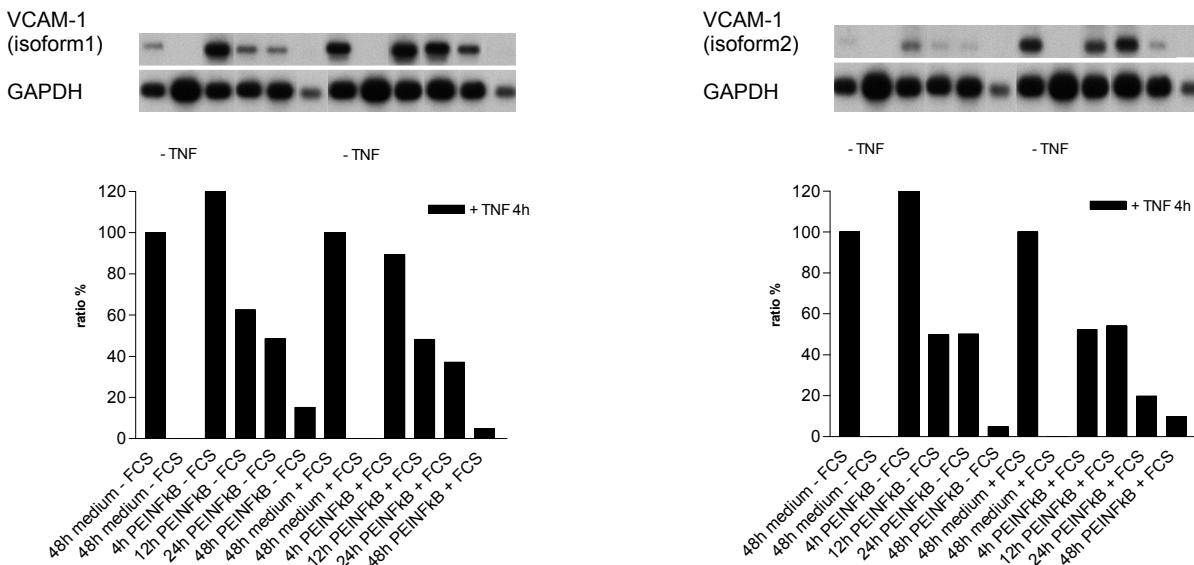
Figure 28: Northern blot experiments performed under addition of bioPEGPEI/NF-κB drug to medium for several incubation times of 4h, 12h, 24h, and 48h. Incubation of bEnd5 cells with medium +/-10% FCS and +/-TNFα (50ng/ml) served as starting points for treatment studies. Expression patterns of VCAM-1 isoform1 and isoform2 are described in two separate diagrams. On the x-axis treatment and incubation times are shown, the y-Axis describes the percentage of activation compared to the original value (100%). ratio = VCAM-1/GAPDH.

As the second part of our investigations we performed concentration-effect studies using 0.1μM, 0.5μM, 1μM, 2μM, and 5μM of NF-κB complexed with bioPEGPEI (N/P = 6:1). The experiments were carried out with FCS deprived medium. (see **Figure 29**). bEnd5 cells were incubated for 24h. At this time point we saw a significant inhibition of activation by bioPEGPEI/NF-κB. Surprisingly, after incubation of cells with 0.1μM and 0.5μM of oligodeoxynucleotide a slight increase, up to 40% for isoform1 and 20% for isoform2 at a concentration of 0.1μM, was detected, decreasing to 20% for isoform1 and 3% for isoform2 of the original value after incubation with 5μM of NF-κB decoy. The signals for isoform2 were weaker than the signals for isoform1 as already seen in **Figure 28**.

Figure 29: Evaluation of concentration curves using bioPEGPEI/NF-κB 6:1 with different concentrations of NF-κB of 0.1μM, 0.5μM, 1μM, 2μM, and 5μM at a time point of 24h. Incubation of bEnd5 cells with medium without FCS and +/-TNFα (50ng/ml) served as starting points for treatment studies. Expression patterns of VCAM-1 isoform1 and isoform2 are described in two separate diagrams. On the x-axis treatment and incubation times are shown, the y-Axis describes the percentage of activation compared to the original value (100%). ratio = VCAM-1/GAPDH. Results represent one of two experiments carried out with similar treatment.

Repeating experiments with similar formulation of a question were carried out to control a possible toxic effect leading to an activation of VCAM-1 expression by bioPEGPEI/NF-κB or NF-κB alone without TNFα activation **Figure 30**. Concentrations of 0.1μM were chosen, because of their stimulating effects seen in the previous studies. Neither bioPEGPEI/NF-κB nor NF-κB showed any activating effect when applied without

following TNFα activation, suggesting no toxic effect of bioPEGPEI or NF-κB at this concentration. The expression values of different oligodeoxynucleotide concentrations behaved similar to values seen in **Figure 29**. Concentrations of 5μM were able to completely suppress activation of VCAM-1 isoforms.

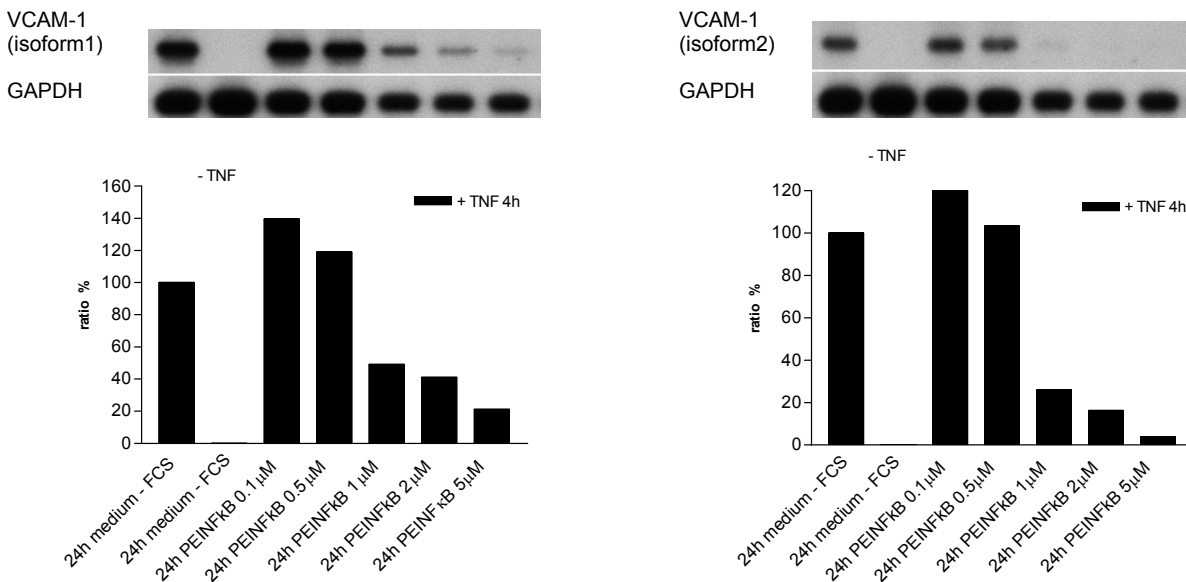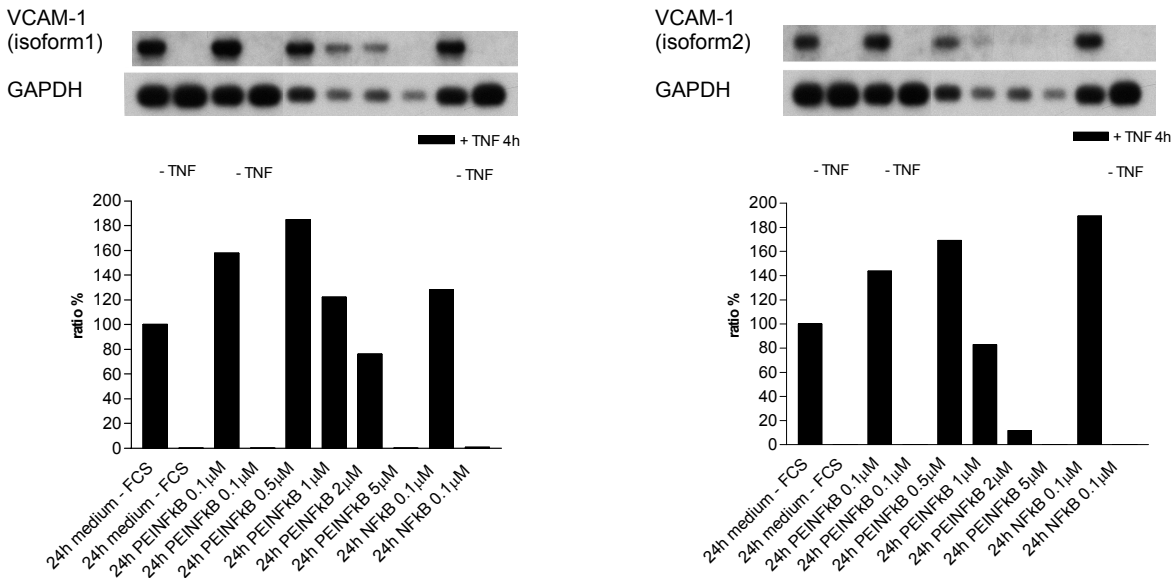**Figure 30:** Evaluation of concentration curves using bioPEGPEI/NF-κB 6:1 with different concentrations of NF-κB of 0.1μM, 0.5μM, 1μM, 2μM, and 5μM at a time point of 24h. Incubation of bEnd5 cells with medium without FCS and +/-TNFα (50ng/ml) served as starting points for treatment studies. In addition, for studies of toxic effects cells were treated with 0.1μM NF-κB complexed with bioPEGPEI or NF-κB alone. Expression patterns of VCAM-1 isoform1 and isoform2 are described in two separate diagrams. On the x-axis treatment and incubation times are shown, the y-Axis describes the percentage of activation compared to the original value (100%). ratio = VCAM-1/GAPDH. Results represent one of two experiments carried out with similar treatment.

In our next studies the bioPEGPEI/NF-κB (6:1) complex was conjugated with the 8D3 anti-transferrin receptor MAb to compare uptake seen in preliminary experiments and using the targeted vector **Figure 31**. The 8D3 streptavidin conjugate was incubated with bioPEGPEI/NF-κB for 15min for coupling and bEnd5 cells were treated as described above. We depicted early time points (8h) and concentrations of 0.5μM and 1μM to show significant differences in inhibition patterns. For VCAM-1 isoform1 a reduction of expression at a concentration of NF-κB decoy of 0.5μM was seen for the targeted delivery – 117% 0.5μM bioPEGPEI/NF-κB, and 60% 0.5 μM 8D3SAbioPEGPEI/NF-κB compared to the original value set to 100%. This was a difference of 57%. The same

picture was observed for a concentration of 1μM NF-κB – 107% bioPEGPEI/NF-κB, and 53% 1μM 8D3SAbioPEGPEI/NF-κB – a difference of 54%. For VCAM-1 isoform2 a stronger inhibition could be reached. However, the differences between targeted and non-targeted delivery were less distinct than for isoform1. With bioPEGPEI/NF-κB 0.5μM an inhibition to 58% was reached, compared to 31% for the vector-mediated delivery (difference 27%). For concentrations of 1μM bioPEGPEI/NF-κB an inhibition to 50% could be shown compared to 27% for the targeted delivery (difference 23%). Even incubation of bEnd5 cells with NF-κB decoy concentrations of 5μM under the same conditions did not reveal a reduction of activation comparable to the tissue directed delivery.
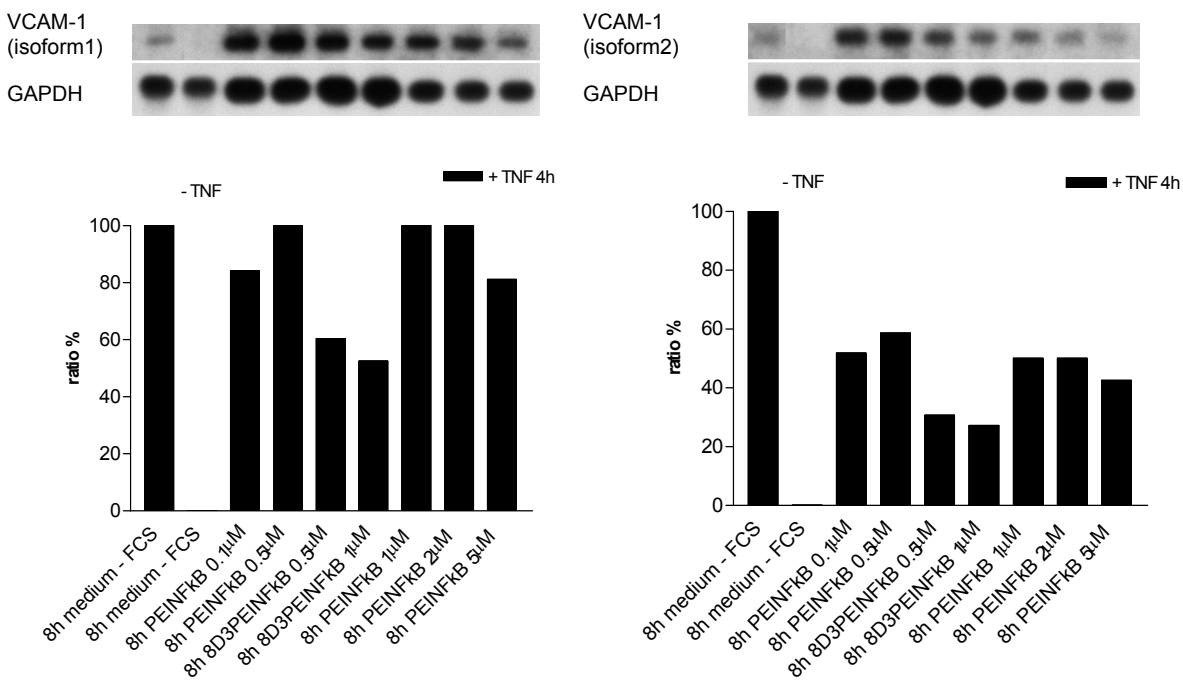
Figure 31: Influence of targeted delivery with 8D3SAbioPEGPEI/NF-κB complex at concentrations of 0.5μM and 1μM compared to non-targeted delivery at the same or higher concentrations after 8h of incubation. Incubation of bEnd5 cells with medium without FCS and +/- TNFα (50ng/ml) served as starting points for treatment studies. Expression patterns of VCAM-1 isoform1 and isoform2 are described in two separate diagrams. On the x-axis treatment and incubation times are shown, the y-Axis describes the percentage of activation compared to the original value (100%). ratio = VCAM-1/GAPDH.

3.4.   i.v. pharmacokinetics of bioPEGPEI/NF-κB and 8D3SA-bioPEGPEI/ NF-κB

In order to investigate the pharmacological behavior of bioPEGPEI/NF-κB after i.v. injection into BALB/c mice, we labeled NF-κB decoy with ^{3}H and added non-labeled ODN for complex formation at different N/P ratios. Complexes with and without vector were injected into the jugular vein and blood samples were collected from 25sec to 60min to determine the plasma concentration time course.

Figure 32 shows the plasma concentration time course and TCA precipitability of the various tracers in the corresponding plasma samples. All plasma concentrations represent only the TCA precipitable fraction. They were fitted with a bi-exponential disposition function. The initial, rapid distribution phase (α-phase) is characterized by half lives between 1.9min and 3min. During that phase (until approximately 10 min after injection) the plasma concentrations in all groups declined by one order of magnitude or more from their initial values at t = 0. Plasma concentrations in the following β-phase (also called elimination phase) are low and contribute only a minor fraction to the area under the curve (AUC). The AUC is the most relevant parameter from the viewpoint of drug delivery, because its value represents the concentration of a drug in the circulation, which is available for transport into organs (e.g., brain). **Table 6** gives the AUC over the sampling period (0-60 min) as calculated for the different groups. Variance analysis revealed that the complex with bioPEGPEIODN at N/P ratio of 6:1 had a significantly higher AUC (by a factor of 2) compared to the other complexes (N/P = 3:1 or 10:1) and to free oligodeoxynucleotide. The conjugate of the 6:1 complex with the vector, 8D3SA, decreased its AUC.

The results of the TCA precipitation indicated rapid degradation of the labeled NF-κB decoy in the circulation. By 30 min and 60 min, the precipitable fraction had decreased to less than 50% and 25%, respectively, in all groups. Compared to free ODN, complex formation with bioPEGPEI improved metabolic stability moderately, as seen for the 3:1 and 6:1 complexes.
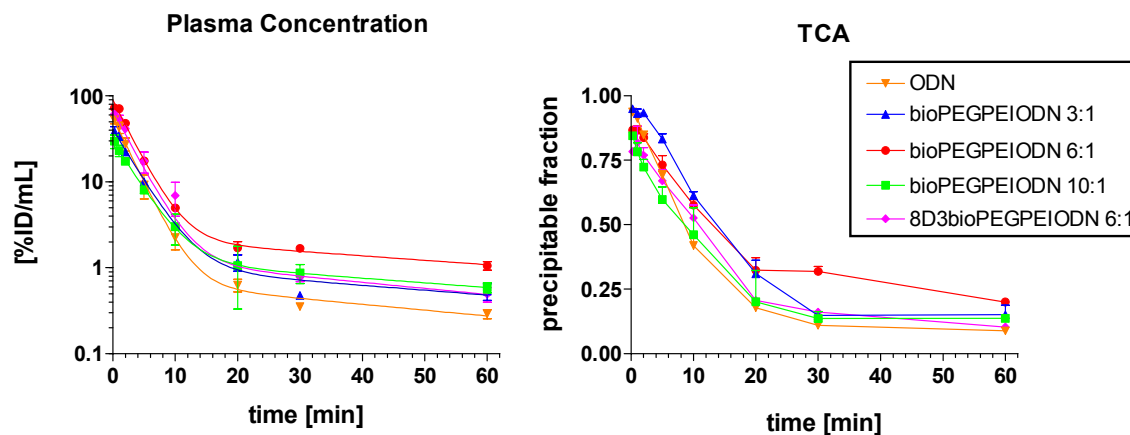
Figure 32: Comparison of AUCs (area under the plasma curve) of bioPEGPEI/NF-κB complexed with different amino to phosphate ratios after i.v. bolus injection into the jugular vein of a BALB/c mouse. On the x-axis the blood sampling times are plotted, on the y-axis the log of plasma concentration values is shown.

	ODN	bioPEGPEI/ ODN N/P=3:1	bioPEGPEI/ ODN N/P=6:1	bioPEGPEI/ ODN N/P=10:1	8D3SAbioPEGPEI/ ODN N/P=6:1
AUC$_{(0 - 60min)}$ [% ID · min/ml]	185 ± 33	183 ± 11	364 ± 8*	160 ± 16	255 ± 19*
% of control (NF-κB decoy)	100	99	197	86	138

Table 6: Comparison of pharmacokinetic parameters of free ODN, bioPEGPEI/ODN at different N/P ratios and 8D3SA-bioPEGPEI/ODN at a N/P ratio of 6:1. AUC – area under the plasma curve; calculated by nonlinear regression fitting to a bi-exponential disposition function (WinNonlin).
*significantly different with $p < 0.05$

4.   Discussion

All studies performed during the present dissertation are embedded in an ongoing effort to improve targeted DNA delivery using non-viral vectors, specifically the cationic polymer polyethylenimine (PEI). PEI and DNA form polyplexes, which are intensively studied as non-viral gene delivery vehicles, efficiently transfect plasmid DNA or oligodeoxynucleotides (ODNs) into a variety of cells and enable nuclear translocation of DNA. We used the rat anti mouse monoclonal antibody 8D3 for targeting of these polyplexes, to transferrin receptors. The streptavidin-biotin technology was applied for coupling of polyplex and vector. Synthesis and pharmacokinetic properties of 8D3-SA were thoroughly evaluated. A custom synthesized PEI was utilized, which carries a biotin-PEG moiety in a 1:1 molar ratio. The polyplexes formed with bioPEGPEI and ODN were intensively studied with regard to their physicochemical characteristics. The polyplexes had suitable size and displayed good *in vitro* stability under various conditions, including the presence of plasma.

A brain-derived endothelial cell line (bEnd5) served as an in vitro model of the BBB, because the endothelial cells are the anatomical substrate of the BBB and represent the cellular drug target of our approach. The potential to pharmacologically modify gene expression at the BBB could be of considerable therapeutic interest in a multitude of brain diseases. Here, a phospodiester ODN decoy for the transcription factor NF-κB was used as drug. The decoy ODN should exert its therapeutic effects by occupying the binding site of activated NF-κB, thereby preventing or decreasing the transcription of genes with the κB response element in their promoter and inhibiting inflammatory reactions. EMSA for NF-κB and quantitative Northern blots for inflammatory markers have been established as tools for evaluating pharmacological effects on bEnd5 cells.

Both the binding/uptake of bioPEGPEI/ODN polyplexes by bEnd5 cells and effects on inflammatory markers were analyzed. A complex, concentration and time dependent pattern of stimulation or inhibition by bioPEGPEI/ODN of the TNFα-stimulated expression of mRNA for VCAM-1 was seen. This shows for the first time that PEI-mediated delivery of transcription factor decoys results in pharmacological activity. Notably, a good correlation was found between the increase in cellular uptake mediated by the 8D3-SA vector and the concentration required for inhibition of VCAM-1 gene expression.

Finally, the pharmacokinetic behavior of the free ODN and the polyplexes was studied in mice. Depending on the N/P ratio of the polyplexes, an up to 2-fold increase in plasma AUC of intact ODN was seen in comparison to ODN administered in free form.

4.1.   8D3-SA as vector for drug delivery

The pharmacokinetic results obtained with the 8D3-SA conjugate are well compatible with published data of vectors for drug delivery based on transferrin receptor-antibodies. Particularly, the mouse anti rat monoclonal anti-transferrin receptor antibody OX26 has been widely used in recent years (for a listing see **Table 1**, Introduction). The 8D3 rat anti mouse monoclonal antibody was generated by immunization with a brain-derived endothelial cell line and was subsequently characterized as specific for the TfR (Kissel et al., 1998). It recognizes transferrin receptors in concentrations, which were 10fold lower than the commercially available antibody C2F2 (Kemp et al., 1987; Kissel et al., 1998).

Kissel et al. showed in immunocytochemical studies staining of brain parenchymal endothelial cells only, but not endothelial cells of fenestrated capillaries of the choroid plexus or the circumventricular organs. 8D3 also recognizes TfRs at the blood-testis barrier consisting of the Sertoli cells. In that case endothelial cells remained unstained. Important for its use as a vector for in vivo drug delivery is the fact that 8D3 apparently does not compete for Tf binding sites. This can be concluded from the absence of inhibitory effects on cell proliferation even at high concentrations (Kissel et al., 1998).

It is known that rapidly proliferating cells express a high number of transferrin receptors, such as hepatocytes (Hirose-Kumagai et al., 1984) and erythroblasts (Morgan and Baker, 1988). This abundant expression was also found on endothelial cells of the BBB, showing that the cerebral endothelium has a key role in mediating transport of iron into the cell and into brain, respectively.

The brain uptake of the MAb 8D3 was evaluated by pharmacokinetic studies in mice (Lee et al., 2000). In our studies we compared the recently obtained results for the brain uptake of the 8D3 antibody with the 8D3-SA (streptavidin) conjugate. Coupling of the antibody to streptavidin enables for delivery of biotinylated drugs. The avidin-biotin linker strategy is a well established method, leading to very tight binding because of the binding affinity of $10^{15}[M^{-1}]$ between streptavidin and biotin. The use of the neutral bacterial homolog streptavidin or neutralized avidin is favored over the native cationic avidin due to its extended half life in the circulation, resulting in increased AUC and brain uptake. Because of its charge, cationic avidin is cleared rapidly from the bloodstream by

the liver and kidneys with a half life of less than 1min (Pardridge et al., 1993). A neutral form of avidin has been published (Hiller et al., 1987; Wilchek and Bayer, 1993), which was obtained by removal of the carbohydrate moiety from Asn[17] and neutralization of the residues of basic amino acids within the avidin sequence. Comparative pharmacokinetic experiments in rats performed with neutral avidin-OX26 antibody conjugates and the same conjugates with cationic avidin showed a 5-fold greater AUC for ^{3}H-biotin/neutral avidin-OX26 (Kang and Pardridge, 1994).

The 8D3 antibody demonstrated high uptake into brain tissue of up to 3.1 %ID/g (percent of the injected dose per g). In contrast, the OX26 antibody against the rat transferrin receptor, showed no brain uptake (0.06 ± 0.01 % ID/g), but behaved like a vascular marker in mice. Confirming the receptor-mediated character of BBB transport, saturation at very high doses (1 and 4mg/kg) co-administered with the tracer dose of [125]I-8D3 (approx. 15 µg/kg) could be found (Lee et al., 2000). However, for the intended use as drug delivery vector it is important to point out that 8D3 at a dose of 1 mg/kg still reached a total brain concentration of 2.46 %ID/g, corresponding to an average brain tissue concentration of 4.1 nM (molecular weight of 8D3 = 150kDa) (Lee et al., 2000). Coupling of 8D3 to streptavidin only slightly changed the pharmacokinetic behavior. The amount of the injected dose per gram body weight was 3.1 ± 0.4 %ID/g for the free 8D3 and 2.5 ± 0.3 %ID/g for 8D3-SA. Almost the same results were obtained for the PS products, showing PS values of 3.3 ± 0.1 μl/min^{-1}g^{-1} for the 8D3 antibody and 2.5 ± 0.3 μl/min^{-1}g^{-1} for the 8D3-SA conjugate. The AUC and the volume of distribution remained nearly constant (**Figure 6, Table 5**). These initial *in vivo* experiments provided evidence that the 8D3-SA conjugate can be used as a brain drug transport vector. Moreover, capillary depletion studies performed with this vector showed binding and uptake of 33% of the total brain concentration of vector to the brain capillaries. One hour after bolus injection into BALB/c mice (**Figure 7**). The endothelial cell volume represents only 0.1% of the brain volume, i.e. 1μl/g (Farrell and Pardridge, 1991). Therefore, the local concentration of 8D3-SA conjugate associated with brain microvascular endothelial cells (membrane bound and internalized) can be estimated to be as high as 0.7µM, if an i.v. dose of 25 μg per mouse (1mg/kg body weight) was injected.

To evaluate the ability of the 8D3-SA conjugate for binding/internalization *in vitro*, the endothelioma cell line bEnd5 was used and immunocytochemical and tracer binding studies were performed. To our knowledge no uptake studies of the 8D3 antibody on cultured cells were carried out previously. Immunocytochemical studies showed similar

staining patterns for the free 8D3 antibody and the 8D3-SA conjugate (both at a concentration of 10µg/ml) on bEnd5 cells and confirmed results, which were obtained on cryostat sections of mouse brains (Kissel et al., 1998) (**Figure 8**). The conjugation of streptavidin to this antibody did not influence its binding characteristics. In order to differentiate between binding and internalization of antibody conjugate we used tracer binding experiments in combination with a mild acid wash step to remove all surface associated 8D3. After a 1h incubation of 8D3-SA on bEnd5 cells a binding/uptake of 2.7%/mg protein could be observed. Further studies showed an internalization of ^{3}H-biotin labeled 8D3-SA conjugate to 70% of the cell-associated activity already after 15min of incubation (**Figure 9**). Increasing incubation times up to 60min did not alter the amount of internalized antibody, which is in good agreement with *in vivo* data published by Fishman (Fishman et al., 1987). These authors perfused rat brains with ^{125}I-Tf and reported a receptor-mediated uptake of the labeled protein, rapid over the first 10-15min and approaching a steady-state by 60min. The specificity of uptake was confirmed in our studies by competing the labeled antibody conjugate with a 240fold molar excess of 8D3 by 90%. The mouse anti-rat specific anti transferrin receptor antibody OX26 was not able to compete the binding.

4.2.   Physico-chemical characteristics of the bioPEGPEI/ODN complex and cell uptake

NF-κB decoys complexed by bioPEGPEI served as our biotinylated ligand for the 8D3-SA vector. ODNs with a natural phosphodiester backbone need to be protected against nucleases in plasma for *in vivo* application to prevent degradation. Cationic polymers, especially polyethylenimine (PEI), are widely used as carriers for DNA, due to their ability to form compact complexes (polyplexes) and transfect cells efficiently by adsorptive endocytosis. Polyplexes with other cationic polymers have also been studied intensively for gene transfer, such as polyspermine (Vinogradov et al., 1998), poly-L-lysine (Lollo et al., 2002), polyamidoamine dendrimers (Maksimenko et al., 2003). The very property of these polyplexes, which enables them to undergo absorptive endocytosis, causes the principal problem for prospective *in vivo* use: nonspecific cellular uptake in various organs, particularly liver, spleen, kidney, and lung (Kunath et al., 2002; Merdan et al., 2002a). PEGylation is a modification known from protein-based drugs (Veronese and Harris, 2002) and the liposome field (Papahadjopoulos et al., 1991) to improve pharmacokinetics. In the case of PEI it has been demonstrated to

reduce interactions with plasma proteins and blood cellular elements (Ogris et al., 1999; Vinogradov et al., 1999). For our purposes the linkage of biotin-PEG (MW = 3,400 Da) was performed at a 1:1 molar ratio with the low molecular weight (LMW) PEI (2,700 Da). The linear PEG chain carried a reactive N-hydroxysuccinimide ester group (NHS), which attached to amino groups of PEI. This introduces simultaneously the shielding PEG-group and the coupling moiety, biotin. The synthesis used in our project is a simple one step procedure, taking advantage of the commercially available biotin-PEG reagent.

We investigated the ability of bioPEGPEI to condense DNA by incubating PEI and NF-κB decoys at different molar N/P ratios in 10mM PBS at pH 7.4 and performing retardation assays (**Figure 11A**) First, this method allowed finding of the N/P ratio where the complete complexation was achieved, and second, the stability of complexes under various incubation conditions could be tested. It should be noted that the method cannot provide the value of the surface charge of a certain complex, which could only be measured exactly by determining the ζ potential.

bioPEGPEI/ODN complexes were formed at N/P ratios from 1:1 to 7:1, and free ODN served as a control. With increasing PEI/DNA ratios the fraction of DNA migrating into the agarose gel was reduced and was not visible at a ratio of 3:1 and above. The detection of ethidium bromide stained DNA in the gel pockets proved the presence of the complex. With increasing N/P ratios the intercalation of ethidium bromide into the DNA is restricted (Bieber et al., 2002), which can be observed by the lack of DNA staining in the pockets at ratios > 4:1. At the N/P ratio of 3:1, where complexation of DNA is just complete as judged from the agarose gel analysis, the interaction between cationic polymer and negatively charged DNA does not yet seem to be very strong, because of detectable free DNA, when these samples were analyzed on a 20% non-denaturating polyacrylamide gel (**Figure 11B**). However, complexes investigated at a ratio of 6:1 and 10:1 gave identical results on either agarose or polyacrylamide gels. With respect to stability issues the addition of 20% human plasma to complexes at a N/P ratio of 6:1 and 10:1 and incubation at 37°C for different time periods (0min to 120min) did not change the stability behavior of complexes (**Figure 11C**).

A similar method was applied to test the ability of the 8D3-SA conjugate to effectively bind the ligand bioPEGPEI/ODN (**Figure 12**). The 8D3-SA conjugate was incubated with bioPEGPEI/ODN at different molar ratios (1/1, 1/3, 1/9, 1/27). A shift of measured radioactivity towards the starting point of electrophoresis compared to antibody-conjugate migration itself revealed a binding of both components. [3]H-8D3-SA peaks and

^{32}P-bioPEGPEI/ODN peaks were counted and radioactivity accumulated in gel slice #7 and #8, respectively (vs. #9 for 8D3-SA alone). Counting the ^{32}P-activity, we observed that increasing molar excess of PEI (e.g. 1/27) caused an accumulation of 8D3SA-bioPEGPEI/ODN in the slice containing the application pocket (**Figure 15**). This could be due to corresponding differences in the shielding of the cationic charge of bioPEGPEI in the polyplex by 8D3-SA. Shielding of surface charges of polyplexes by protein (transferrin) has been described by Kircheis et al. (Kircheis et al., 2001b).

Cell binding and uptake studies were carried out with the brain endothelial cell line bEnd5. The uptake of free ODN, bioPEGPEIODN and 8D3SA-bioPEGPEIODN at an antibody to bioPEGPEI ratio of 1:1 was compared (**Figure 16**). The incubation of free ODN on bEnd5 was used as a negative control. Our tracer uptake studies showed an uptake of only 0.2% of free ODN after 60min of incubation. Due to their phosphate groups oligodeoxynucleotides have a strong negative charge and repelling interaction with the negatively charged cell membrane prevents their uptake into the cell. The positively charged PEI showed higher internalization and increased cellular accumulation in cells due to adsorptive-mediated endocytosis (Ogris et al., 2001). Shielding of PEI with PEG masks the surface charge of the polymer and reduces the non-specific binding to cell membranes (Kircheis et al., 2001a). We observed internalization of complex without 8D3-SA of up to 2%, most likely due to absorptive mediated endocytosis. A 3-fold increase in uptake was achieved by targeting the transferrin receptors on these bEnd5. The overall increase in cellular uptake mediated by the vector and bioPEGPEI compared to free ODN is therefore more than 50-fold after 60 min. For comparison, the group of Kabanov measured *in vitro* uptake of transferrin-targeted PEGPEI/ODN by various carcinoma cells and reported an 80-fold enhancement after 6h in the uptake of fluorescent labeled phosphorothioate antisense ODN compared to PEGPEI/ODN complexes without transferrin (Vinogradov et al., 1999).

We extended our uptake experiments with a fluorescence microscopy study on bEnd5 cells, which revealed no uptake of free ODN ($0.5\mu M$ or $2\mu M$) during time periods up to 8h. In contrast, uptake of bioPEGPEI/ODN complexes was readily detected. The cells displayed a staining of the plasma membranes after 30min and clearly visible staining of the nuclei after 8h of incubation, suggesting an endosomal escape of DNA or complexed DNA, respectively (**Figure 17**). Our results with the doublestranded ODN decoy fit well with studies in which plasmid DNA or synthetic ribozymes were used. Pollard and colleagues (Pollard et al., 1998) investigated the transport of naked and PEI-complexed

plasmid DNA into the nucleus. They reported a hardly detectable nuclear uptake of naked DNA compared to PEI associated DNA after direct injection into the cytoplasm of various mammalian cell lines. Recently Bieber et al. (2002) showed colocalization of plasmid DNA complexed with PEI in perinuclear granular structures at 3-5h after transfection of cells using confocal laser scanning microscopy. Merdan et al. (2002b) used confocal laser scanning microscopy on living cells to demonstrate endosomal release and nuclear uptake of a fluorescently labeled ribozyme, which was also delivered to cells as a PEI complex.

The physico-chemical characterization of bioPEGPEI/ODN polyplexes was expanded by size measurements at different N/P ratios using dynamic light scattering. The size of a cationic complex strongly depends on the N/P ratio, and modification of polymer and buffer, in which the complex was formed. Complex formation was carried out in 10mM PBS at pH 7.4 at N/P ratios from 3:1 to 60:1 (**Figure 17**). Notably, there were no major changes in size observed over the range of N/P ratios. At a ratio of 3:1 complex sizes started at about 130nm and remained stable over a time period of at least one week. Complexes slightly smaller (about 120nm) were observed at a ratio of 6:1 with a narrower Gaussian distribution than obtained for 3:1 complexes. These results suggest a tighter condensation between DNA and PEI at a ratio of 6:1. Even for 60:1 complexes complex sizes were estimated at 160-200nm. The reason for the stability in complex sizes may be that the effect of the PEG moiety offsets the increasing N/P ratio, which would otherwise cause complexes to be more compact. Ogris and colleagues reported that there is a tendency for aggregation of non-modified complexes at low N/P ratios near electroneutrality. This aggregation can be prevented by increasing of N/P ratio > 6:1 or higher (Ogris et al., 1998). PEGylation has also been shown to have an influence on aggregation characteristics of PEI. PEG exerts its effects by its nonionic water-soluble chains (Vinogradov et al., 1998). The stabilizing effect of PEG was confirmed in our studies, even at low N/P ratios we observed constant size measurements over extended time periods.

The coupling of the 8D3-SA conjugate to bioPEGPEI/NF-κB at a molar 8D3SA/bioPEGPEI ratio of 1:1 increased the particle size by about 40nm to 160nm (**Figure 19**), which was stable for at least 24h. The same experiments carried out in complete DMEM medium without FCS showed a size of 160nm for bioPEGPEI/ODN complexes after 10min of incubation, increasing over time to 280nm after one week due to additional salt binding to the complex (**Figure 20**). Size measurements in the

presence of serum or plasma proteins would be desirable, however these are notoriously difficult with dynamic light scattering. The presence of lipoprotein particles and macromolecules interferes with the signal and requires multimodal size analysis, which is prone to artifacts.

A combination of stability tests, consisting of ultrafiltration and TCA precipitation, was used to investigate the behavior of bioPEGPEI/DNA complexes after incubation in 10mM PBS at pH 7.4 or in cell culture medium (DMEM+ with 10% FCS) for periods up to 24h at 37°C (**Figure 21**). The complex was TCA precipitable to nearly 100% (in PBS) and 88% (in DMEM+ with 10% FCS) directly after labeling, proving the initial integrity of bioPEGPEI/ODN. When PBS was used as the incubation medium, 100% of free ODN passed through the filtration membrane, as opposed to complete retention of bioPEGPEI/ODN. In the case of DMEM+ with 10% FCS as the incubation medium for free ODN, still 70% passed through the membrane, suggesting only minor plasma protein binding. A 24h incubation in either PBS or DMEM+ with FCS did not increase the filterable fraction to more than 3.4%, and the stability was confirmed by TCA precipitation studies. Interestingly, results obtained for incubation of bioPEGPEI/DNA complex on bEnd5 cells for the same periods showed a different picture (**Figure 22**). The filterable ^{32}P radioactivity after 24h incubation of complexes on cells was almost the same as the filterable fraction of free ODN in medium with serum. This clearly indicates a gradual decay of the complexes in the presence of cells. Moreover, the low TCA precipitability of 34% after 24h also shows susceptibility to metabolic degradation. A potential explanation of this behavior could be the observation that cationic polyplexes interact with negatively charged cell surface proteoglycans (Mislick and Baldeschwieler, 1996), and the interaction could disrupt the complexes over time.

4.3. NF-κB gel shift assays for analysis of activation pattern after stimulation with LPS/TNFα or LPS

The starting point of our investigations on the induction of an inflammatory response *in vitro* was the activation of the transcription factor NF-κB by TNFα and LPS. Signals generated by ligand receptor interactions at the plasma membrane ultimately cause an alteration of gene expression of effector molecules, such as cytokines and adhesion molecules (Ghosh and Karin, 2002; Ghosh et al., 1998). In its resting state, NF-κB is associated with its inhibitory component IκB in cytoplasm. After receptor activation, an

IκB kinase (IKK) complex is responsible for phosphorylation of IκB. IκB is then specifically ubiquitinated, dissociates from NF- κB and is digested by the proteasome. The free dimeric NF-κB translocates into the nucleus.

In recent years efforts have been made to inhibit the NF-κB pathway at different levels of activation. Specific inhibition of NF-κB was initially explored in studies with IκBα mutants (Baldwin, 1996; Ghosh et al., 1998) lacking the ability for phosphorylation and degradation by the proteasome. However, a therapeutic use would require the transfection of cells with genes coding for dominant negative IκB mutants (Yamamoto and Gaynor, 2001).

Alternatively, the transcription factor decoy approach could be a viable strategy for clinical use (Dzau, 2002). ODN decoys for NF-κB have recently been evaluated in human brain derived endothelial cell culture by Hess et al. (2000) with the goal to inhibit inflammatory reactions associated with brain ischemia/reperfusion. The murine brain derived bEnd5 cells, which we chose, have been previously utilitized for lymphocyte transmigration assays, and their expression of adhesion molecules has been measured (Laschinger and Engelhardt, 2000). Because the activation pattern of NF-κB has not been studied before in bEnd5, we wanted to demonstrate first its stimulation in nuclear extracts using EMSA.

We could show that NF-κB was constitutively active at low levels under control conditions, and that the signals increased strongly after 1min and 5min of TNFα/LPS stimulation. A second peak of activity appeared after 60min to 120min (**Figure 23**). Similar time courses of NF-κB activation have been reported in another tissue (pancreas acini) (Gukovsky et al. 1998) and in different cell lines (Hoffmann et al., 2002) and were attributed to a differential degradation of IκBα and IκBβ. The inflammatory stimuli used here, were in the range commonly applied, for example the LPS concentrations of 1μg/ml for stimulation correspond to a study with HUVEC by Madan et al. (2000). Similarly, TNFα concentrations of 50ng/ml were in the range of 10-100ng/ml as used by others (Botella et al., 2000; Madan et al., 2000).

NF-κB gel shift assays after LPS stimulation alone showed a different, monophasic stimulation pattern, with increasing activity after 5min and peak activity after 10min, and a gradual decline from 30 to 120min (**Figure 24**).

4.4.   mRNA expression of inflammatory markers after LPS, TNFα, and LPS/TNFα stimulation

The gene expressions of IκBα and IκBβ, of adhesion molecules, such as VCAM-1 and ICAM-1, and of enzymes involved in inflammatory reactions (COX-2, iNOS) gives us a read-out suitable for quantitative evaluation of pharmacological effects at the cellular level. Therefore, the time course of mRNA expression for these markers after defined stimuli (LPS, TNFα, and a combination of LPS/TNFα) was established. bEnd5 cells were treated over a time frame of 360min and the extent and the profile of up-regulation of markers was compared.

Due to its role as a negative feedback regulator, measurements of IκBα at the mRNA or protein level can be used as surrogate markers of activity of the NF-κB system. This has also been applied to brain microvessel endothelial cells in situ (Quan et al., 1997; Laflamme and Rivest, 1999). In our Northern blots (**Figures 25-27**) we could see robust stimulation of IκBα expression. TNFα and the combination TNFα/LPS stimulated the message earlier (by 30 min) and stronger than LPS alone. Interestingly, the mRNA of IκBβ was also significantly increased at later time points (120min and later) under TNFα and TNFα/LPS treatment, but not under LPS alone. Because the promoter for IκBβ lacks a κB element, it is generally assumed that IκBβ is not subject to regulation by NF-κB (Hoffmann et al., 2002). The pattern of upregulation of both isoforms, IκBα and IκBβ, in bEnd5 cells has recently been fully confirmed in our lab by real time RT-PCR measurements of these messages. However, a confirmation at the protein level will also be required (Western blots of cytosolic and nuclear extracts), and these studies are currently in progress.

In MS the recruitment of autoaggressive T lymphocytes from the blood across the BBB is mediated through interactions of adhesion molecules (ICAM-1, VCAM-1) on the endothelial cells and their counterparts LFA-1 and VLA-4, respectively, on lymphocytes. After passing the endothelial barrier T-lymphocytes may encounter CNS myelin antigens, which results in stimulation of helper T lymphocytes, lymphocyte proliferation, macrophage activation, and cytokine secretion.

We found on our bEnd5 cells under control conditions that ICAM-1 mRNA is present at low levels, which is in good agreement with published data (Dietrich, 2002; van de Stolpe and van der Saag, 1996). At the concentrations we used, TNFα (50ng/ml) was a strong and LPS (1μg/ml) was a moderate inducer of ICAM-1. mRNA levels rose

continuously over the covered period of 6h for TNFα, but peaked at 120min under stimulation with LPS. A combination of LPS/TNFα stimulation neither increased the levels obtained after TNFα activation alone, nor changed the stimulation profile, suggesting a predominant role of TNFα in mediating the up-regulation of ICAM-1 under the conditions used here. The same pattern can be reported for the VCAM-1 mRNA.

The increased gene expression observed for iNOS (after LPS and/or TNFα) and COX-2 (after TNFα and LPS/TNFα) corresponded with the data published on neuroinflammtory conditions. In EAE models, mRNA levels for iNOS in brain rise after induction of the disease. It could be shown that the induction of iNOS mRNA coincided with the severity of clinical signs, and in some cases with the presence of inflammatory cells in the brain (Koprowski et al., 1993). Confirming a function of iNOS in the disease process, an amelioration of EAE with a selective inhibitor of the inducible nitric oxide synthase (iNOS) could be achieved (Hooper et al., 1997). Previous studies have also indicated that the prostaglandin producing COX-2 is increased in cerebral endothelial cells of EAE-affected rats, which was closely linked to disease progression (Deininger and Schluesener, 1999).

4.5.   Effect of NF-κB decoy on the expression of VCAM-1

The treatment of bEnd5 cells with the bioPEGPEI/ODN drug (**Figures 28-31**) can be summarized as follows: (a) VCAM-1 mRNA (isoform1 and 2) is downregulated in a time dependent manner by treatment of cells for 4h to 48h before stimulation with TNFα for 4h. (b) The treatment effect was seen in the presence or absence of serum. (c) the polyplex itself (without subsequent TNFα stimulation) did not stimulate VCAM-1 gene expression. (d) A clear dose-response relation over the concentration range $0.1\mu M$ to $5\mu M$ was observed. (e) The vector, 8D3-SA, enhanced the potency by about an order of magnitude ($0.5 \mu M$ with 8D3-SA was more effective than $5 \mu M$ without vector).

These results show for the first time that a phosphodiester ODN decoy delivered by modified PEI has specific pharmacological activity at submicromolar concentrations. Obviously the ODN-drug is able to reach the effect compartment inside the cell (cytosol and/or nucleus) where it can bind to activated NF-κB. Previously, effects with ODN-based drugs after delivery with PEI have only been shown for a phosphorothioate antisense ODN (Vinogradov et al., 1999), and recently for a ribozyme (Aigner et al., 2002). In the first case an antisense ODN to mdr-1 was delivered to human epidermoid

carcinoma cells, and a suppression of p-glycoprotein was seen after 48h of treatment at 0.5μM. The delivery system was based on a biotinylated PEG-PEI coupled to biotinylated transferrin as targeting vector via an avidin bridge. In the second case, an unmodified ribozyme against fibroblast growth factor binding protein (FGF-BP) was delivered with low molecular weight PEI to carcinoma cells in vitro and to tumor xenografts *in vivo*. The ribozyme was active at low concentrations in vitro (0.1-1 μg/mL) and *in vivo* (0.4 mg/kg), but only in complex with PEI, not in free form.

The inhibitory effect on stimulated expression of mRNA for VCAM-1 as observed in the present study is comparable to the effect of interferon-β as recently described by Floris and colleagues (Floris et al., 2002). These authors also utilized brain-derived endothelial cell cultures. Interferon β is the most potent drug currently available for therapy of MS.

Our present results provide preliminary evidence that the proposed hypothesis for a new treatment strategy in neuroinflammatory disease may hold true. Obviously, further detailed studies into the cellular mechanism of action are required. For example, the stimulatory effect on VCAM-1 mRNA seen at low concentrations remains currently unexplained, and the potential of cellular toxicity needs to be investigated over a wider range of concentrations and incubation times. Also, controls of the specifity of the pharmacological activity need to be performed by the use of different, unrelated ODNs (or scrambled sequences) and by analysis of different parameters (e.g. ICAM-1, iNOS, IκBα).

4.6.   Pharmacokinetic characteristics of bioPEGPEI/NF-κB

The interpretation of the results of the pharmacokinetic study can be based on the underlying hypothesis: The complexation of ODN by PEI should prevent the degradation of DNA in the circulation. Moreover, shielding of the DNA/polymer complex with PEG should further improve stability and lead to an increase of the AUC in plasma, equivalent to a decrease in systemic clearance. Here, the effect on oligodeoxynucleotide stability was found to be significant with an increase of AUC by 98% (N/P = 6:1 complex vs. free ODN). Recently, collaborators reported a 62% increase in AUC for PEGylated copolymers with 25kDa PEI (Kunath et al., 2002). However, a direct comparison is not possible, because PEI was radiolabeled in the cited work, and the pharmacokinetic of free ODN could not be measured. Characterizing the elimination of the ODN moiety, as

performed here, may be more relevant with regard to the intended use of these polymer/ODN complexes as drug delivery vehicles for DNA-based drugs.

Despite similar complex sizes in physiological buffer (**Figure 17**), physicochemical differences may be responsible for the lower AUCs observed for the 3:1 and 10:1 complexes compared to the 6:1 complexes. Complexes formed at N/P= 3:1 are just able to completely bind DNA (**Figure 15**) and would be expected to have limited stability in high salt solutions. Complexes at N/P =10:1 have a larger excess of cationic charge compared to the 6:1 complexes, which may be insufficiently shielded by the PEG tails. More cationic particles will interact more strongly with the anionic cell surfaces and would be cleared from the circulation faster.

While there was a significant change in the plasma AUC for the 6:1 complexes versus free ODN, the protection from metabolic breakdown of ODN was limited. The TCA precipitable fractions (**Figure 31**) show that most of the ODN in plasma was degraded within 10-20min. This behavior could not be predicted from the *in vitro* studies. As shown in **Figure 21**, the labeled NF-κB decoy was stable when incubated in cell culture media with plasma addition, and it was fully protected from degradation for at least 1 hour in the presence of endothelial cells. On the other hand, the present *in vivo* results correspond well to recent *in vivo* data with dual labeled complexes of PEGylated PEI (MW=25kDa) and ODN (unpublished data from our laboratory).

Although organs had been sampled from the animals at the end of the 60 min period, evaluations of individual organ uptake were not performed. The fact that the major fraction of plasma radioactivity must be attributed to low molecular weight metabolites (free nucleotides, water) indicated that evaluation of total tissue radioactivity would be meaningless. Detailed analysis of tissue associated radioactivity using DNA extraction and PAGE, will be pweformed in future studies. Modifications of the PEGPEI co-polymer may be required to achieve further improvements in the pharmacokinetic behavior of the polyplexes.

5.   Summary

In this project a vector for drug delivery into brain endothelial cells, consisting of an anti-transferrin receptor antibody and a complex of polyethylenimine (PEI) and an oligodeoxynucleotide (ODN) drug was evaluated. NF-κB decoys are short double-stranded ODNs, which contain a recognition sequence for binding to the transcription factor. By binding to the transcription factor NF-κB they prevent the transcription of several genes involved in inflammatory processes, such as adhesion molecules and pro-inflammatory enzymes. Adhesion molecules promote the transmigration of activated T lymphocytes across the blood-brain barrier (BBB), leading to demyelination of nerve fibers within the brain, as seen in inflammatory diseases like Multiple Sclerosis (MS). Inhibition of lymphocyte transmigration by downregulation of the expression of these genes may be therapeutically beneficial.

The rat anti mouse anti-transferrin receptor antibody 8D3 was purified from hybridoma supernatant and was conjugated to recombinant streptavidin (SA) in order to bind to biotinylated ligands. *In vivo* pharmacokinetics and *in vitro* binding studies were performed to evaluate the 8D3-SA vector. Pharmacokinetic studies showed a comparable half-life and area under the curve (AUC) of antibody conjugate and free 8D3 antibody in plasma. Immunohistochemistry with a brain endothelioma cell line (bEnd5) revealed a similar binding behavior for both, antibody and its streptavidin conjugate. The specificity of uptake of ^{3}H-biotin-8D3SA by bEnd5 cells could be observed in experiments carried out either with an acid wash step to remove all surface bound antibody, or by using the mouse anti rat transferrin receptor antibody OX26.

The biotinylated drug applied in this project was a polymer – polyethylenimine (PEI), which is able to complex a double-stranded 20bp ODN sequence (NF-κB decoy). The low molecular weight PEI (LMW PEI) of 2,700 Da was chosen due to such favorable properties as low cytotoxicity, high transfection efficiency, and narrow size distribution. A co-polymer of PEI and biotinylated PEG was synthesized to allow coupling to the vector. Stability studies were carried out to examine the characteristics of bioPEGPEI/ODN complexes in salt solution, under addition of 10% or 20% plasma, or by incubation of complex in medium over a long time frame. Particle size measurements in PBS pH 7.4 revealed an optimal size distribution of bioPEGPEI/NF-κB complex at a ratio PEI-amine/ODN-phosphate of 6:1 with an average particle size of 120nm, which was stable for at least 1 week. Gel retardation assays also showed a complete complexation of

bioPEGPEI and ODN at this ratio. The addition of 8D3-SA increased the complex size by 40nm.

In vitro pharmacological effects of bioPEGPEI/NF-κB could be observed after treatment of bEnd5 cells with different concentrations of NF-κB decoy over a time frame of 48 hours. An inhibition of VCAM-1 (isoform 1 and 2) expression was already visible after 12 hours with a steady increase of this inhibitory effect to 48 hours. ODN-drug concentrations of 5μM in complex with bioPEGPEI showed a nearly complete suppression of VCAM-1 expression. Coupling of bioPEGPEI/NF-κB decoy to the vector decreased the concentration required for a reduction of VCAM-1 mRNA to 0.5μM - 1μM, suggesting an increase in potency by targeting to the transferring receptor.

Pharmacokinetic studies in mice showed the behavior of bioPEGPEI/NF-κB complexes with different N/P ratios. At a N/P ratio of 6:1 the AUC (area under the plasma curve) could be increased 2-fold compared to free NF-κB. A coupling to the targeting vector did not further change the pharmacokinetic characteristics.

The drug targeting approach investigated in this project promises to be an excellent model for *in vitro* applications. The in vivo administration must be further evaluated with the goal to improve the pharmacokinetic behavior (enhance AUC). This may require additional modifications of the bioPEGPEI copolymer.

6. Zusammenfassung

In diesem Projekt sollte ein Vektor zur "Drug delivery" an Hirnendothelzellen, bestehend aus einem monoklonalen Antikörper gegen den Transferrinrezeptor und einem Komplex aus Polyethylenimin (PEI) / Oligodeoxynukleotid (ODN) untersucht werden. NF-κB "decoys" sind kurze doppelsträngige Oligodeoxynukleotide, welche eine Erkennungssequenz für die Bindung des Transkriptionsfaktors enthalten. Durch die Bindung an den Transkriptionsfaktor NF-κB verhindern sie die Transkription von verschiedenen, in entzündliche Prozesse involvierte Genen. Adhäsionsmoleküle fördern die Transmigration von aktivierten T-Lymphozyten über die Blut-Hirn-Schranke (BHS), die zu Entzündung und zu einer Demyelinisierung von Axonen im Gehirn führt. Dieser Zustand wurde in entzündlichen Erkrankungen wie der Multiplen Sklerose (MS) gesehen. Die Hemmung der Transkription dieser Gene kann durch verminderte Lymphozytentransmigration zu therapeutischen Effekten führen.

Der Ratte-anti-Maus-Antikörper 8D3 gegen den Transferrinrezeptor wurde aus Hybridommedium gereinigt und an Streptavidin gekoppelt, um biotinylierte Liganden binden zu können. Zur Vektoranalyse wurden *in vivo* Pharmakokinetikstudien und *in vitro* Bindungsstudien durchgeführt. Die Pharmakokinetikstudien zeigten eine vergleichbare Halbwertszeit und Fläche unter der Plasmakurve (Area under the plasma curve = AUC) des Antikörperkonjugates und freien 8D3 Antikörpers im Plasma. Immunhistochemie an der Hirnendothelzelllinie bEnd5 zeigte ein ähnliches Bindungsverhalten für den Antikörper und das Streptavidinkonjugat. Die Spezifität der Aufnahme von ^{3}H-Biotin-8D3-SA durch die bEnd5 Zellen wurde in Experimenten bestätigt, die entweder mit einem Säurewaschschritt zur Entfernung aller oberflächengebundenen Antikörper oder durch Anwendung des Maus-anti Ratte-Transferrinrezeptor-Antikörpers OX26 durchgeführt wurden.

Der biotinylierte Ligand, der in diesem Projekt verwendet wurde, war ein Polymer – Polyethylenimin (PEI), das in der Lage ist, eine doppelsträngige 20 Basenpaare lange Sequenz (NF-κB "decoy") zu komplexieren. Das PEI mit niedrigem Molekulargewicht (low molecular weight = LMW PEI) mit 2700Da wurde für dieses Projekt gewählt, weil es durch solche positiven Eigenschaften wie geringe Zytotoxizität, hohe Transfektionsraten und enge Größenverteilung bekannt ist. PEI wurde kovalent mit einem biotinylierten PEG modifiziert, um die Kopplung an den Vector zu ermöglichen.

Wir führten Stabilitätsstudien zur Analyse der Komplexeigenschaften in Salzlösungen unter Zusatz von 10% oder 20% Plasma und Inkubation des Komplexes in Medium über einen längeren Zeitraum durch. Partikelgrößenmessungen in PBS mit einem pH-Wert von 7.4 zeigten eine optimale Größenverteilung des bioPEGPEI/NF-κB-decoy Komplexes mit einem PEI-Amino/ODN-Phosphat (N/P) Verhältnis von 6:1 und eine durchschnittliche Partikelgröße von 120nm, welche für mindestens eine Woche stabil war. Gelretardationsassays zeigten bei diesem N/P-Verhältnis ebenfalls eine vollständige Komplexierung von PEI und ODN. Die Zugabe des 8D3-SA erhöhte die Komplexgröße um 40nm.

Pharmakologische Effekte von bioPEGPEI/NF-κB decoy *in vitro* konnten nach der Behandlung der bEnd5 Zellen mit verschiedenen Konzentrationen der NF-κB "decoys" über einen Zeitrahmen von 48 Stunden beobachtet werden. Eine Hemmung der mRNA für VCAM-1 (Isoform1 und 2) war bereits nach 12 Stunden sichtba,r mit einem stetigen Anstieg des inhibitorischen Effektes bis zu 48 Stunden. Die Pharmakonkonzentrationen von 5μM zeigten eine nahezu vollständige Supprimierung der VCAM-1-Expression. Kopplung des Pharmakons an den Vektor führte zu einer Reduktion der Konzentration auf 0,5μM - 1μM, die zur Hemmung der Genexpression benötigt wird. Diese Ergebnisse sprechen für eine Erhöhung der Potenz des Pharmakon-Komplexes durch "targeting" an den Transferrinrezeptor.

Pharmakokinetikstudien zeigten das Verhalten des bioPEGPEI/NF-κB-Komplexes mit verschiedenen N/P Verhältnissen. Bei einem N/P Verhältnis von 6:1 konnte die AUC im Vergleich zu freiem NF-κB verdoppelt werden. Die Kopplung an den Vektor veränderte die pharmakokinetischen Eigenschaften des Komplexes nicht wesentlich.

Die "drug targeting" Methode, die in diesem Projekt untersucht wurde, stellt ein exzellentes Modell für *in vitro* Anwendungen dar. Weitere Untersuchungen zur *in vivo* Anwendung sind notwendig, mit dem Ziel einer weiteren Verbesserung der pharmakokinetischen Parameter (Erhöhung der AUC). Hierzu können weitere Modifikationen des bioPEGPEI erforderlich sein.

7. Bibliography

Abdallah, B., Hassan, A., Benoist, C., Goula, D., Behr, J. P., and Demeneix, B. A.: A powerful nonviral vector for in vivo gene transfer into the adult mammalian brain: polyethylenimine. Hum Gene Ther **7** (16)**:** 1947-54., 1996.

Ahn, J. D., Morishita, R., Kaneda, Y., Lee, S. J., Kwon, K. Y., Choi, S. Y., Lee, K. U., Park, J. Y., Moon, I. J., Park, J. G., Yoshizumi, M., Ouchi, Y., and Lee, I. K.: Inhibitory effects of novel AP-1 decoy oligodeoxynucleotides on vascular smooth muscle cell proliferation in vitro and neointimal formation in vivo. Circ Res **90** (12)**:** 1325-32, 2002.

Albeck, D. S., Backman, C., Veng, L., Friden, P., Rose, G. M., and Granholm, A.: Acute application of NGF increases the firing rate of aged rat basal forebrain neurons. Eur J Neurosci **11** (7)**:** 2291-304, 1999.

Albeck, D. S., Hoffer, B. J., Quissell, D., Sanders, L. A., Zerbe, G., and Granholm, A. C.: A non-invasive transport system for GDNF across the blood-brain barrier. Neuroreport **8** (9-10)**:** 2293-8, 1997.

Al-Omaishi, J., Bashir, R., and Gendelman, H. E.: The cellular immunology of multiple sclerosis. J Leukoc Biol **65** (4)**:** 444-52, 1999.

Azmin, M. N., Stuart, J. F., and Florence, A. T.: The distribution and elimination of methotrexate in mouse blood and brain after concurrent administration of polysorbate 80. Cancer Chemother Pharmacol **14** (3)**:** 238-42, 1985.

Backman, C., Biddle, P. T., Ebendal, T., Friden, P. M., Gerhardt, G. A., Henry, M. A., Mackerlova, L., Soderstrom, S., Stromberg, I., Walus, L., and et al.: Effects of transferrin receptor antibody-NGF conjugate on young and aged septal transplants in oculo. Exp Neurol **132** (1)**:** 1-15, 1995.

Backman, C., Rose, G. M., Hoffer, B. J., Henry, M. A., Bartus, R. T., Friden, P., and Granholm, A. C.: Systemic administration of a nerve growth factor conjugate reverses age-related cognitive dysfunction and prevents cholinergic neuron atrophy. J Neurosci **16** (17)**:** 5437-42, 1996.

Baeuerle, P. A., and Baichwal, V. R.: NF-kappa B as a frequent target for immunosuppressive and anti-inflammatory molecules. Adv Immunol **65:** 111-37, 1997.

Baeuerle, P. A., and Baltimore, D.: NF-kappa B: ten years after. Cell **87** (1)**:** 13-20, 1996.

Baeuerle, P. A., and Henkel, T.: Function and activation of NF-kappa B in the immune system. Annu Rev Immunol **12:** 141-79, 1994.

Baldwin, A. S., Jr.: The NF-kappa B and I kappa B proteins: new discoveries and insights. Annu Rev Immunol **14:** 649-83, 1996.

Baldwin, D. A., De Sousa, D. M., and Von Wandruszka, R. M.: The effect of pH on the kinetics of iron release from human transferrin. Biochim Biophys Acta **719** (1)**:** 140-6, 1982.

Barger, S. W., Horster, D., Furukawa, K., Goodman, Y., Krieglstein, J., and Mattson, M. P.: Tumor necrosis factors alpha and beta protect neurons against amyloid beta-peptide toxicity: evidence for involvement of a kappa B-binding factor and attenuation of peroxide and Ca2+ accumulation. Proc Natl Acad Sci U S A **92** (20)**:** 9328-32, 1995.

Beg, A. A., and Baldwin, A. S., Jr.: The I kappa B proteins: multifunctional regulators of Rel/NF-kappa B transcription factors. Genes Dev **7** (11)**:** 2064-70, 1993.

Begley, D. J.: The blood-brain barrier: principles for targeting peptides and drugs to the central nervous system. J Pharm Pharmacol **48** (2)**:** 136-46, 1996.

Behl, C., Davis, J. B., Klier, F. G., and Schubert, D.: Amyloid beta peptide induces necrosis rather than apoptosis. Brain Res **645** (1-2)**:** 253-64, 1994.

Behr, J. P.: Systemic linear polyethylenimine (L-PEI)-mediated gene delivery in the mouse. J Gene Med **2** (2)**:** 128-34, 2000.

Beltinger, C., Saragovi, H. U., Smith, R. M., LeSauteur, L., Shah, N., DeDionisio, L., Christensen, L., Raible, A., Jarett, L., and Gewirtz, A. M.: Binding, uptake, and intracellular trafficking of phosphorothioate-modified oligodeoxynucleotides. J Clin Invest **95** (4)**:** 1814-23, 1995.

Bennett, C. F., Chiang, M. Y., Chan, H., Shoemaker, J. E., and Mirabelli, C. K.: Cationic lipids enhance cellular uptake and activity of phosphorothioate antisense oligonucleotides. Mol Pharmacol **41** (6)**:** 1023-33, 1992.

Benns, J. M., Mahato, R. I., and Kim, S. W.: Optimization of factors influencing the transfection efficiency of folate-PEG-folate-graft-polyethylenimine. J Control Release **79** (1-3)**:** 255-69, 2002.

Bickel, U., Kang, Y. S., and Pardridge, W. M.: In vivo cleavability of a disulfide-based chimeric opioid peptide in rat brain. Bioconjug Chem **6** (2)**:** 211-8, 1995.

Bickel, U., Kang, Y. S., Yoshikawa, T., and Pardridge, W. M.: In vivo demonstration of subcellular localization of anti-transferrin receptor monoclonal antibody-colloidal gold conjugate in brain capillary endothelium. J Histochem Cytochem **42** (11)**:** 1493-7, 1994a.

Bickel, U., Yamada, S., and Pardridge, W. M.: Synthesis and bioactivity of monobiotinylated DALDA: a mu-specific opioid peptide designed for targeted brain delivery. J Pharmacol Exp Ther **268** (2)**:** 791-6, 1994b.

Bickel, U., Yoshikawa, T., Landaw, E. M., Faull, K. F., and Pardridge, W. M.: Pharmacologic effects in vivo in brain by vector-mediated peptide drug delivery. Proc Natl Acad Sci U S A **90** (7)**:** 2618-22, 1993.

Bickel, U., Yoshikawa, T., and Pardridge, W. M.: Delivery of peptides and proteins through the blood-brain barrier. Adv Drug Deliv Rev **46** (1-3)**:** 247-79, 2001.

Bieber, T., Meissner, W., Kostin, S., Niemann, A., and Elsasser, H.: Intracellular route and transcriptional competence of polyethylenimine- DNA complexes. J Control Release **82** (2-3)**:** 441., 2002.

Bielinska, A., Shivdasani, R. A., Zhang, L. Q., and Nabel, G. J.: Regulation of gene expression with double-stranded phosphorothioate oligonucleotides. Science **250** (4983)**:** 997-1000, 1990.

Bjorbaek, C., Elmquist, J. K., Michl, P., Ahima, R. S., van Bueren, A., McCall, A. L., and Flier, J. S.: Expression of leptin receptor isoforms in rat brain microvessels. Endocrinology **139** (8)**:** 3485-91, 1998.

Blessing, T., Kursa, M., Holzhauser, R., Kircheis, R., and Wagner, E.: Different strategies for formation of pegylated EGF-conjugated PEI/DNA complexes for targeted gene delivery. Bioconjug Chem **12** (4)**:** 529-37, 2001.

Bodor, N., and Simpkins, J. W.: Redox delivery system for brain-specific, sustained release of dopamine. Science **221** (4605)**:** 65-7, 1983.

Boletta, A., Benigni, A., Lutz, J., Remuzzi, G., Soria, M. R., and Monaco, L.: Nonviral gene delivery to the rat kidney with polyethylenimine. Hum Gene Ther **8** (10)**:** 1243-51, 1997.

Borst, P., Schinkel, AH: Introduction to the Blood-Brain Barrier : Methodology, Biology and Pathology, Cambridge University Press, Cambridge, 1998.

Botella, L. M., Puig-Kroger, A., Almendro, N., Sanchez-Elsner, T., Munoz, E., Corbi, A., and Bernabeu, C.: Identification of a functional NF-kappa B site in the platelet endothelial cell adhesion molecule-1 promoter. J Immunol **164** (3)**:** 1372-8, 2000.

Boussif, O., Lezoualc'h, F., Zanta, M. A., Mergny, M. D., Scherman, D., Demeneix, B., and Behr, J. P.: A versatile vector for gene and oligonucleotide transfer into cells in culture and in vivo: polyethylenimine. Proc Natl Acad Sci U S A **92** (16)**:** 7297-301., 1995.

Bragonzi, A., Boletta, A., Biffi, A., Muggia, A., Sersale, G., Cheng, S. H., Bordignon, C., Assael, B. M., and Conese, M.: Comparison between cationic polymers and lipids in mediating systemic gene delivery to the lungs. Gene Ther **6** (12)**:** 1995-2004., 1999.

Charles, V., Mufson, E. J., Friden, P. M., Bartus, R. T., and Kordower, J. H.: Atrophy of cholinergic basal forebrain neurons following excitotoxic cortical lesions is reversed by intravenous administration of an NGF conjugate. Brain Res **728** (2)**:** 193-203, 1996.

Chavany, C., Le Doan, T., Couvreur, P., Puisieux, F., and Helene, C.: Polyalkylcyanoacrylate nanoparticles as polymeric carriers for antisense oligonucleotides. Pharm Res **9** (4)**:** 441-9, 1992.

Chemin, I., Moradpour, D., Wieland, S., Offensperger, W. B., Walter, E., Behr, J. P., and Blum, H. E.: Liver-directed gene transfer: a linear polyethlenimine derivative mediates highly efficient DNA delivery to primary hepatocytes in vitro and in vivo. J Viral Hepat **5** (6)**:** 369-75, 1998.

Chen, Z. J., Parent, L., and Maniatis, T.: Site-specific phosphorylation of IkappaBalpha by a novel ubiquitination-dependent protein kinase activity. Cell **84** (6)**:** 853-62, 1996.

Chollet, P., Favrot, M. C., Hurbin, A., and Coll, J. L.: Side-effects of a systemic injection of linear polyethylenimine-DNA complexes. J Gene Med **4** (1)**:** 84-91, 2002.

Claudio, L., Kress, Y., Norton, W. T., and Brosnan, C. F.: Increased vesicular transport and decreased mitochondrial content in blood-brain barrier endothelial cells during experimental autoimmune encephalomyelitis. Am J Pathol **135** (6)**:** 1157-68, 1989.

Collins, T., Read, M. A., Neish, A. S., Whitley, M. Z., Thanos, D., and Maniatis, T.: Transcriptional regulation of endothelial cell adhesion molecules: NF-kappa B and cytokine-inducible enhancers. Faseb J **9** (10)**:** 899-909, 1995.

Cordon-Cardo, C., O'Brien, J. P., Casals, D., Rittman-Grauer, L., Biedler, J. L., Melamed, M. R., and Bertino, J. R.: Multidrug-resistance gene (P-glycoprotein) is expressed by endothelial cells at blood-brain barrier sites. Proc Natl Acad Sci U S A **86** (2)**:** 695-8, 1989.

Crowe, A., and Morgan, E. H.: Iron and transferrin uptake by brain and cerebrospinal fluid in the rat. Brain Res **592** (1-2)**:** 8-16, 1992.

Cybulsky, M. I., Fries, J. W., Williams, A. J., Sultan, P., Eddy, R., Byers, M., Shows, T., Gimbrone, M. A., Jr., and Collins, T.: Gene structure, chromosomal location, and basis for alternative mRNA splicing of the human VCAM1 gene. Proc Natl Acad Sci U S A **88** (17)**:** 7859-63, 1991.

Daaka, Y., and Wickstrom, E.: Target dependence of antisense oligodeoxynucleotide inhibition of c-Ha-ras p21 expression and focus formation in T24-transformed NIH3T3 cells. Oncogene Res **5** (4)**:** 267-75, 1990.

Daniel, P. M., Lam, D. K., and Pratt, O. E.: Relation between the increase in the diffusional permeability of the blood-central nervous system barrier and other changes during the development of experimental allergic encephalomyelitis in the Lewis rat. J Neurol Sci **60** (3)**:** 367-76, 1983.

de Vries, H. E., Hoogendoorn, K. H., van Dijk, J., Zijlstra, F. J., van Dam, A. M., Breimer, D. D., van Berkel, T. J., de Boer, A. G., and Kuiper, J.: Eicosanoid

production by rat cerebral endothelial cells: stimulation by lipopolysaccharide, interleukin-1 and interleukin-6. J Neuroimmunol **59** (1-2)**:** 1-8, 1995.

de Vries, H. E., Kuiper, J., de Boer, A. G., Van Berkel, T. J., and Breimer, D. D.: The blood-brain barrier in neuroinflammatory diseases. Pharmacol Rev **49** (2)**:** 143-55, 1997.

Deguchi, Y., Kurihara, A., and Pardridge, W. M.: Retention of biologic activity of human epidermal growth factor following conjugation to a blood-brain barrier drug delivery vector via an extended poly(ethylene glycol) linker. Bioconjug Chem **10** (1)**:** 32-7, 1999.

Deininger, M. H., and Schluesener, H. J.: Cyclooxygenases-1 and -2 are differentially localized to microglia and endothelium in rat EAE and glioma. J Neuroimmunol **95** (1-2)**:** 202-8, 1999.

Diamond, J. M., and Wright, E. M.: Molecular forces governing non-electrolyte permeation through cell membranes. Proc R Soc Lond B Biol Sci **171** (28)**:** 273-316, 1969.

Dietrich, J.B.: The adhesion molecule ICAM-1 and its regulation in relation with the blood-brain barrier. J Neuroimmunol **128** (1-2): 58-68, 2002

Dunlap, D. D., Maggi, A., Soria, M. R., and Monaco, L.: Nanoscopic structure of DNA condensed for gene delivery. Nucleic Acids Res **25** (15)**:** 3095-101, 1997.

Dzau, V. J.: Transcription factor decoy. Circ Res **90** (12)**:** 1234-6, 2002.

Ehsan, A., Mann, M. J., Dell'Acqua, G., and Dzau, V. J.: Long-term stabilization of vein graft wall architecture and prolonged resistance to experimental atherosclerosis after E2F decoy oligonucleotide gene therapy. J Thorac Cardiovasc Surg **121** (4)**:** 714-22, 2001.

Farrell, C. L., and Pardridge, W. M.: Blood-brain barrier glucose transporter is asymmetrically distributed on brain capillary endothelial lumenal and ablumenal membranes: an electron microscopic immunogold study. Proc Natl Acad Sci U S A **88** (13)**:** 5779-83, 1991.

Fischer, D., Bieber, T., Li, Y., Elsasser, H. P., and Kissel, T.: A novel non-viral vector for DNA delivery based on low molecular weight, branched polyethylenimine: effect of molecular weight on transfection efficiency and cytotoxicity. Pharm Res **16** (8)**:** 1273-9, 1999.

Fishman, J. B., Rubin, J. B., Handrahan, J. V., Connor, J. R., and Fine, R. E.: Receptor-mediated transcytosis of transferrin across the blood-brain barrier. J Neurosci Res **18** (2): 299-304, 1987.

Floris, S., Ruuls, S.R., Wierinckx, A., van der Pol, S.M., Dopp, E., van der Meide, P.H., Dijkstra, C.D., and De Vries, H.E.: Interferon-beta directly influences monocyte infiltration into the central nervous system. J Neuroimmunol **127** (1-2): 69-79, 2002

Frank, H. J., Pardridge, W. M., Morris, W. L., Rosenfeld, R. G., and Choi, T. B.: Binding and internalization of insulin and insulin-like growth factors by isolated brain microvessels. Diabetes **35** (6)**:** 654-61, 1986.

Friden, P. M., Walus, L. R., Musso, G. F., Taylor, M. A., Malfroy, B., and Starzyk, R. M.: Anti-transferrin receptor antibody and antibody-drug conjugates cross the blood-brain barrier. Proc Natl Acad Sci U S A **88** (11)**:** 4771-5, 1991.

Gambarotta, G., Boccaccio, C., Giordano, S., Ando, M., Stella, M. C., and Comoglio, P. M.: Ets up-regulates MET transcription. Oncogene **13** (9)**:** 1911-7, 1996.

Godbey, W. T., Wu, K. K., Hirasaki, G. J., and Mikos, A. G.: Improved packing of poly(ethylenimine)/DNA complexes increases transfection efficiency. Gene Ther **6** (8)**:** 1380-8., 1999a.

Godbey, W. T., Wu, K. K., and Mikos, A. G.: Poly(ethylenimine) and its role in gene delivery. J Control Release **60** (2-3)**:** 149-60., 1999b.

Golden, P. L., Maccagnan, T. J., and Pardridge, W. M.: Human blood-brain barrier leptin receptor. Binding and endocytosis in isolated human brain microvessels. J Clin Invest **99** (1)**:** 14-8, 1997.

Ghosh, S., and Karin, M.: Missing pieces in the NF-kappaB puzzle. Cell **109 Suppl:** S81-96, 2002.

Ghosh, S., May, M. J., and Kopp, E. B.: NF-kappa B and Rel proteins: evolutionarily conserved mediators of immune responses. Annu Rev Immunol **16:** 225-60, 1998.

Goula, D., Remy, J. S., Erbacher, P., Wasowicz, M., Levi, G., Abdallah, B., and Demeneix, B. A.: Size, diffusibility and transfection performance of linear PEI/DNA complexes in the mouse central nervous system. Gene Ther **5** (5)**:** 712-7., 1998.

Gref, R., Minamitake, Y., Peracchia, M. T., Trubetskoy, V., Torchilin, V., and Langer, R.: Biodegradable long-circulating polymeric nanospheres. Science **263** (5153)**:** 1600-3, 1994.

Gukovsky, I., Gukovskaya, A.S., Blinman, T.A., Zaninovic, V., and Pandol, S.J.: Early NF-kappaB activation is associated with hormone-induced pancreatitis. Am J Physiol **275** (6 Pt 1): G1402-14, 1998

Guo, W., and Lee, R. J.: Efficient gene delivery via non-covalent complexes of folic acid and polyethylenimine. J Control Release **77** (1-2)**:** 131-8, 2001.

Hafler, D. A., and Weiner, H. L.: Immunologic mechanisms and therapy in multiple sclerosis. Immunol Rev **144:** 75-107, 1995.

Henninger, D. D., Panes, J., Eppihimer, M., Russell, J., Gerritsen, M., Anderson, D. C., and Granger, D. N.: Cytokine-induced VCAM-1 and ICAM-1 expression in different organs of the mouse. J Immunol **158** (4)**:** 1825-32, 1997.

Hess, D. C., Howard, E., Cheng, C., Carroll, J., Hill, W. D., and Hsu, C. Y.: Hypertonic mannitol loading of NF-kappaB transcription factor decoys in human brain microvascular endothelial cells blocks upregulation of ICAM-1. Stroke **31** (5)**:** 1179-86, 2000.

Higuchi, T., and Davis, S. S.: Thermodynamic analysis of structure-activity relationships of drugs. Prediction of optimal structure. J Pharm Sci **59** (10)**:** 1376-83, 1970.

Hiller, Y., Gershoni, J. M., Bayer, E. A., and Wilchek, M.: Biotin binding to avidin. Oligosaccharide side chain not required for ligand association. Biochem J **248** (1)**:** 167-71, 1987.

Hirose-Kumagai, A., Sakai, H., and Akamatsu, N.: Increase of transferrin receptors in hepatocytes during rat liver regeneration. Int J Biochem **16** (6)**:** 601-5, 1984.

Hoffmann, A., Levchenko, A., Scott, M. L., and Baltimore, D.: The IkappaB-NF-kappaB signaling module: temporal control and selective gene activation. Science **298** (5596)**:** 1241-5, 2002.

Hooper, D. C., Bagasra, O., Marini, J. C., Zborek, A., Ohnishi, S. T., Kean, R., Champion, J. M., Sarker, A. B., Bobroski, L., Farber, J. L., Akaike, T., Maeda, H., and Koprowski, H.: Prevention of experimental allergic encephalomyelitis by targeting nitric oxide and peroxynitrite: implications for the treatment of multiple sclerosis. Proc Natl Acad Sci U S A **94** (6)**:** 2528-33, 1997.

Huwyler, J., Wu, D., and Pardridge, W. M.: Brain drug delivery of small molecules using immunoliposomes. Proc Natl Acad Sci U S A **93** (24)**:** 14164-9, 1996.

Jain, R. K.: Tumor physiology and antibody delivery. Front Radiat Ther Oncol **24:** 32-46; discussion 64-8, 1990.

Jefferies, W. A., Brandon, M. R., Hunt, S. V., Williams, A. F., Gatter, K. C., and Mason, D. Y.: Transferrin receptor on endothelium of brain capillaries. Nature **312** (5990)**:** 162-3, 1984.

Jing, S. Q., and Trowbridge, I. S.: Nonacylated human transferrin receptors are rapidly internalized and mediate iron uptake. J Biol Chem **265** (20)**:** 11555-9, 1990.

Kabanov, A. V., Vinogradov, S. V., Suzdaltseva, Y. G., and Alakhov, V.: Water-soluble block polycations as carriers for oligonucleotide delivery. Bioconjug Chem **6** (6)**:** 639-43, 1995.

Kaltschmidt, B., Uherek, M., Volk, B., Baeuerle, P. A., and Kaltschmidt, C.: Transcription factor NF-kappaB is activated in primary neurons by amyloid beta peptides and in neurons surrounding early plaques from patients with Alzheimer disease. Proc Natl Acad Sci U S A **94** (6)**:** 2642-7, 1997.

Kaltschmidt, C., Kaltschmidt, B., Lannes-Vieira, J., Kreutzberg, G. W., Wekerle, H., Baeuerle, P. A., and Gehrmann, J.: Transcription factor NF-kappa B is activated in microglia during experimental autoimmune encephalomyelitis. J Neuroimmunol **55** (1)**:** 99-106, 1994.

Kang, Y. S., Boado, R. J., and Pardridge, W. M.: Pharmacokinetics and organ clearance of a 3'-biotinylated, internally [32P]-labeled phosphodiester oligodeoxynucleotide coupled to a neutral avidin/monoclonal antibody conjugate. Drug Metab Dispos **23** (1)**:** 55-9, 1995.

Kang, Y. S., and Pardridge, W. M.: Use of neutral avidin improves pharmacokinetics and brain delivery of biotin bound to an avidin-monoclonal antibody conjugate. J Pharmacol Exp Ther **269** (1)**:** 344-50, 1994.

Kantarci, O. H., de Andrade, M., and Weinshenker, B. G.: Identifying disease modifying genes in multiple sclerosis. J Neuroimmunol **123** (1-2)**:** 144-59, 2002.

Kemp, J. D., Thorson, J. A., McAlmont, T. H., Horowitz, M., Cowdery, J. S., and Ballas, Z. K.: Role of the transferrin receptor in lymphocyte growth: a rat IgG monoclonal antibody against the murine transferrin receptor produces highly selective inhibition of T and B cell activation protocols. J Immunol **138** (8)**:** 2422-6, 1987.

Killian, D. M., Gharat, L., and Chikhale, P. J.: Modulating blood-brain barrier interactions of amino acid-based anticancer agents. Drug Deliv **7** (1)**:** 21-5, 2000.

Kinashi, T., St Pierre, Y., and Springer, T. A.: Expression of glycophosphatidylinositol-anchored and -non-anchored isoforms of vascular cell adhesion molecule 1 in murine stromal and endothelial cells. J Leukoc Biol **57** (1)**:** 168-73, 1995.

Kircheis, R., Blessing, T., Brunner, S., Wightman, L., and Wagner, E.: Tumor targeting with surface-shielded ligand--polycation DNA complexes. J Control Release **72** (1-3)**:** 165-70, 2001a.

Kircheis, R., Wightman, L., Schreiber, A., Robitza, B., Rossler, V., Kursa, M., and Wagner, E.: Polyethylenimine/DNA complexes shielded by transferrin target gene expression to tumors after systemic application. Gene Ther **8** (1)**:** 28-40, 2001b.

Kircheis, R., Schuller, S., Brunner, S., Ogris, M., Heider, K. H., Zauner, W., and Wagner, E.: Polycation-based DNA complexes for tumor-targeted gene delivery in vivo. J Gene Med **1** (2)**:** 111-20., 1999.

Kircheis, R., Wightman, L., and Wagner, E.: Design and gene delivery activity of modified polyethylenimines. Adv Drug Deliv Rev **53** (3)**:** 341-58, 2001b.

Kissel, K., Hamm, S., Schulz, M., Vecchi, A., Garlanda, C., and Engelhardt, B.: Immunohistochemical localization of the murine transferrin receptor (TfR) on

blood-tissue barriers using a novel anti-TfR monoclonal antibody. Histochem Cell Biol **110** (1)**:** 63-72, 1998.

Koppelhus, U., and Nielsen, P. E.: Cellular delivery of peptide nucleic acid (PNA). Adv Drug Deliv Rev **55** (2)**:** 267-80, 2003.

Koprowski, H., Zheng, Y. M., Heber-Katz, E., Fraser, N., Rorke, L., Fu, Z. F., Hanlon, C., and Dietzschold, B.: In vivo expression of inducible nitric oxide synthase in experimentally induced neurologic diseases. Proc Natl Acad Sci U S A **90** (7)**:** 3024-7, 1993.

Kordower, J. H., Charles, V., Bayer, R., Bartus, R. T., Putney, S., Walus, L. R., and Friden, P. M.: Intravenous administration of a transferrin receptor antibody-nerve growth factor conjugate prevents the degeneration of cholinergic striatal neurons in a model of Huntington disease. Proc Natl Acad Sci U S A **91** (19)**:** 9077-80, 1994.

Kreuter, J., Shamenkov, D., Petrov, V., Ramge, P., Cychutek, K., Koch-Brandt, C., and Alyautdin, R.: Apolipoprotein-mediated transport of nanoparticle-bound drugs across the blood-brain barrier. J Drug Target **10** (4)**:** 317-25, 2002.

Kumar, A. G., Dai, X. Y., Kozak, C. A., Mims, M. P., Gotto, A. M., and Ballantyne, C. M.: Murine VCAM-1. Molecular cloning, mapping, and analysis of a truncated form. J Immunol **153** (9)**:** 4088-98, 1994.

Kunath, K., von Harpe, A., Petersen, H., Fischer, D., Voigt, K., Kissel, T., and Bickel, U.: The structure of PEG-modified poly(ethylene imines) influences biodistribution and pharmacokinetics of their complexes with NF-kappaB decoy in mice. Pharm Res **19** (6)**:** 810-7, 2002.

Kurihara, A., Deguchi, Y., and Pardridge, W. M.: Epidermal growth factor radiopharmaceuticals: 111In chelation, conjugation to a blood-brain barrier delivery vector via a biotin-polyethylene linker, pharmacokinetics, and in vivo imaging of experimental brain tumors. Bioconjug Chem **10** (3)**:** 502-11, 1999.

Lacroix, S., Feinstein, D., and Rivest, S.: The bacterial endotoxin lipopolysaccharide has the ability to target the brain in upregulating its membrane CD14 receptor within specific cellular populations. Brain Pathol **8** (4)**:** 625-40, 1998.

Laflamme, N., and Rivest, S.: Effects of systemic immunogenic insults and circulating proinflammatory cytokines on the transcription of the inhibitory factor kappaB alpha within specific cellular populations of the rat brain. J Neurochem **73** (1)**:** 309-21, 1999.

Laschinger, M., and Engelhardt, B.: Interaction of alpha4-integrin with VCAM-1 is involved in adhesion of encephalitogenic T cell blasts to brain endothelium but not in their transendothelial migration in vitro. J Neuroimmunol **102** (1)**:** 32-43, 2000.

Laurel, C., and Ingelman, B.: The iron-binding protein of swine serum. Acta Chem. Scand. **1:** 770-776, 1947.

Lee, H. J., Engelhardt, B., Lesley, J., Bickel, U., and Pardridge, W. M.: Targeting rat anti-mouse transferrin receptor monoclonal antibodies through blood-brain barrier in mouse. J Pharmacol Exp Ther **292** (3)**:** 1048-52, 2000.

Lee, H. J., Boado, R. J., Braasch, D. A., Corey, D. R., and Pardridge, W. M.: Imaging gene expression in the brain in vivo in a transgenic mouse model of Huntington's disease with an antisense radiopharmaceutical and drug-targeting technology. J Nucl Med **43** (7)**:** 948-56, 2002a.

Lee, H. J., Zhang, Y., Zhu, C., Duff, K., and Pardridge, W. M.: Imaging brain amyloid of Alzheimer disease in vivo in transgenic mice with an Abeta peptide radiopharmaceutical. J Cereb Blood Flow Metab **22** (2)**:** 223-31, 2002b.

Lemkine, G. F., Goula, D., Becker, N., Paleari, L., Levi, G., and Demeneix, B. A.: Optimisation of polyethylenimine-based gene delivery to mouse brain. J Drug Target **7** (4)**:** 305-12., 1999.

Leonetti, J. P., Degols, G., and Lebleu, B.: Biological activity of oligonucleotide-poly(L-lysine) conjugates: mechanism of cell uptake. Bioconjug Chem **1** (2)**:** 149-53, 1990.

Lin, L., and Ghosh, S.: A glycine-rich region in NF-kappaB p105 functions as a processing signal for the generation of the p50 subunit. Mol Cell Biol **16** (5)**:** 2248-54, 1996.

Lipinski, C. A., Lombardo, F., Dominy, B. W., and Feeney, P. J.: Experimental and computational approaches to estimate solubility and permeability in drug discovery and development settings. Adv Drug Deliv Rev **46** (1-3)**:** 3-26, 2001.

Lollo, C. P., Banaszczyk, M. G., Mullen, P. M., Coffin, C. C., Wu, D., Carlo, A. T., Bassett, D. L., Gouveia, E. K., and Carlo, D. J.: Poly-L-lysine-based gene delivery systems. Synthesis, purification, and application. Methods Mol Med **69:** 1-13, 2002.

Madan, B., Batra, S., and Ghosh, B.: 2'-hydroxychalcone inhibits nuclear factor-kappaB and blocks tumor necrosis factor-alpha- and lipopolysaccharide-induced adhesion of neutrophils to human umbilical vein endothelial cells. Mol Pharmacol **58** (3)**:** 526-34, 2000.

Maher, L. J., 3rd, and Dolnick, B. J.: Comparative hybrid arrest by tandem antisense oligodeoxyribonucleotides or oligodeoxyribonucleoside methylphosphonates in a cell-free system. Nucleic Acids Res **16** (8)**:** 3341-58, 1988.

Maksimenko, A. V., Mandrouguine, V., Gottikh, M. B., Bertrand, J. R., Majoral, J. P., and Malvy, C.: Optimisation of dendrimer-mediated gene transfer by anionic oligomers. J Gene Med **5** (1)**:** 61-71, 2003.

Mann, M. J., and Dzau, V. J.: Therapeutic applications of transcription factor decoy oligonucleotides. J Clin Invest **106** (9)**:** 1071-5, 2000.

Mann, M. J., Whittemore, A. D., Donaldson, M. C., Belkin, M., Conte, M. S., Polak, J. F., Orav, E. J., Ehsan, A., Dell'Acqua, G., and Dzau, V. J.: Ex-vivo gene therapy of human vascular bypass grafts with E2F decoy: the PREVENT single-centre, randomised, controlled trial. Lancet **354** (9189)**:** 1493-8, 1999.

Max, E. E., Maizel, J. V., Jr., and Leder, P.: The nucleotide sequence of a 5.5-kilobase DNA segment containing the mouse kappa immunoglobulin J and C region genes. J Biol Chem **256** (10)**:** 5116-20, 1981.

McDonald, W. I., Compston, A., Edan, G., Goodkin, D., Hartung, H. P., Lublin, F. D., McFarland, H. F., Paty, D. W., Polman, C. H., Reingold, S. C., Sandberg-Wollheim, M., Sibley, W., Thompson, A., van den Noort, S., Weinshenker, B. Y., and Wolinsky, J. S.: Recommended diagnostic criteria for multiple sclerosis: guidelines from the International Panel on the diagnosis of multiple sclerosis. Ann Neurol **50** (1)**:** 121-7, 2001.

Merdan, T., Kopecek, J., and Kissel, T.: Prospects for cationic polymers in gene and oligonucleotide therapy against cancer. Adv Drug Deliv Rev **54** (5)**:** 715-58, 2002a.

Merdan, T., Kunath, K., Fischer, D., Kopecek, J., and Kissel, T.: Intracellular processing of poly(ethylene imine)/ribozyme complexes can be observed in living cells by using confocal laser scanning microscopy and inhibitor experiments. Pharm Res **19** (2)**:** 140-6, 2002b.

Meresse, S., Delbart, C., Fruchart, J. C., and Cecchelli, R.: Low-density lipoprotein receptor on endothelium of brain capillaries. J Neurochem **53** (2)**:** 340-5, 1989.

Miller, D. H., Khan, O. A., Sheremata, W. A., Blumhardt, L. D., Rice, G. P., Libonati, M. A., Willmer-Hulme, A. J., Dalton, C. M., Miszkiel, K. A., and O'Connor, P. W.: A controlled trial of natalizumab for relapsing multiple sclerosis. N Engl J Med **348** (1)**:** 15-23, 2003.

Mislick, K. A., and Baldeschwieler, J. D.: Evidence for the role of proteoglycans in cation-mediated gene transfer. Proc Natl Acad Sci U S A **93** (22)**:** 12349-54, 1996.

Moos, T., and Morgan, E. H.: Transferrin and transferrin receptor function in brain barrier systems. Cell Mol Neurobiol **20** (1)**:** 77-95, 2000.

Morgan, E. H., and Baker, E.: Role of transferrin receptors and endocytosis in iron uptake by hepatic and erythroid cells. Ann N Y Acad Sci **526:** 65-82, 1988.

Morishita, R., Higaki, J., Tomita, N., and Ogihara, T.: Application of transcription factor "decoy" strategy as means of gene therapy and study of gene expression in cardiovascular disease. Circ Res **82** (10)**:** 1023-8, 1998.

Nadal, A., Fuentes, E., Pastor, J., and McNaughton, P. A.: Plasma albumin is a potent trigger of calcium signals and DNA synthesis in astrocytes. Proc Natl Acad Sci U S A **92** (5)**:** 1426-30, 1995.

Nadeau, S., and Rivest, S.: Effects of circulating tumor necrosis factor on the neuronal activity and expression of the genes encoding the tumor necrosis factor receptors (p55 and p75) in the rat brain: a view from the blood-brain barrier. Neuroscience **93** (4)**:** 1449-64, 1999.

Nau, R., Sorgel, F., and Prange, H. W.: Pharmacokinetic optimisation of the treatment of bacterial central nervous system infections. Clin Pharmacokinet **35** (3)**:** 223-46, 1998.

Neuwelt, E. A., and Rapoport, S. I.: Modification of the blood-brain barrier in the chemotherapy of malignant brain tumors. Fed Proc **43** (2)**:** 214-9, 1984.

Ogris, M., Steinlein, P., Carotta, S., Brunner, S., and Wagner, E.: DNA/polyethylenimine transfection particles: influence of ligands, polymer size, and PEGylation on internalization and gene expression. AAPS PharmSci **3** (3)**:** E21, 2001.

Ogris, M., Brunner, S., Schuller, S., Kircheis, R., and Wagner, E.: PEGylated DNA/transferrin-PEI complexes: reduced interaction with blood components, extended circulation in blood and potential for systemic gene delivery. Gene Ther **6** (4)**:** 595-605., 1999.

Ogris, M., Steinlein, P., Kursa, M., Mechtler, K., Kircheis, R., and Wagner, E.: The size of DNA/transferrin-PEI complexes is an important factor for gene expression in cultured cells. Gene Ther **5** (10)**:** 1425-33., 1998.

Oksenberg, J. R., and Hauser, S. L.: New insights into the immunogenetics of multiple sclerosis. Curr Opin Neurol **10** (3)**:** 181-5, 1997.

Olivier, J. C., Huertas, R., Lee, H. J., Calon, F., and Pardridge, W. M.: Synthesis of pegylated immunonanoparticles. Pharm Res **19** (8)**:** 1137-43, 2002.

O'Neill, L. A., and Kaltschmidt, C.: NF-kappa B: a crucial transcription factor for glial and neuronal cell function. Trends Neurosci **20** (6)**:** 252-8, 1997.

Osburg, B., Peiser, C., Domling, D., Schomburg, L., Ko, Y. T., Voigt, K., and Bickel, U.: Effect of endotoxin on expression of TNF receptors and transport of TNF-alpha at the blood-brain barrier of the rat. Am J Physiol Endocrinol Metab **283** (5)**:** E899-908, 2002.

Oupicky, D., Ogris, M., Howard, K. A., Dash, P. R., Ulbrich, K., and Seymour, L. W.: Importance of lateral and steric stabilization of polyelectrolyte gene delivery vectors for extended systemic circulation. Mol Ther **5** (4)**:** 463-72, 2002.

Papahadjopoulos, D., Allen, T. M., Gabizon, A., Mayhew, E., Matthay, K., Huang, S. K., Lee, K. D., Woodle, M. C., Lasic, D. D., Redemann, C., and et al.: Sterically stabilized liposomes: improvements in pharmacokinetics and antitumor therapeutic efficacy.PG - 11460-4. Proc Natl Acad Sci U S A **88** (24), 1991.

Pardridge, W. M.: Recent advances in blood-brain barrier transport. Annu Rev Pharmacol Toxicol **28:** 25-39, 1988.

Pardridge, W. M.: CNS drug design based on principles of blood-brain barrier transport. J Neurochem **70** (5)**:** 1781-92, 1998.

Pardridge, W. M.: Targeting neurotherapeutic agents through the blood-brain barrier. Arch Neurol **59** (1)**:** 35-40, 2002.

Pardridge, W. M., Boado, R. J., and Kang, Y. S.: Vector-mediated delivery of a polyamide ("peptide") nucleic acid analogue through the blood-brain barrier in vivo. Proc Natl Acad Sci U S A **92** (12)**:** 5592-6, 1995.

Pardridge, W. M., Boado, R. J., and Buciak, J.: Drug delivery of antisense oligonucleotides or peptides to tissues in vivo using an avidin-biotin system. Drug Target. Del. **1:** 43-50, 1993.

Pardridge, W. M., Buciak, J. L., and Friden, P. M.: Selective transport of an anti-transferrin receptor antibody through the blood-brain barrier in vivo. J Pharmacol Exp Ther **259** (1)**:** 66-70, 1991.

Pardridge, W. M., Eisenberg, J., and Yang, J.: Human blood-brain barrier transferrin receptor. Metabolism **36** (9)**:** 892-5, 1987a.

Pardridge, W. M., Kang, Y. S., and Buciak, J. L.: Transport of human recombinant brain-derived neurotrophic factor (BDNF) through the rat blood-brain barrier in vivo using vector-mediated peptide drug delivery. Pharm Res **11** (5)**:** 738-46, 1994.

Pardridge, W. M., Kumagai, A. K., and Eisenberg, J. B.: Chimeric peptides as a vehicle for peptide pharmaceutical delivery through the blood-brain barrier. Biochem Biophys Res Commun **146** (1)**:** 307-13, 1987b.

Pardridge, W. M., and Mietus, L. J.: Transport of steroid hormones through the rat blood-brain barrier. Primary role of albumin-bound hormone. J Clin Invest **64** (1)**:** 145-54, 1979.

Pardridge, W. M., Wu, D., and Sakane, T.: Combined use of carboxyl-directed protein pegylation and vector-mediated blood-brain barrier drug delivery system optimizes brain uptake of brain-derived neurotrophic factor following intravenous administration. Pharm Res **15** (4)**:** 576-82, 1998.

Petersen, H., Fechner, P. M., Martin, A. L., Kunath, K., Stolnik, S., Roberts, C. J., Fischer, D., Davies, M. C., and Kissel, T.: Polyethylenimine-graft-Poly(ethylene glycol) Copolymers: Influence of Copolymer Block Structure on DNA Complexation and Biological Activities as Gene Delivery System. Bioconjug Chem **13** (4)**:** 845-54., 2002.

Pollard, H., Remy, J. S., Loussouarn, G., Demolombe, S., Behr, J. P., and Escande, D.: Polyethylenimine but not cationic lipids promotes transgene delivery to the nucleus in mammalian cells. J Biol Chem **273** (13)**:** 7507-11, 1998.

Quan, N., Whiteside, M., and Herkenham, M.: Cyclooxygenase 2 mRNA expression in rat brain after peripheral injection of lipopolysaccharide. Brain Res **802** (1-2)**:** 189-97, 1998a.

Quan, N., Whiteside, M., and Herkenham, M.: Time course and localization patterns of interleukin-1beta messenger RNA expression in brain and pituitary after peripheral administration of lipopolysaccharide. Neuroscience **83** (1)**:** 281-93, 1998b.

Quan, N., Whiteside, M., Kim, L., and Herkenham, M.: Induction of inhibitory factor kappaBalpha mRNA in the central nervous system after peripheral lipopolysaccharide administration: an in situ hybridization histochemistry study in the rat. Proc Natl Acad Sci U S A **94** (20)**:** 10985-90, 1997.

Raub, T. J., and Newton, C. R.: Recycling kinetics and transcytosis of transferrin in primary cultures of bovine brain microvessel endothelial cells. J Cell Physiol **149** (1)**:** 141-51, 1991.

Reiss, Y., and Engelhardt, B.: T cell interaction with ICAM-1-deficient endothelium in vitro: transendothelial migration of different T cell populations is mediated by endothelial ICAM-1 and ICAM-2. Int Immunol **11** (9)**:** 1527-39, 1999.

Robaczewska, M., Guerret, S., Remy, J. S., Chemin, I., Offensperger, W. B., Chevallier, M., Behr, J. P., Podhajska, A. J., Blum, H. E., Trepo, C., and Cova, L.: Inhibition of hepadnaviral replication by polyethylenimine-based intravenous delivery of antisense phosphodiester oligodeoxynucleotides to the liver. Gene Ther **8** (11)**:** 874-81., 2001.

Rohnelt, R. K., Hoch, G., Reiss, Y., and Engelhardt, B.: Immunosurveillance modelled in vitro: naive and memory T cells spontaneously migrate across unstimulated microvascular endothelium. Int Immunol **9** (3)**:** 435-50, 1997.

Rosati, G.: The prevalence of multiple sclerosis in the world: an update. Neurol Sci **22** (2)**:** 117-39, 2001.

Rungeler, P., Lyss, G., and Merfort, I.: Zentraler Mediator im Immunsystem und Entzundungsgeschehen. Pharm Ztg. **2:** 100-8, 1999.

Sagara, K., and Kim, S. W.: A new synthesis of galactose-poly(ethylene glycol)-polyethylenimine for gene delivery to hepatocytes. J Control Release **79** (1-3)**:** 271-81, 2002.

Saito, Y., Buciak, J., Yang, J., and Pardridge, W. M.: Vector-mediated delivery of 125I-labeled beta-amyloid peptide A beta 1-40 through the blood-brain barrier and binding to Alzheimer disease amyloid of the A beta 1-40/vector complex. Proc Natl Acad Sci U S A **92** (22)**:** 10227-31, 1995.

Sakamoto, A., and Ido, T.: Liposome targeting to rat brain: effect of osmotic opening of the blood-brain barrier.PG - 171-5. Brain Res **629** (1), 1993.

Salahuddin, T. S., Johansson, B. B., Kalimo, H., and Olsson, Y.: Structural changes in the rat brain after carotid infusions of hyperosmolar solutions. An electron microscopic study. Acta Neuropathol (Berl) **77** (1)**:** 5-13, 1988.

Sands, H., Gorey-Feret, L. J., Cocuzza, A. J., Hobbs, F. W., Chidester, D., and Trainor, G. L.: Biodistribution and metabolism of internally 3H-labeled oligonucleotides. I. Comparison of a phosphodiester and a phosphorothioate. Mol Pharmacol **45** (5)**:** 932-43, 1994.

Schackert, G., Fan, D., Nayar, R., and Fidler, I. J.: Arrest and retention of multilamellar liposomes in the brain of normal mice or mice bearing experimental brain metastases.PG - 73-9. Sel Cancer Ther **5** (2), 1989.

Scherer, D. C., Brockman, J. A., Chen, Z., Maniatis, T., and Ballard, D. W.: Signal-induced degradation of I kappa B alpha requires site-specific ubiquitination. Proc Natl Acad Sci U S A **92** (24)**:** 11259-63, 1995.

Schlingensiepen, K. H., and Heilig, M.: Gene function analysis and therapeutic prospects in neurobiology. *In* Antisense - from Technology to Therapy, ed. by R. Schlingensiepen, W. Brysch, and K. H. Schlingensiepen, pp. 186-223, Blackwell Science, Berlin, 1997.

Schlingensiepen, R., and Schlingensiepen, K. H.: Antisense oligodeoxynucleotides - highly specific tools for basic research and pharmacotherapy. *In* Antisense - from

Technology to Therapy, ed. by R. Schlingensiepen, W. Brysch, and K. H. Schlingensiepen, pp. 186-223, Blackwell Science, Berlin, 1997.

Schmedtje, J. F., Jr., Ji, Y. S., Liu, W. L., DuBois, R. N., and Runge, M. S.: Hypoxia induces cyclooxygenase-2 via the NF-kappaB p65 transcription factor in human vascular endothelial cells. J Biol Chem **272** (1)**:** 601-8, 1997.

Schroeder, U., Sommerfeld, P., Ulrich, S., and Sabel, B. A.: Nanoparticle technology for delivery of drugs across the blood-brain barrier. J Pharm Sci **87** (11)**:** 1305-7, 1998.

Sen, R., and Baltimore, D.: Multiple nuclear factors interact with the immunoglobulin enhancer sequences. Cell **46** (5)**:** 705-16, 1986.

Shashoua, V. E., and Hesse, G. W.: N-docosahexaenoyl, 3 hydroxytyramine: a dopaminergic compound that penetrates the blood-brain barrier and suppresses appetite.PG - 1347-57. Life Sci **58** (16), 1996.

Shaw, J. P., Kent, K., Bird, J., Fishback, J., and Froehler, B.: Modified deoxyoligonucleotides stable to exonuclease degradation in serum. Nucleic Acids Res **19** (4)**:** 747-50, 1991.

Shi, N., and Pardridge, W. M.: Noninvasive gene targeting to the brain. Proc Natl Acad Sci U S A **97** (13)**:** 7567-72, 2000.

Shi, N., Zhang, Y., Zhu, C., Boado, R. J., and Pardridge, W. M.: Brain-specific expression of an exogenous gene after i.v. administration. Proc Natl Acad Sci U S A **98** (22)**:** 12754-9, 2001.

Smith, Q. R. *In* Frontiers in Cerebral Vascular Biology: Transport and its Regulation, ed. by L. R. Drewes, Betz, A.L., pp. 83-93, Plenum Press, New York, 1993.

Smith, Q. R.: Transport of glutamate and other amino acids at the blood-brain barrier. J Nutr **130** (4S Suppl)**:** 1016S-22S, 2000.

Soda, R., and Tavassoli, M.: Liver endothelium and not hepatocytes or Kupffer cells have transferrin receptors. Blood **63** (2)**:** 270-6, 1984.

Soker, S., Svahn, C. M., and Neufeld, G.: Vascular endothelial growth factor is inactivated by binding to alpha 2-macroglobulin and the binding is inhibited by heparin. J Biol Chem **268** (11)**:** 7685-91, 1993.

Somia, N., and Verma, I. M.: Gene therapy: trials and tribulations. Nat Rev Genet **1** (2)**:** 91-9, 2000.

Song, B. W., Vinters, H. V., Wu, D., and Pardridge, W. M.: Enhanced neuroprotective effects of basic fibroblast growth factor in regional brain ischemia after conjugation to a blood-brain barrier delivery vector. J Pharmacol Exp Ther **301** (2)**:** 605-10, 2002.

Sorensen, T. L., and Ransohoff, R. M.: Etiology and pathogenesis of multiple sclerosis. Semin Neurol **18** (3)**:** 287-94, 1998.

Suh, J., Paik, HJ, Hwang, BK: Ionization of polyethylenimine and polyallylamine at various pHs. Bioorg. Chem. **22:** 318-27, 1994.

Tadayoni, B. M., Friden, P. M., Walus, L. R., and Musso, G. F.: Synthesis, in vitro kinetics, and in vivo studies on protein conjugates of AZT: evaluation as a transport system to increase brain delivery. Bioconjug Chem **4** (2)**:** 139-45, 1993.

Takada, Y., Vistica, D. T., Greig, N. H., Purdon, D., Rapoport, S. I., and Smith, Q. R.: Rapid high-affinity transport of a chemotherapeutic amino acid across the blood-brain barrier. Cancer Res **52** (8)**:** 2191-6, 1992.

Tang, M. X., and Szoka, F. C.: The influence of polymer structure on the interactions of cationic polymers with DNA and morphology of the resulting complexes. Gene Ther **4** (8)**:** 823-32., 1997.

Taylor, E. M., and Morgan, E. H.: Developmental changes in transferrin and iron uptake by the brain in the rat. Brain Res Dev Brain Res **55** (1)**:** 35-42, 1990.

Terry, R. W., Kwee, L., Levine, J. F., and Labow, M. A.: Cytokine induction of an alternatively spliced murine vascular cell adhesion molecule (VCAM) mRNA encoding a glycosylphosphatidylinositol-anchored VCAM protein. Proc Natl Acad Sci U S A **90** (13)**:** 5919-23, 1993.

Troster, S. D., Muller, U., and Kreuter, J.: Modification of the body distribution of poly(methyl methaacrylate) nanoparticles in rats by coating with surfactants. Int. J. Pharm. **61:** 85-100, 1990.

Tsuzuki, N., Hama, T., Kawada, M., Hasui, A., Konishi, R., Shiwa, S., Ochi, Y., Futaki, S., and Kitagawa, K.: Adamantane as a brain-directed drug carrier for poorly absorbed drug. 2. AZT derivatives conjugated with the 1-adamantane moiety.PG - 481-4. J Pharm Sci **83** (4), 1994.

van der Eb, M. M., Cramer, S. J., Vergouwe, Y., Schagen, F. H., van Krieken, J. H., van der Eb, A. J., Rinkes, I. H., van de Velde, C. J., and Hoeben, R. C.: Severe hepatic dysfunction after adenovirus-mediated transfer of the herpes simplex virus thymidine kinase gene and ganciclovir administration. Gene Ther **5** (4)**:** 451-8, 1998.

van de Stolpe, A., and van der Saag, P. T.: Intercellular adhesion molecule-1. J Mol Med **74** (1)**:** 13-33, 1996.

van Houten, M., and Posner, B. I.: Insulin binds to brain blood vessels in vivo. Nature **282** (5739)**:** 623-5, 1979.

Veronese, F. M., and Harris, J. M.: Introduction and overview of peptide and protein pegylation. Adv Drug Deliv Rev **54** (4)**:** 453-6, 2002.

Vinogradov, S., Batrakova, E., Li, S., and Kabanov, A.: Polyion complex micelles with protein-modified corona for receptor- mediated delivery of oligonucleotides into cells. Bioconjug Chem **10** (5)**:** 851-60., 1999.

Vinogradov, S. V., Bronich, T. K., and Kabanov, A. V.: Self-assembly of polyamine-poly(ethylene glycol) copolymers with phosphorothioate oligonucleotides. Bioconjug Chem **9** (6)**:** 805-12., 1998.

Wade, L. A., and Katzman, R.: Rat brain regional uptake and decarboxylation of L-DOPA following carotid injection. Am J Physiol **228** (2)**:** 352-9, 1975.

Whitesell, L., Geselowitz, D., Chavany, C., Fahmy, B., Walbridge, S., Alger, J. R., and Neckers, L. M.: Stability, clearance, and disposition of intraventricularly administered oligodeoxynucleotides: implications for therapeutic application within the central nervous system. Proc Natl Acad Sci U S A **90** (10)**:** 4665-9, 1993.

Wilchek, M., and Bayer, E. A.: Avidin-biotin immobilisation systems. *In* Application of Immobilized Macromolecules, ed. by U. B. Sleytr, P. Messner, D. Pum, and M. Sara, pp. 51-60, Springer-Verlag, New York, 1993.

Wong, M. L., Rettori, V., al-Shekhlee, A., Bongiorno, P. B., Canteros, G., McCann, S. M., Gold, P. W., and Licinio, J.: Inducible nitric oxide synthase gene expression in the brain during systemic inflammation. Nat Med **2** (5)**:** 581-4, 1996.

Wu, D., Boado, R. J., and Pardridge, W. M.: Pharmacokinetics and blood-brain barrier transport of [3H]-biotinylated phosphorothioate oligodeoxynucleotide conjugated to a vector-mediated drug delivery system. J Pharmacol Exp Ther **276** (1)**:** 206-11, 1996.

Wu, D., and Pardridge, W. M.: Central nervous system pharmacologic effect in conscious rats after intravenous injection of a biotinylated vasoactive intestinal peptide analog coupled to a blood-brain barrier drug delivery system. J Pharmacol Exp Ther **279** (1)**:** 77-83, 1996.

Wu, D., and Pardridge, W. M.: Neuroprotection with noninvasive neurotrophin delivery to the brain. Proc Natl Acad Sci U S A **96** (1)**:** 254-9, 1999.

Wu, D., Song, B. W., Vinters, H. V., and Pardridge, W. M.: Pharmacokinetics and brain uptake of biotinylated basic fibroblast growth factor conjugated to a blood-brain barrier drug delivery system. J Drug Target **10** (3)**:** 239-45, 2002.

Wu, D., Yang, J., and Pardridge, W. M.: Drug targeting of a peptide radiopharmaceutical through the primate blood-brain barrier in vivo with a monoclonal antibody to the human insulin receptor. J Clin Invest **100** (7)**:** 1804-12, 1997.

Yamamoto, Y., and Gaynor, R. B.: Therapeutic potential of inhibition of the NF-kappaB pathway in the treatment of inflammation and cancer. J Clin Invest **107** (2)**:** 135-42, 2001.

Yeoman, L. C., Danels, Y. J., and Lynch, M. J.: Lipofectin enhances cellular uptake of antisense DNA while inhibiting tumor cell growth. Antisense Res Dev **2** (1)**:** 51-9, 1992.

Zalipsky, S., Puntambekar, B., Boulikas, P., Engbers, C. M., and Woodle, M. C.: Peptide attachment to extremities of liposomal surface grafted PEG chains: preparation of the long-circulating form of laminin pentapeptide, YIGSR. Bioconjug Chem **6** (6)**:** 705-8, 1995.

Zelphati, O., Zon, G., and Leserman, L.: Inhibition of HIV-1 replication in cultured cells with antisense oligonucleotides encapsulated in immunoliposomes. Antisense Res Dev **3** (4)**:** 323-38, 1993.

Zhang, Y., Jeong Lee, H., Boado, R. J., and Pardridge, W. M.: Receptor-mediated delivery of an antisense gene to human brain cancer cells. J Gene Med **4** (2)**:** 183-94, 2002.

Zhang, Y., and Pardridge, W. M.: Conjugation of brain-derived neurotrophic factor to a blood-brain barrier drug targeting system enables neuroprotection in regional brain ischemia following intravenous injection of the neurotrophin. Brain Res **889** (1-2)**:** 49-56, 2001a.

Zhang, Y., and Pardridge, W. M.: Neuroprotection in transient focal brain ischemia after delayed intravenous administration of brain-derived neurotrophic factor conjugated to a blood-brain barrier drug targeting system. Stroke **32** (6)**:** 1378-84, 2001b.

Zhu, C., Zhang, Y., and Pardridge, W. M.: Widespread expression of an exogenous gene in the eye after intravenous administration. Invest Ophthalmol Vis Sci **43** (9)**:** 3075-80, 2002.

Zou, S. M., Erbacher, P., Remy, J. S., and Behr, J. P.: Systemic linear polyethylenimine (L-PEI)-mediated gene delivery in the mouse. J Gene Med **2** (2)**:** 128-34., 2000.

Academic teachers

My academic teachers at the Phillips University Marburg were the Drs. and Profs.:

Aumüller, Aurich, Beato, Besedovsky, Bickel, del Rey, Elsässer, Engelhardt, Feuser, Fruhstorfer, Garten, Grzeschik, Habermehl, Hartmann, Herrler, Jungclas, Kern, Kirchner, Knöller, Koolman, Lammel, Lang, Lefkovits, Löffler, Mandrek, Maser, McGregor, Müller, Niessing, Risau, Rogausch, Röhm, Schachtschabel, Schäfer, Schrimpf, Schulz, Schwee, Sedlacek, Seitz, Seitz, Steininger, Suske, Voigt, von Löw, Walter, Waßmuth, Westermann, Westphal

Publications

Abstracts and Posters

Osburg B., Bickel U.
Characterization of an Anti-Transferrin Receptor Monoclonal Antibody -
Streptavidin Conjugate for Drug Delivery to Brain in Mice, AAPS Annual Meeting,
Indianapolis, Indiana, USA, Oct.-Nov. 2000

Bickel U., **Osburg B**.
A Vector for Brain Drug Delivery in Mouse Models
Cerebral Vascular Biology IVth International Conference, Cambridge, UK. April 1-5th
2001

Bickel U., **Osburg B.**
Differential expression of IκBα and IκBβ transcripts in a mouse brain-derived endothelial
cell line
32th Annual Neuroscience Meeting, Orlando, Florida, USA, November 2-7th, 2002

Articles

Osburg, B., Shi J., Bickel U.
Differential regulation of IκB isoforms in brain endothelial cells
(in preparation for Neuroscience letters)

Osburg, B., Bickel U.
Transferrin receptor uptake of a polyethylenimine PEG co-polymer enhances the
effect of a transcription factor decoy
(in preparation for Journal of Controlled Release)